Masters

Built Environment

2006-01-01

# The Extraction of a Road Centre Line from Airborne Laser Scanning Data

Patrick Doyle
*Technological University Dublin*

## Recommended Citation

# The Extraction of a Road Centre Line from Airborne Laser Scanning Data

Patrick Doyle B.Sc. (Geomatics)

M.Phil

Dublin Institute of Technology

Dr Ken Boyle      Mr Kevin Mooney

School of Spatial Planning

January 2006

# Abstract

Due to its speed and accuracy the Global Positioning System (GPS) is widely used as a data collection tool. Problems however can occur when this GPS data is used in conjunction with existing National Mapping Agencies (NMA) vector databases that are not of comparable accuracy. Shifts and misalignments of the datasets can occur. In talks with the Irish mapping agency, Ordnance Survey Ireland (OSi), prior to this project, it viewed with interest the possibility of using Airborne Laser Scanning (ALS) data as a general quality indicator of existing vector databases.

The aim of this research was to extract the centre line of a small segment of straight road from triangulated ALS ground points. ALS data with a point density of 2 points per square metre was processed using TerraScan® to yield a set of ground points. The extraction process was based on the creation and analysis of cross-sections taken at regular intervals from the triangulated ALS data.

The cross-section widths and intervals were based on a search template developed from the start and end coordinates of an assumed centre line taken from an existing vector database. The cross-sections developed were based on individual triangles of the triangulation, groups of triangles and on interpolated data. Parameters of gradient, intensity and interpolated height are investigated.

Algorithms were developed in Matlab® to create and semi-automatically analyse the cross-sections. Cross-sections were generated for two different road sections and a ground truth survey was conducted for one of the roads.

The most useful cross-sections were those based on Interpolated Heights from the triangulated ALS data using the road width as an additional parameter. Results demonstrated that it was possible to define the true road extent from the ALS data with an accuracy equal to its point density of 2m by using a linear Least Squares best-fit algorithm.

The Intensity of the return pulse was not used in the extraction process and formed a separate piece of research. The findings were that the most useful cross-sections were those based on the Intensity Standard Deviations of the vertices of individual triangles in the triangulated ALS data and on Interpolated Intensity. Results show that it is possible to detect road markings from this information.
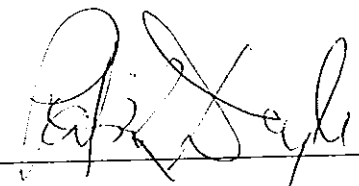
# Declaration

I certify that this thesis which I now submit for examination for the award of Master of Philosophy, is entirely my own work and has not been taken from the work of others save and to the extent that such work has been cited and acknowledged within the text of my work.

This thesis was prepared according to the regulations for postgraduate study by research of the Dublin Institute of Technology and has not been submitted in whole or in part for an award in any other Institute or University.

The work reported on in this thesis conforms to the principles and the requirements of the Institute's guidelines for ethics in research.

The Institute has permission to keep, to lend or to copy this thesis in whole or in part, on condition that any such use of the material of the thesis be duly acknowledged.

Signature _____ Date _____

Candidate

# Acknowledgements

Over the past two years I have received a great deal of support and assistance from many people. I would like to thank the DIT for providing me with the resources necessary to carry out my research, Frank Prendergast and all his staff in the Department of Spatial Information Sciences and my supervisors, Dr Ken Boyle and Mr Kevin Mooney.

In particular I would like to acknowledge the assistance received from my immediate supervisor Mr Kevin Mooney. Kevin was always available to discuss progress and problems and his positive attitude always inspired. Thank you Kevin for your advice, encouragement, kindness and patience.

As the research was not just a day job it did have an impact on home life, so a special thank you to my wife, Catherine, always supportive of my efforts, and my two daughters Aisling and Cliona.

And finally thanks to Margaret and Jim, my parents.

# Abbreviations

ALS                 Airborne Laser Scanning

DGPS                Differential Global Positioning System

DSM                 Digital Surface Model

DTM                 Digital Terrain Model

GPS                 Global Positioning System

IMU                 Inertial Management Unit

LIDAR               Light Detection and Ranging

NMA                 National Mapping Agency

OSi                 Ordnance Survey Ireland

POS                 Positioning and Orientation System

# List of Tables

# TABLE OF CONTENTS

# 1. Introduction

Over the past decade the demand for spatial information has increased dramatically. Advances in computer technology coupled with the reduction in costs have broadened the market for spatially related products. Geographic Information Systems (GIS) are now widely used by many and diverse industries. For example insurance companies use GIS to identify high risks areas, utility companies for maintenance scheduling and upgrading, communication companies for selecting suitable antennae sites, transport and emergency services for optimised route planning, banks and supermarket chains for selecting suitable regions for new branches and stores. This list could be expanded into many other areas of planning, investment and development.

The new areas of vehicle navigation and driver assistance warning systems also require spatial data. These systems are progressing from informing drivers not only where they are, but what potential hazards to expect, sharp curves, inclines and obstructed visibility. The mobile phone network and the Internet are another two areas that will probably see a sharp increase in the demand for spatial information in the future.

The foundation layer for most GIS systems is a map. Up to recently technologies were not widely available that could determine an absolute position anywhere on the earth's surface with a high degree of accuracy. With Global Positioning Systems (GPS) this is now possible. Many of the applications mentioned above utilise GPS as a positional data collection technique in the creation of layers in a GIS. As an example a utility company might use GPS to locate the position of lampposts. Displaying this

layer on a foundation map that was not of comparable positional accuracy to the GPS collected data, can result in shifts and misalignments.

A consequence of the positional differences between user collected GPS data and base mapping is an increased demand for improved accuracy data from national mapping agencies. The positional inaccuracy of some base maps arises from map revision based on revision, often referred to as legacy mapping. In the past preserving the relative accuracy of features took precedence. But today absolute position using GPS can be achieved with a high degree of accuracy.

As a response to supplying the increased demand for accurate spatial data many national mapping agencies have embarked on campaigns to completely re-map their countries. If one considers that in many cases, large archives of vector databases exist, which must be viewed as an asset, it would prove useful to assess the quality of these.

In discussions with the Irish National Mapping Agency, Ordnance Survey Ireland (OSi) prior to starting this research, highlighted a particular problem that it was about to confront. This was the requirement to provide a nation-wide Digital Terrain Model (DTM) with a grid spacing of one meter. Having looked at the options available OSi decided that using an Airborne Laser Scanner (ALS) would be the most time-effective means of acquiring and maintaining this data. Owing to the high cost of the laser system, OSi would seek to maximise their investment by exploring other contributions ALS could make to its operations.

In common with the other national mapping agencies OSi is also addressing the problem of positional accuracy improvement of its existing mapping and viewed with interest the possibility of using the laser scanner data as a general quality indicator of its existing vector map database. It was therefore decided that this research would explore the possibility of extracting an improved road centre line vector from an Airborne Laser Scanning point cloud, using a vector stored in the existing database as a starting candidate.

The basic concept was to take the centre line coordinates of a section of an existing road vector, use these to find an improved road position in the laser scanner data, and determine any misalignment present. Chapter 3 details the methodology used and includes detailed analysis of the processing stages that resulted in a solution for two research test areas. Chapter 4 provides an analysis of the outcomes of the study and Chapter 5 covers the Conclusions and Recommendations.

The remainder of this Chapter1 describes the Airborne Laser Scanner system, potential sources of errors in the data, expected planimetric and height accuracy and a review of literature detailing various approaches adopted by researchers to process the laser scanner data, concentrating mainly on the area of feature extraction.

Chapter 2 introduces the research area for this study and details the two primary data sets used, the ALS data and the pre-processing required to arrive at a set of ground points, and the ground truth data.

## 1.1 Airborne Laser Scanning

Airborne Laser Scanning (ALS) also referred to as LIDAR (Light Detection and Ranging), is a remote sensing technology usually from a fixed-wing aircraft or helicopter. It is an active system using its own electromagnetic radiation in the form of a laser and does not rely on incident light. This implies that ALS missions can be flown at night increasing its versatility.

The choice of aircraft is dependant on the density of data required and the type of area covered. Point densities are related to flying height. Therefore a much higher point density, typically 14 points per square metre, can be achieved in helicopter surveys. Due to their higher operational altitude, fixed-wing aircraft provide point densities of 1 to 3 points per square metre. The above point densities relate to the Flimap system and are not general ALS point spacings for high and low altidudes, other systems may differ. (http://www.flimap.com-uploads-LiDARMisconceptions.pdf.url).

Helicopters are normally used for corridor surveys e.g. roads, railways, power lines, where point density is a higher priority than area coverage. For surveys of a larger area with lower point density requirements the most economical option is to use a fixed-wing aircraft.

The principle of ALS is that a sensor, in this case a laser, determines the distance to the ground or to some object. If the beam direction angle to the object is known, along with the 3D positional coordinates of the sensor, the coordinates of the object can be calculated (Katzenbeisser, 2003b).

Three systems are involved to achieve this outcome, GPS, an Inertial Measurement Unit (IMU) and the Laser Scanner in conjunction with computer control and software.

GPS is comprised of three entities, often referred to as, the space segment, control segment and user segment. The space segment consists of 24 satellites orbiting the earth at a height of 20200km in six near-circular orbital planes inclined at 55 degrees to the equator. The control segment consists of five earth bound monitoring stations, a master station at Colorado Spring's USA, and four other stations located at, Ascension Island, Diego Garcia, Kwajalein and Hawaii. Each station tracks the satellites and relays their positions to the master station that determines the precise location of the satellite constellation. The user segment consists of an antenna and a receiver. By using the range from a receiver antenna mounted on the aircraft to the satellite constellation, and triangulation techniques, the antenna position is calculated. GPS is normally operated in a differential mode whereby additional receivers are positioned over ground stations of known coordinates. This produces a more accurate result as a number of errors in the satellite signal are minimised by combining the ground receiver results with those from the aircraft.

The IMU consists of gyroscopes and accelerometers that detect changes in the angular rate and velocities of the sensor caused by the aircraft motion. When initialised with a known GPS position the software solves Newton's laws of motion from inputs provided by the IMU, which it integrates to calculate the incremental change in position.

7

The IMU has good dynamic accuracy and GPS has good absolute accuracy they are complimentary. By combining both data sets in a Kalman filter a blended position is achieved (Mostafa et al, 2001).

The laser scanner is comprised of two main components, the laser ranger, and a scanning mechanism to deflect the beam across the surface. There are three principal types of deflection devices in use, the oscillating mirror, rotating polygon mirror and fibre scanner. As the laser signal cannot be used directly to measure the range to the surface it must first be modulated. Two modulation techniques are used in laser scanning, pulsed ranging and continuous wave (CW), with pulsed ranging being the most widely used. The outputs from the scanner are the range vector to the surface and direction angle. Combining of the data from the GPS, IMU and the laser scanner geo-references the point cloud in three dimensions.

The operation of the ALS system is illustrated in figure 1.1. The system collects data in a strip fashion as the aircraft flies over the terrain. Area coverage, distribution and density of points, are determined by flying height, the type of scanner used and the scan rate.
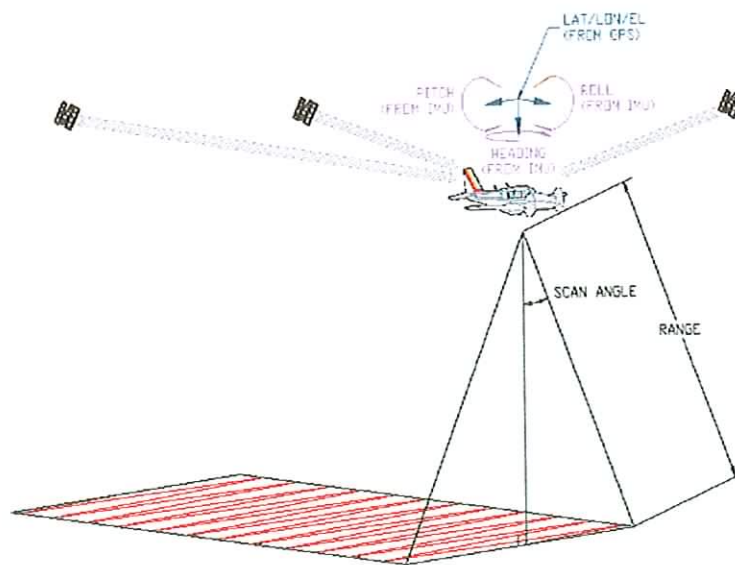


Figure: 1.1 ALS System in Operation        (Leica Geosystems)

8

A scanner using the swivelling mirror principle will collect points distributed in a sinusoidal pattern, with a greater density of points appearing at the edges (the maximum and minimum part of the sine pattern figure 1.2) compared to the areas leading to these. Points from these edge areas are unusable due to angle errors (Katzenbeisser, 2003b).
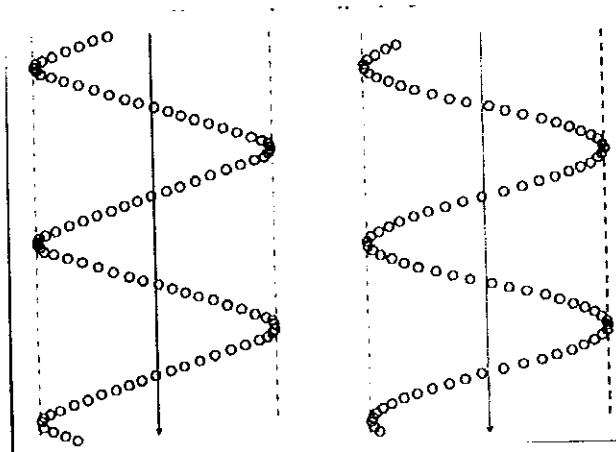
Figure 1.2 Swivelling Mirror Scan Pattern    (TopoSys GmbH)

The rotating polygon mirror deflects the laser beam linearly from one side of the strip to the other producing a polygon point distribution shape (figure 1.3). Using this system no measured values can be collected at the corners of the polygon.
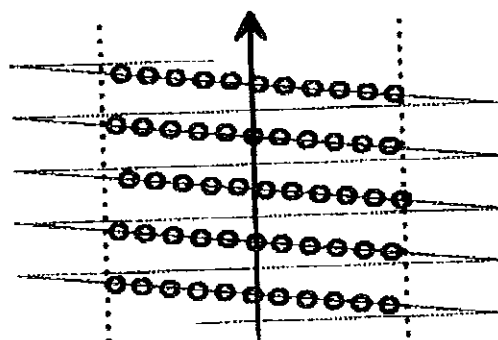
Figure 1.3 Rotating Polygon Mirror Scan Pattern  (TopoSys GmbH)

9

Fibre optic scanners would appear to offer the best performance. Identical fibre arrays are mounted in the focal plane of the receiving and transmitting lenses. By using two rotating mirrors transmitting and receiving paths are scanned sequentially and synchronously giving an exact match. The pattern of points collected is zig-zag (figure 1.4) and all points are useable (Wehr and Lohr, 1999).
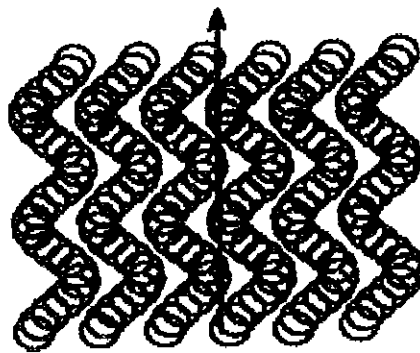


Figure 1.4 Fibre Scanner Scan Pattern (TopoSys GmbH)

Two important additional characteristics of modern ALS systems are multiple returns and return intensity information. Owing to the fact that the laser energy is not totally absorbed by an object in its path, there is a back scattering of some of the laser radiation to the receiver resulting in multiple returns from the same object. Figure 1.5 shows an example of multiple returns where a first return is recorded from the upper branches of a tree followed by successive returns as the signal pulse progresses towards the ground.
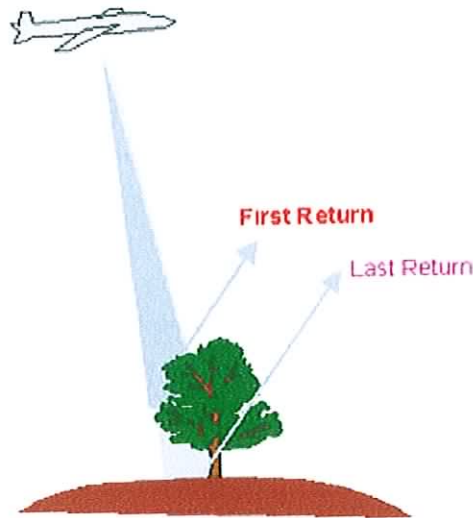
Figure: 1.5 ALS Multiple Return Signals         (http://www.gisdevelopment.net)

Multiple returns can provide useful information. Normally they are indicative of penetrable objects (typically natural vegetation) and could be used to identify and segment such areas for further analysis or removal from the point cloud. Another use could be to determine the heights of individual trees, or a tree stand. First return pulses are used to determine a Digital Surface Model (DSM), a profile of features projecting above the ground, while last return pulses determine the actual ground, a Digital Terrain Model (DTM). In a forested area the difference in height between these two models can be used to calculate tree heights or groups of trees. The fact that tree foliage can be penetrated and a return signal detected from the ground below is important for creating DTM's of wooded areas. Traditional methods, such as photogrammetry, may require the interpolation of ground heights over large areas depending on the density of the ground cover. As the distance between determinable ground points increases, the accuracy of the DTM decreases. A high penetration of the ALS data in such an area could be very useful but will depend on the nature of the vegetation.

11

Intensity is also an important property that can be used to identify features and objects present in the ALS data, but to date has not been used extensively (Toth, 2000). Intensity analysis works on the principle of comparing the energy value of the emitted signal with the return signal. The amount of energy absorbed by a surface or object depends on its material make-up.

Materials that are more reflective will show a higher intensity return value than those that are not. For example a dark asphalt road surface will absorb more energy than surrounding grass, vegetation or concrete. Therefore it could be used to classify man-made objects from natural objects. There are however no absolute values for a particular material. It is the relativity of intensity values within a point cloud that one must work with and this may require some training data from the scene to determine value ranges for natural materials compared to man-made.

In this research ALS data was available from OSi which was gathered using a Leica ALS 50 rotating mirror scanner. The data was processed using Applanix POS software to integrate the GPS and IMU information. The output from the Applanix software was then processed by the ALS 50 Post Processor. This integrates the scanner timing, range and scan angles with the GPS/IMU data to produce a coordinated 3D point cloud. The data was collected at a flying height of 1200m resulting in an average point density of 2 points per square metre. Multiple return and intensity data were also provided.

## 1.2 Sources of Error

In accessing the accuracy of Airborne Laser Scanner data it is important that the user has an awareness of the potential sources of systematic errors and the procedures adopted by the data provider to identify them and minimise their effects on the delivered data.

The accuracy of the ALS system is influenced by the error contributions from each of its subsystems, the laser scanner, GPS system, IMU and the time synchronization of these data collection tools.

The GPS system is responsible for determining the position of the sensor. By adopting best practice in using this equipment positional accuracy can be greatly improved. This would include:

- Mission planning to insure optimum satellite coverage and therefore good geometry for position fixing (low PDOP).

- Positioning of ground antennae such that they will not be influenced by multipath errors.

- Ensuring that the operational distance between ground stations and the rover in the aircraft does not exceed 25 kilometres.

Katzenbeisser (2003a) states that using a dual frequency GPS receiver in differential mode the expected position accuracy should be within .05 metres in all directions providing the following conditions are met:

- Satellite coverage evenly distributed to give a PDOP of less than 2.5.

- No disruption of the satellite signals

13

- Ground stations positioned no more than 25 kilometres from the rover

As the distance from the laser scanner to the ground cannot be measured directly it becomes a time measuring problem. The time taken between the broadcast of a pulse and its reception is recorded and combined with the speed of light to determine the distance. The speed of light changes with the density of the atmosphere, which in turn varies depending on pressure, humidity and temperature. An atmospheric model based on the expected conditions at a particular flying height is applied to correct the speed of light. Weather conditions at the time of flight must be known as the model will assume that the flight took place in clear conditions and would not compensate for errors arising due to rain, mist, fog, cloud or snow which would have a very negative affect on the accuracy of the data due to scattering and absorption of the laser signal (Lemmens and Mathias, 1997).

A further source of error in the distance measurement occurs due to the nature of the topography and the laser-scanning angle. The laser scanner is an opto-electric device that deflects the laser beam across the flight path. This scanning action creates varying angles between the ground and the scanner. Errors occur as the scanning motion extents out from the nadir position to the left and right edges of the swath (Morin, 2002). The distributions of these errors are parabolic in shape and are often referred to as the "smiley" effect. These errors affect both height and planimetric coordinates and are evident even over very level terrain (Alharthy et al, 2004; Lohani and Mason, 2001). A mathematical model can be used to straighten the parabolic effect but whether it could be used over an entire area would be very dependant on the type of

topography present. Over a very level surface the model should minimise the effects of these errors.

It must also be realised that the laser beam itself is not perfectly collimated but widens as the distance to the object increases (beam divergence) (Katzenbeisser, 2003a). This can result, depending on terrain slope and scan angle, as a splash on the surface whereby part of the laser footprint hits the ground earlier than others, resulting in an erroneous height for that particular point (Lemmens and Mathias, 1997).

The IMU determines the orientation of the sensor. It is essential to transfer the angles of the beam deflection into the direction of the IMU in order to precisely align both scanner and IMU. This boresight alignment must stay stable throughout the flight. Katzenbeisser (2003a) demonstrates by an example how critical this alignment is.

A hypothetical alignment error, due to temperature or baseplate deformation, results in a misalignment between the two devices of 1mm. Translating this error at 1000m flying height into the point determination on the surface results in a displacement error of approximately 3m. As the GPS recorded position is at the antenna there will normally be an offset distance from there to the laser sensor. This must also remain stable during the flight.

With adequate calibration procedures potential errors due to boresight alignment and antenna offset should be minimised. There should be data available to show the results of calibration flights taken before and after data collection. This should give an indication of how stable the calibration remained during the data collection phase.

Timing of measurements is of critical importance in post-processing the ALS data set and relies on strict time synchronization between components of the system. The time difference and time coincidence of events must be measured precisely.

Measurements of position, orientation, distance and beam deflection are taken by different parts of the system and not taken at the same instance (Katzenbeisser, 2003a) but ultimately must be combined to give a solution. Time synchronization is normally stable but delays can occur during sharp manoeuvres at the end of a strip or due to heavy buffeting in windy conditions. Knowledge of the flying conditions on the day and the nature of area flown will indicate these are a potential source of error.

As the GPS data is normally captured in the WGS84 coordinate reference system, transformation errors from this system to a local coordinate system may be caused by errors in reference points or by human error (Maas, 2002). If orthometric heights are required the selection and use of the correct geoid model to transform from ellipsoidal heights could also be a source of error.

Maas (2002) states that the accuracy of airborne laser scanner data, as usually quoted by system providers, is between 10-20cm in height and between 20-70cm in planimetry at flying heights of 500m to 700m.

Errors in planimetry and height are not constant throughout the area and are influenced by terrain slope, terrain type, flying height and scan angle. Therefore the manufacturers quoted accuracy figures may relate to the most level areas in the scene or be the result of averaging across the swath width (Baltasivias, 1999).

Theoretically airborne laser scanning can provide 3D data automatically in ideal conditions. This, however, is not always the case and un-modelled errors will lead to shifts and tilts in the overlapping strips. These errors become more apparent as the density of the points increase. A strip adjustment similar to that used in photogrammetry can be applied to the overlapping areas. Without ground control this procedure can pose problems, as it may be difficult to identify tie points in adjacent regions due to the scan pattern of the system (Baltsavias, 1999).

Strip adjustment is an option available to improve the accuracy of the laser scanner data. This makes use of the redundant data in the overlapping strip area, together with ground control, as input into a mathematical model of the sensor errors which are solved in a Least Squares adjustment (Behan et al, 2000). However as the supplier will probably have done some adjustment already, the data user must know the whole processing chain if the benefits from additional adjustments are to be evaluated (Maas, 2002).

As the effort involved in acquiring suitable ground control may prove prohibitive procedures have been developed to successfully adjust strips while keeping control points to a minimum (Vosselmann and Maas, 2001). With a minimum of four control points in the corners of a large region a Least Squares matching of data points in a triangulated irregular network (TIN) structure has achieved good results. The triangulated irregular network is used to detect common planar patches in the laser scanner data. As patches with gradients are also required the authors suggest the use

of building detection algorithms, or the use of a GIS to identify common buildings in both strips. These are then used as inputs into the least squares mathematical model.

Practical tests conducted at the Purdue University (Alharthy et al, 2004) on accuracy of laser scanning data confirm the non-homogenous nature of the accuracy across the swath width. Accuracy decreases with increasing scan angles, as stated by Baltasavias. Over a test area of approximately 3.5 square kilometres using 1m spaced laser data with ground control in both flat and undulating locations their results show a high variability between the middle of the swath width compared to the left and right outer edges. The average planimetric offset observed ranged from 30cm (middle of strip) to 60cm (edge of strip) and height differences of 3cm (middle of strip) to 23 cm (edge of strip). Tests on a much larger scale in the Netherlands show height errors in the region of 15cm and planimetric error of 65cm (Maas, 2002).

In conclusion the accuracy figures reported in the literature are in accordance with the manufactures specifications. Knowledge of potential systematic error sources is important in order to access what steps have been taken by the data provider to minimise their effects. Based on this appraisal it may be possible to improve the accuracy of the data by further strip adjustment. Generally the height accuracy is better than planimetric accuracy. Planimetric accuracy degrades with increasing flying heights (Maas, 2002). Accuracy is also affected by the nature of the terrain. Large gradient changes may affect the accuracy of all three coordinates and although the height coordinate is generally good over flat areas, it will deteriorate if the region is covered with heavy scrub vegetation or includes wetlands (Lemmens and Mathias, 1997).

To satisfy the demand for data and to ensure the updating of existing systems, priority must be given to developing automatic extraction methods or at least semi-automated methods that can aid manual procedures.

One of the first applications of ALS data was in the production of high-density digital elevation models (DTM's). As the laser point cloud described the whole surface as a digital surface model (DSM), it was necessary to extract only those points that were part of the bare earth, ground points. To create a ground model it was necessary to filter out from the data set all points above ground. Various methodologies were developed to achieve this.

Some preliminary filtering was done by analysing the height differences between first and second pulse returns. Points showing a large difference above a set threshold could be considered above surface and discarded. Grey scale images based on height were produced enabling image processing techniques such as morphological filtering to detect for example building shapes, which could also safely be categorised as not belonging to ground points. Images based on intensity could also be used as an aid to identifying whether points were above or on the surface (Hu et al, 2003 and Clode et al, 2004). Methods were also used to analyse the geometry of points within a triangulated irregular network (TIN) structure (Maas and Vosselman, 1999).

Development of filtering algorithms is a very large ongoing field of research and is only briefly mentioned here in the context of demonstrating the development of possible strategies to deal with the vast amount of points present in an ALS data set.

The early processing algorithms concentrated on stripping all above surface points to arrive at a bare earth surface. Now there is much interest in the data that was discarded. Maas and Vosselman (1999) refer to this as "inverse filtering" as a means of arriving at a region of interest.

The generation of a DTM from the point cloud is one way of dividing the data into two broad categories. If the features of interest belong to the surface then they are part of the DTM data set. Alternatively if the region of interest is above the surface subtracting the DTM points from the total data set (DSM) will yield all the above ground points (often referred to as a normalised DSM) (Haala and Brenner, 1999).

These reduced data sets will require further processing in order to detect the required feature or object. This will involve segmenting the data into sets based on some similarity criteria, identifying and classifying the object or feature class they belong to, and finally perhaps modelling them based on real world parametric models (Axelsson, 1999).

Alharty et al. (2004) adopted a tiered approach to processing the ALS data with the aim of extracting building footprints. A DTM was created which was then subtracted from the DSM, to give all possible building points. Of course these points also represent other features rising above the surface, which must be dealt with. Alharty et al, exploited the first and second return readings to establish criteria for eliminating some of these. If the height difference between first and second return of points with the same X and Y values was not zero, then this signified a penetratable object, such as a tree. These points were further refined by the application of a height and size

thresholding algorithm. The purpose of this was to remove as many small objects as possible (vehicles, people etc) from the scene. A raster image was then produced and using image processing a linear filter (convolution) was used to define the building outlines. The resulting polygons were then re-registered with the original data.

Maas and Vosselmann (1999) also advocate the technique of using the DSM minus DTM as a means of obtaining a set of points describing buildings from the point cloud. They also suggest other possible methods such as intensity data to distinguish man made materials from natural vegetation. If the terrain is relatively smooth the analysis of height histograms could be used to determine building boundaries, or alternatively a 2D GIS can be used to give building footprints.

Using a correctly registered 2D GIS with the ALS data would be very useful as the areas containing building points would be fenced off by the polygon shapes. However if the GIS are not up to date its use could result in buildings being overlooked. Potential building points are triangulated using a Delaunay triangulation. Each triangle is then checked for a planar condition. If the triangle belonged to the same plane they are part of the roof surface. The building outlines are found by a straight line connecting algorithm, and the roof shape, by intersecting planes, to show ridgelines. Finally vertical walls are constructed to intersect the roof planes and the outline to form the house model.

A different approach to building extraction is to use the DSM altimetry data in a raster format and analyse vertical slices taken through it (Zhan et al, 2005). The authors take slices at one-metre vertical intervals and create a binary image from each. They then reason that a building should demonstrate near vertical walls, so there should be very

little deviation between each of the slices. Determining the best building footprint however is very arbitrary. This is due to noise in the data close to ground level and requires the user to decide which of the vertical slices best describes the building. Better results may have been achieved if some of the procedures implemented by Alherty et al. (2004) (i.e. height thresholding, first and second return analysis, surface smoothness) were applied to the DSM first.

Hoffmann et al. (2002) demonstrate a method to extract roof shapes from laser scanner data. Points belonging to buildings are taken from the point cloud. A Delaunay triangulation was then used to structure these points. For each triangle a plane was calculated from which parameters of slope, orientation and height could be determined. Triangles exhibiting similar properties were clustered and then further analysed to determine if the orientation of the clusters suggested a roof type. For example two clusters having similar slope values with a difference in orientation of 180 degrees identifies a gable roof. The method has shown very promising results particularly in relation to reconstructing gable roofs with smaller roofs and smaller roof detail such as dormers presenting problems mainly due to the low-density point cloud.

As Hoffmann et al. (2002) have shown there are limitations to the amount of detail that can be reconstructed from the point cloud due to its under-sampling of the surface. Katzenbeisser (2003b) illustrates this problem by using the analogy of Shannon's Theorem in electrical engineering "if a signal is scanned with equidistant increments, the step width must be less than half the smallest form one wishes to

recognise". Applying this in a geomatic sense if one wants to recognise a 1m wide retaining wall the ALS data sampling distance must not be larger than 0.5m.

The concept of how well a continuous surface can be described by a discrete point representation is addressed by Toth and Grejner-Brezezinska (2000). Again the question to be resolved is what is the optimal sampling distance to recover the required amount of detail. The mathematical answer is Shannon's Theorem, but in a very general sense ALS data is quiet good in reconstructing a rural area with modest undulations. However, as the complexity of the scene increases, as in an urban setting, there is a sharp decrease in its ability to define features. This is directly due to the inadequate sampling frequency. It cannot resolve abrupt changes, or break lines, necessary to define features.

This sparse nature of the ALS data and the fact that it is only a cloud of coordinated points with no object information suggests that additional information should be used to realise its full potential. Axelsson (1999) refers to laser scanner data as blind data as it has no semantic or image information and advocates the fusion of data from other sources.

Data fusion will be important in the development of future automatic processes for 3D reconstruction. Rottensteiner (2002) sees the emergence of "multi-sensor-grammetry" whereby data from ALS, SAR, and high- resolution space borne scanners will be combined.

Haala and Brenner (1999) highlight the complementary nature of ALS data with data from other sensors. For example, there is a difficulty when classifying multispectral data that display similar reflectance values such as trees, grass covered areas or streets and buildings. However what does distinguish them is their height above the surface. They use three digital images in the spectral bands, red, green and near infrared co-registered with a DSM to classify the data.

The development of systems that use a combination of laser scanning and digital aerial photography is increasing. The benefits are that a simultaneous visual ortho-coverage of the ALS data is provided. Toth and Grejner-Brzezinska (2000) view these types of systems along with the fusion of data from other sensors as the best means to bring together complementary and redundant information. Existing surface extraction using stereo image matching is not without its flaws, but it has significant expertise built up over the years, which must be viewed as an asset. ALS data can play a vital role in refining and automating these processes. Baltasavias (1999) agrees that the integration of airborne laser scanning with traditional photogrammetric procedures can "open up new revolutionary approaches to the whole photogrammetric production chain".

As roads are part of the bare earth surface a logical starting point for their extraction from ALS data is the creation of an accurate DTM. From this starting position it is then necessary to have some clues that indicate possible road candidates within the scene. Some of these clues may be provided by the ALS data alone (height and intensity for instance) while other sources could be a GIS, aerial imagery, coordinates

from an orthophoto or vector map and finally road parameters such as width or gradient.

The choice of what additional information is needed is dependant on the extent of the road extraction. If the aim of the extraction process is to derive additional detail on an existing road, or road section, it is likely that an approximate location is known already and the problem is now reduced to finding it, based on coordinates for example, within the ALS data and adjusting its position. However the situation changes if a complete network of roads in the scene is required. Additional information such as a GIS, aerial photo or ALS intensity data will be needed. Many of the processes to extract roads on this macro scale rely on image processing techniques.

Hu et al, (2003) demonstrated a method that integrated ALS data with high-resolution imagery to extract a road network in a city environment. Urban scenes pose the most problems when working with aerial photographs due to occlusions and shadowing making it difficult to use image processing as a means of detecting the linear street network. Their approach was to use attributes of the ALS data to segment the point cloud into road and non-road areas. Use was made of height, intensity and first return information. Buildings were removed based on height differences. Some vegetation and trees were detected by looking at the first and second returns from the sensor, the same point having two returns signifying a penetratable object most likely a tree. Intensity data was used to differentiate road surface materials from natural vegetation. In their case the reflectivity of the road material (asphalt with pebbles) appeared to give an almost unique signature.

To refine the removal of low vegetated areas and some trees the optical imagery is used as an aid to the ALS data segmentation. Having removed all unwanted detail from the point cloud the remaining data are converted to a binary image. Image processing is then applied (using a Hough Transform) to detect the street network. A problem encountered with the results of the Hough Transform is the presence of short line segments. Short lines going through large open areas are judged possible parking lots. A morphological operation is performed on the binary image to detect these possible parking areas.

To assess the probability that a car park is present they reason that the presence of vehicles would be a good indicator. By using known car intensity values taken from the Lidar coupled with a shape analysis from the imagery the likelihood that the area is a car park is determined. The short lines within the bounds of this area are then removed

Clode et al. (2004) developed a method to extract a road network in a mixed area of urban, industrial and rural scene. In their case however, no additional sources of information were introduced, the process relying solely on the ALS data. Their approach was to apply a hierarchical classification technique to the data to arrive at a set of most probable road points from which a binary image was created. The first step in the classification is to sample the last pulse ALS data returns into a regular grid. Then using image-processing (morphological grey scale filter) non-terrain objects are removed resulting in a coarse DTM. On the assumption that roads lie on, or near, the DTM a height threshold is applied to the points. Any points whose difference is outside a given tolerance are removed from the data set. The final

selection of points is made from those that have a last pulse intensity value that lies within an acceptable range for the road material used.

Therefore there was a need to investigate the typical ranges for a given material and if this material changed from region to region additional subsets of points would be required. These subsets of points are then used to generate a binary image from which the road network is extracted by connected component analysis. Ground truth for verification purposes was provided by a manually digitised orthophoto. A comparison of the two road networks identified parking areas, short private roads and bridges as mainly affecting the correctness of their method.

Toth et al. (2004) present their research into the complex area of obtaining traffic flow estimates from ALS data. What is of interest is how they extract the road surface detail. The prerequisites for the method are the availability of coarse road data with the minimum requirement being centreline details. With the centre line known the objective of the extraction process changes from finding a road in the ALS data to realigning the road description based on the new ALS measurement of the surface.

Elevation, intensity and scan line analysis are combined to extract the road outline. In common with other authors segmentation of the ALS data based on a plane condition is performed. Patches formed that meet the plane condition are further analysed based on across road slope and longitudinal slope. Across slopes should describe a near horizontal surface. Slopes along the road may show some fluctuation but the rate of change should be consistent.

Scan lines were analysed using an auto-structure function to find straight-line segments. This segmentation works well providing the geometry of the terrain surrounding the road shows large changes. Flat surfaces adjacent to the road (parking lots, pedestrian walkways) cannot be reliably distinguished from the road. Segmentation using the intensity data has proved useful particularly at distinguishing vegetation along the road.

With the road surface approximated from the above procedures a consistency check was used to delineate the road. This utilised a rolling bar, equal to the road width, which checks for similarity across the road profile. Starting at the centre of the road, the bar was rolled parallel to the road direction and stops when the similarity condition ceases, thus indicating the road boundaries.

Hatger and Brenner (2003) also make use of the planar condition to segment the ALS data. But rather than growing regions on a point by point basis, which they felt was computationally expensive, they apply it to entire scan lines. The scan lines were divided into segments and work on the basis that points fulfilling the line equation belonged to the same plane. The process begins with dividing the scan lines into linear segments that fulfil the line equation, a seed region was found in overlapping linear segments of three successive lines, and neighbouring lines were added provided they were part of the same plane. The results from this process showed large planar surfaces most of them belonging to street surfaces while buildings appear as small fragmented regions. However the planar road surfaces were split and it was not possible to determine the left and right boundaries.

To resolve this, another process is reported, i.e. segmentation along a road segment, with the objective of determining the true road extent. Centre line details for the road segment were provided by a GIS and combined with the DSM. Orthogonal profiles were sampled at .5m intervals along the segment and a random consensus algorithm (RANSAC) applied. This resulted in a series of horizontal lines of varying length left and right of the centre line. A median filter was then used to determine the left and right boundaries. Promising results were achieved without the need to include constraints such as maximum or minimum road width.

In the literature review for this project there was a high degree of image analysis involved in the initial processing of the ALS data. Due to the lack of knowledge in this field and the long learning curve to achieve a level of proficiency an alternative route had to be chosen. Available to the project was the commercial ALS processing software Terrascan ®. This was used to filter and classify the point cloud to ground points. In line with other researchers the points were structured using a Delaunay triangulation.

Similar to Toth et al (2004) a prerequisite of the method developed was the requirement of having approximate centre line coordinates. So rather than trying to find a road in the ALS data it becomes a case of using the ALS data to realign an existing road. Toth et al used image processing to analyse the whole surface whereas this research relied on taking representative cross sections of the surface from the triangulated point cloud. The existing centre line coordinates were used to create a grid that was used as a template to sample the triangulation.

Starting with an existing centre line vector, the grid or search template, was formed by coordinating points at one metre intervals along the centre line and at one metre offsets from these points left and right. Overlaying this search template on the triangulated ALS ground points enabled the analysis of cross sections based on the individual bounding triangles, surface patches grown from the single triangles and interpolated data from the triangles. Cross sections based on slope, height and intensity were investigated. No form of image processing was used; the algorithms developed relying on geometric variation and intensity. However, additional parametric information in the form of a known road width was used.

## 2. Research Area / Data

### 2.1 Primary Research Area

Research was undertaken on short sections of two different roads. Road 1 was the regional road connecting the towns of Bray and Greystones to the South of Dublin city and is designated the R761. Road 2, the Southern Cross, is a link road connecting the R761 to the major National route South of Bray, the N11. This road is designated as the R760 (Figure 2.1)
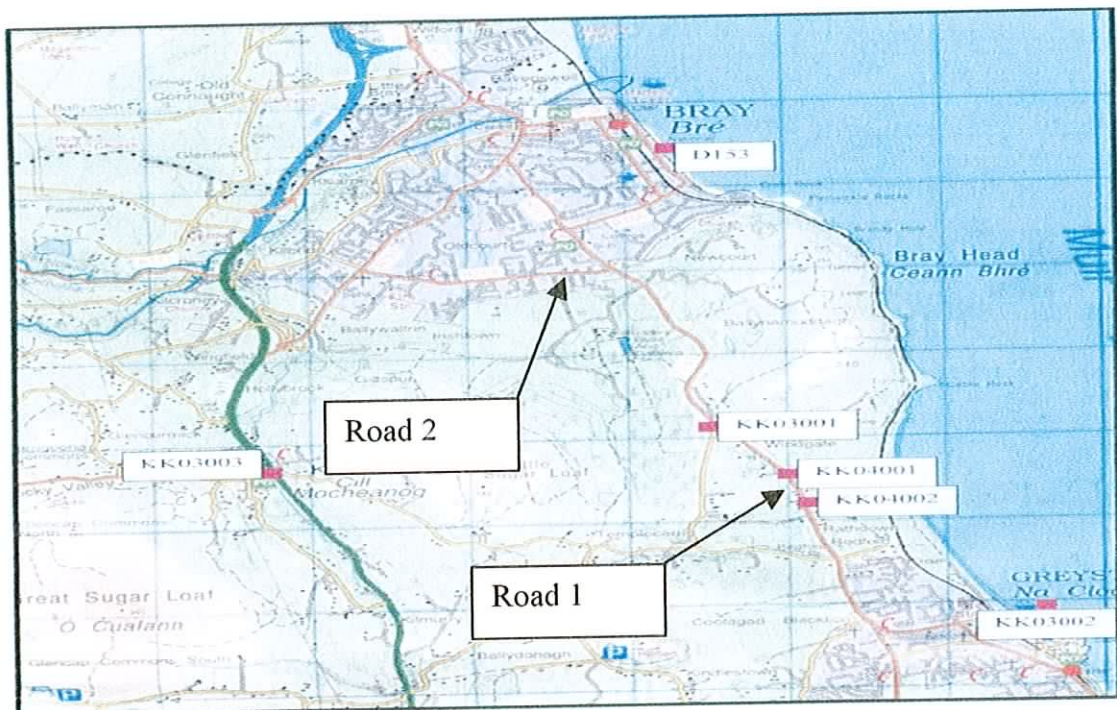


Figure 2.1 Locations of Research Areas. Source (Ordnance Survey Ireland)

Road 1 is constructed from tar macadam and is bounded on either side by a concrete kerb, one side having a small path made from the same road material, the other side a flat verge of rough ground and weeds (Figure 2.2).

There are two sets of road markings, one broken white line and one continuous white line. The area can be described as semi rural, dispersed dwelling with no structures having a road frontage. The road has a North / South direction with an increasing gradient in the Northerly direction. The road width is approximately 10.4m.



Figure: 2.2 R761 Greystones (Road 1)

A generalised schematic of a cross section profile of the road is shown in Figure 2.3.
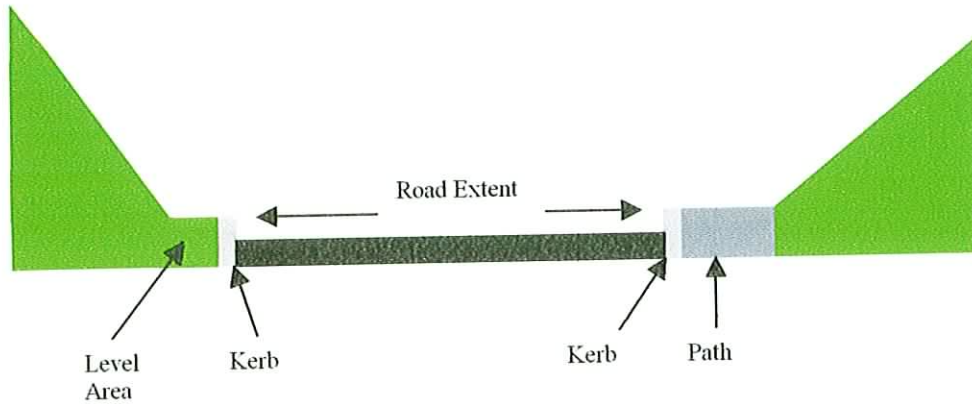
Figure: 2.3. Road Profile Road 1 (R761).

A second test area was needed to conduct repeatability checks on any algorithms developed. The road chosen was the Southern Cross Road that connects Road 1 (R761) with the national route N11. This road lies to the North of Road 1 by a distance of approximately 2 kilometres.

The road material is black asphalt with concrete kerbs on both sides. The distance between these is approximately 11.4m. Immediately adjacent to the kerbs on either side, are grass verges and then concrete footpaths. The road direction is East/West and it has a small gradient rise in the Westerly direction (Figure 2.4)

Figure: 2.4 Southern Cross Road Test Area Two (Road 2)

## 2.2 Airborne Laser Scanning Data

The ALS data for this project was provided by the Irish Mapping Agency, Osi. The Osi contracted Leica in February 2004 to acquire laser scanner data using its ALS50 system. The ALS 50 uses a galvanometer controlled rotating mirror and is capable of recording multiple returns and intensity data. The OSi test area flown was in Co Wicklow covering in total approximately 25 square kilometres extending 5 kilometres southwards from the coastal town of Bray to Greystones and westwards from the coast by 5 kilometres to the N11, the Dublin to Wexford road. This provided a good variety of diverse regions, coastal, urban, rural, industrial, and forestry with a topographic height profile ranging from sea level to high ground. Data was collected from four flying heights, 850 metres, 1100 metres, 1200 metres and 2000 metres giving point densities of 3, 1.5, 2 and 1 points per square metre.

The raw ALS data was calibrated and post processed and calibrated using the Applanix PosPac and Leica Attune software based on the OSi active GPS network

points. There were no DGPS ground stations available in the area at the time the mission was flown. All flight strips were processed in a single adjustment. Any block systematic height error was therefore not removed

The final data sets were delivered as .las files, a standard format for ALS data. Points were coordinated in UTM Zone 29 grid values with ellipsoid heights related to the WGS84 spheroid. Return intensity values were provided for each pulse.

The ALS data set chosen for this research was flown at a height of 1200 metres with an average sampling density of 2 points per square metre. The Road 1 test area was entirely covered by flight strip 120059 flown on 11th February 2004. The Road 2 was entirely covered by strip 121710 flown on the same day.

## 2.3 Ground Truth Data

A ground truth survey was undertaken for Road 1 in order to provide a reference data set against which the extracted road centre line could be compared. The maximum error ($3\sigma$) in the reference data set should not exceed the standard deviation of the ALS points. Expected maximum errors ($3\sigma$) in the ALS data were 15cms in height and 60cms in planimetry (Maas, 2002). Therefore the standard deviation of the ALS data was assumed to be in the order of ± 5cms in height and ± 20 cms in planimetry. These values would require ground truth accuracies of ± 1.7cms in height and ± 7 cms in planimetry.

The ground truth survey consisted of two phases:

1. Creation of a GPS network around the test area, using points D153, KK03003 and KK03002 (Figure 2.5). The survey point D153 is an OSi IRENET passive point of known coordinates. The network was reinforced by including two inter visible points, KK04001 and KK04002, along a section of the Road 1. Post processing of the network would also incorporate baselines to three permanent OSi active GPS stations approximately 20 Kms North of the survey area.

2. A survey of the road section using a total station from point KK04001
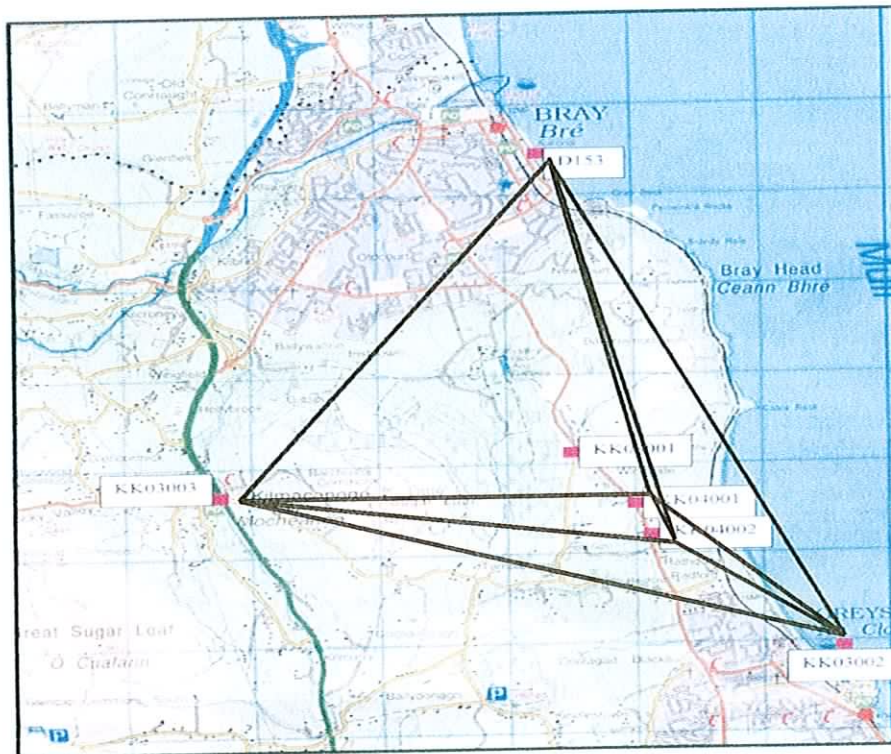


Figure: 2.5 Ground Survey Network. Source (Ordnance Survey Ireland)

The GPS network data was post processed using Trimble Geomatics software. Table 2.1 shows the error report for the adjusted coordinates.

| Point Name | N (Standard error) m | E (Standard error) m | H (Standard error) m |
|---|---|---|---|
| KK04001 | .013 | .013 | .109 |
| KK04002 | .014 | .013 | .109 |
| KK03003 | .013 | .012 | .095 |
| D153 | .010 | .011 | .093 |
| KK03001 | .012 | .012 | .102 |
| KK03002 | .013 | .014 | .115 |

Table 2.1 Error Report Adjusted Coordinates.

A Leica TC500, 7 second total station, and a Psion data logger were used for surveying the road section. As stated above a requirement of the reference data set was that it should be of a higher order of accuracy than the ALS data. Reported errors for the network adjustment showed this to be the case in planimetry but not in height. However, as the ALS data is likely to have a systematic error, and as the research will examine relative height data in a much smaller area compared to the extent of the network, the ground truth was accepted. Approximately 90 detail points were taken over an extent of 40 metres. Features recorded were road edges, kerbs, footpath, road markings and the terrain changes left and right of the road. The ground truth survey data was used solely for verifying the results from the algorithms developed and was not incorporated into any algorithms.

## 2.4 Pre-Processing the ALS Data

The algorithms developed in Matlab to analyse the ALS data rely on having a set of ALS ground points in a TIN structure. It was therefore necessary to do some pre-processing of the data. As the development of filtering algorithms to arrive at a set of ground points was outside the scope of this study, and as the Terrasolid software was available incorporating a set of classification tools, it was decided to use these to extract ground points from the ALS data. The output from this classification step contained over one million points. To reduce this to a more manageable amount the approximate road centre line coordinates were used and an automated routine was developed to replace Terrascan's fence operation, with a bounding box function. In order to evaluate neighbour relationships between adjacent ALS points a TIN structure was created using Delaunay Triangulation.

## 2.5 Terrascan

Terrascan® is part of the main Terrasolid suite of programmes and is widely used to process ALS data. The process of classification is the application of filtering and segmentation operations to identify and separate different classes of objects present in the ALS point cloud. Each object class is colour coded for display purposes. Points can be classified into ground, buildings, low, medium and high vegetation, low points and, if required, user-assigned categories. Each group classified can be taken from the main data set and saved in separate text files for further processing.

The classification procedure commences with the loading of the ALS data into Terrascan. Points are initially classified in a default category and this reduces after

each classification step is carried out. Ground points are the first category to be classified. Prior knowledge of the maximum building size in the area along with an approximate maximum terrain slope angle are required as inputs into the classification routine. Low vegetation classification follows which is based on a height from ground criteria, normally 0 to 1 m. This enables the building classification routine to eliminate these low points as possible structures. Buildings are next and again prior knowledge of maximum and minimum areas of buildings is required. Following this vegetation can be classified as medium and high, each based on a user-inputted height from ground. Two further categories, air and below ground points, are classified. These points may be due to errors in the laser data and are normally few in number. If required Terrascan can also classify railway and power lines.

After the classification it is possible to view statistics on the results. As all points at the start of the process are in the default class and each category is classified from them, the default class is reducing with each classification step and should be close to zero when the final classification step is completed. A large number of points remaining in the default class following the classification process should be investigated. Terrascan has viewing options that allow each individual classification to be switched on or off. For example, if there were many unclassified default points these could be displayed along with ground points. Because each class is assigned its own colour it is possible to see where the default points lie in relation to the ground points to enable a reclassification. Figure 2.6 represents a visualisation of a section of classified ALS data.
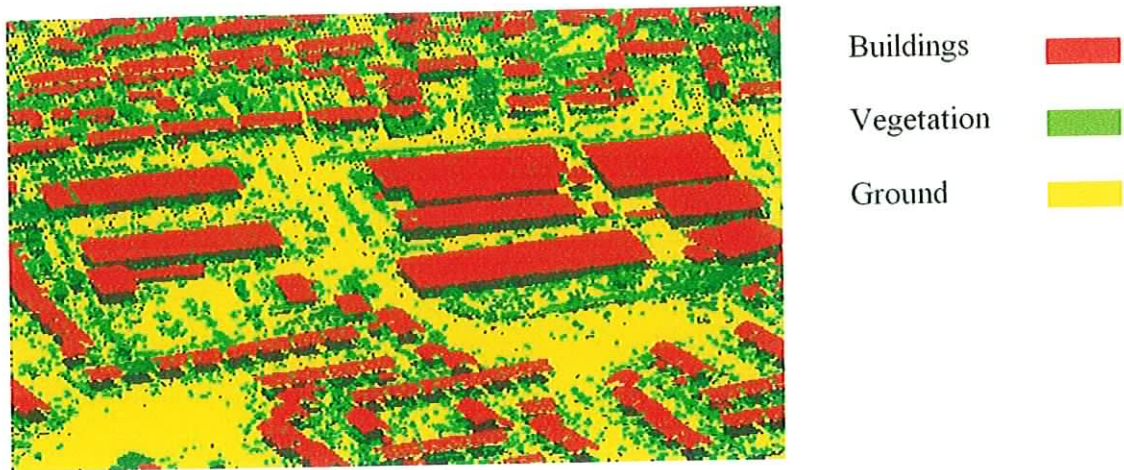
Figure: 2.6 Classified ALS Points using Terrascan

## 2.6 Bounding Box

Once the segment of the existing centre line vector to be evaluated has been selected the ground point data set may be reduced. A bounding box algorithm was developed in Matlab for this purpose.

The bounding box algorithm requires three user inputs:

1. Start coordinates of the road section

2. End coordinates of the road section

3. An offset distance to be applied to these points

The coordinates define the maximum and minimum ranges of the points qualifying as being inside or bounded by these points. The offset distance is important, as it must be large enough to capture enough of the ALS data around the road section, taking into account that there may be significant misalignment between the centre line vector and the actual centre line.

## 2.7 Delaunay Triangulation

With the final reduced data set available it was now necessary to structure the data to enable neighbour and surface analysis. This was achieved using a Delaunay triangulation.
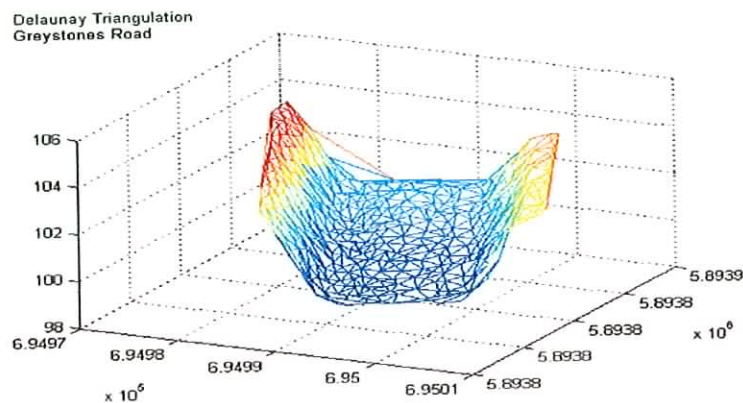


Figure: 2.7 Delaunay Triangulation Road 1

The Matlab Delaunay function was used to create a TIN structure.

The results of the triangulation (Figure: 2.7) should be examined to ensure that it shows some level surface. A highly irregular triangulation surface may be an indication of non-ground points in the data set used for the triangulation. A triangulation showing a regular undulating surface but with no level surface that would constitute a road may indicate incorrect centre line co-ordinates or a situation where the road has been shifted greatly from its assumed position in the vector database. This may be due to major realignment of the ground that has not been revised in the vector database so the parameters of the bounding box are not sufficient to reflect this shift.

# 3. Extraction of Road Centre Line

## 3.1 Introduction to Methodology

The extraction of the actual road centre line from the ALS data was based on the creation and analysis of cross sections from the triangulated ALS ground points taken at regular intervals along the road, using the assumed centre line vector. The proposed strategy was as follows:

```
┌─────────────────────┐
│ Classify the ALS    │ ─┐
│ Data using          │  │
│ Terrascan to get    │  │
│ Ground Points       │  │      ALS Pre-Processing
└──────────┬──────────┘  ├──    (Section 2.4)
           ▼             │
┌─────────────────────┐  │
│ Triangulate Ground  │  │
│ Points using        │ ─┘
│ Delaunay            │
└──────────┬──────────┘
           ▼
┌─────────────────────┐
│ Develop a Search    │
│ Template to take    │
│ Samples from TIN    │
│ At 1m Intervals     │
└──────────┬──────────┘
           ▼
┌─────────────────────┐
│ Develop Algorithms  │
│ In Matlab to Create │
│ and Analyse Cross-  │
│ Sections from the   │
│ TIN                 │
└─────────────────────┘
```
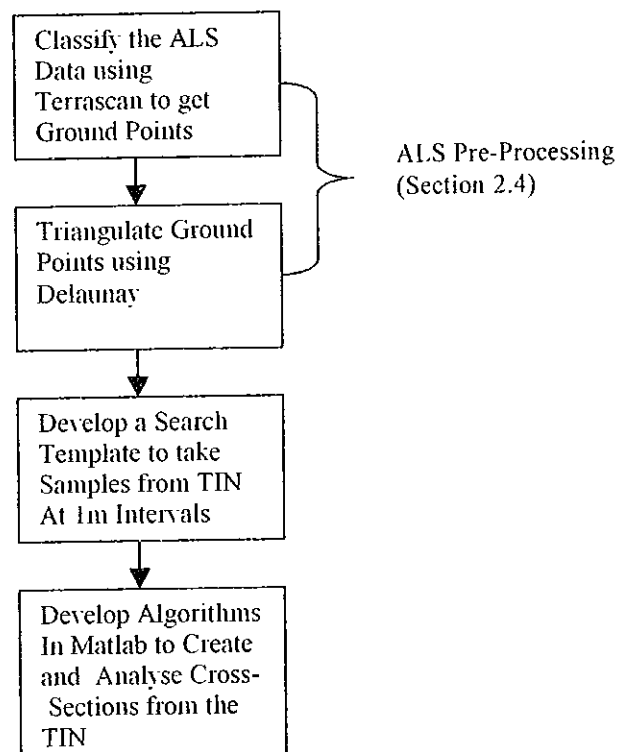
Figure: 3.1 Proposed Strategy to Extract and Analyse Cross-Sections from the Triangulated ALS Ground Points

The first two stages in figure 3.1 are covered in section 2.4, Pre-Processing the ALS data. The Search Template devised to take samples at 1metre intervals from the TIN was based on the coordinates and bearing of the assumed centre line vector. This is detailed in Section 3.3. The algorithms developed in Matlab® to create and analyse the cross-sections are presented in Appendices A, B and C.

43

The cross-sections were based on the properties of single triangles, groups of triangles and on interpolated data. The properties examined were slope, intensity, interpolated heights and interpolated intensity. Section 3.4 gives details of the cross-sections developed. The hypothesis was that the analysis of the cross-sections would enable the true road extent (i.e. detecting the left and right kerbs) to be determined from the ALS data.

## 3.2 Detailed Methodology

Analysis of the ALS data in the form of cross sections remained constant throughout the project. However, differing strategies did evolve on the types of cross sections to be developed and the data on which to base them following the results from initial approaches. It was difficult to set out a methodology that could be used from start to finish but rather decide on an initial strategy; implement it; review the contribution the results made to achieving the final goal; if positive build on it; if negative, choose a new course of action.

In the literature reviewed for this thesis (Chapter 1) there was a consensus among authors that intensity data is under-utilised and, as such, analysis of ALS data would be incomplete without addressing its possible use as an additional information source. Work on intensity cross sections initially ran in parallel with geometric cross section analysis with an emphasis on trying to detect anomalies that might indicate road markings or kerbs. Due to the small size of the test areas and low number of anomalies detected it became clear that the information content from the intensity analysis was not sufficient to be reliably integrated with results from the geometric analysis. As no contribution was made by intensity analysis in the extraction of the road centre line from the ALS data it was decided to group intensity analysis and results achieved as a stand alone section at the end of this chapter.

Road 1 (Figure 2.1) represents the primary research area. As ground truth was available for this road section, the results from algorithms developed could be assessed. By successfully extracting the centre line from Road 1, a tried and tested set of procedures and methodologies could be carried forward and applied to a new set of test data to check their repeatability. The initial workflow is shown in figure 3.2.

```
┌─────────────────────────┐
│ Generate Cross-Sections │
│ from the Road 1         │
│ triangulated            │
│ ALS data                │
└─────────────────────────┘
            │
            ▼
┌─────────────────────────┐
│ Analyse these Cross-    │
│ Sections and develop    │
│ Procedures to Extract   │
│ Road Centre Line        │
└─────────────────────────┘
            │
            ▼
┌─────────────────────────┐
│ Verify Results against  │
│ Ground Truth Data       │
└─────────────────────────┘
            │
            ▼
┌─────────────────────────┐
│ Decide a Methodology    │
│ To Carry Forward        │
└─────────────────────────┘
            │
            ▼
┌─────────────────────────┐
│ Apply this Method to a  │
│ New Test Area to Test   │
│ For Consistency         │
└─────────────────────────┘
```
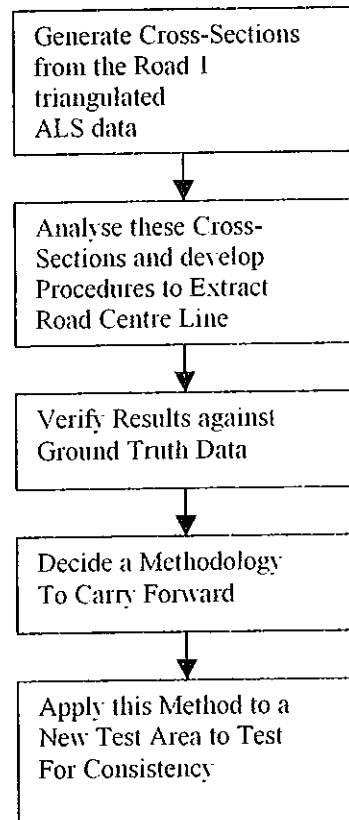
Figure: 3.2 Proposed Workflow for the Centre Line Extraction

The usefulness of the cross-sections was assessed against a central question, "Is there enough information from the analysis of these cross-sections to determine the true road extent?" If it were possible to determine the true road extent the centre line could easily be calculated. The analysis of Road 1 was brought to a successful conclusion and a methodology formulated to carry forward to a new test area, Road 2.

45

Unfortunately the repeatability of the algorithms was not successful and investigations into the cause of the failure began. Reasons for the failure were identified and algorithms changed. In making these changes it was necessary to see what impact they would have on the results for Road 1. It became necessary to go back and forth between the two test areas, implementing any changes made in the new test area to both data sets, until a situation was arrived at where a common set of algorithms worked successfully on both road sections.

## 3.3 Search Template

As stated earlier, for the purpose of generating the cross-sections a search template was constructed using the start and end coordinates of a straight segment of the assumed road centre line vector and its bearing. Intervals of 1 m along the length of the centre line were co-ordinated. From each of these coordinated points offsets of 1 m to the left and right were also coordinated. In general the number of these points will depend on the area to be covered. A sample template is shown in Figure 3.3 to clarify this process. This template will generate eight cross-sections spaced at 1 m intervals. Each cross-section samples a ground width of 19 metres

**Search Template**
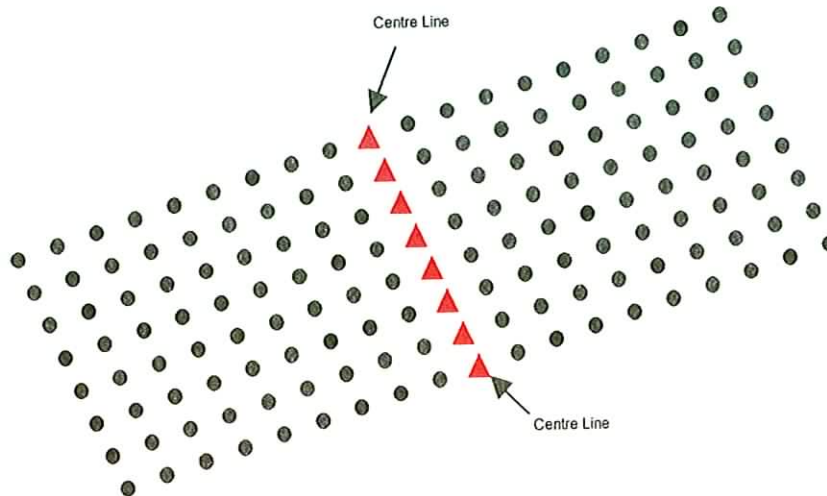


Figure: 3.3 Search Template

## 3.4 Cross-Sections

The use of the search template to locate individual triangles in the TIN structure is the basis for all the cross-sections created. Figure 3.4 shows the search template for the left side of Road 1 superimposed on the triangulated ALS ground points.
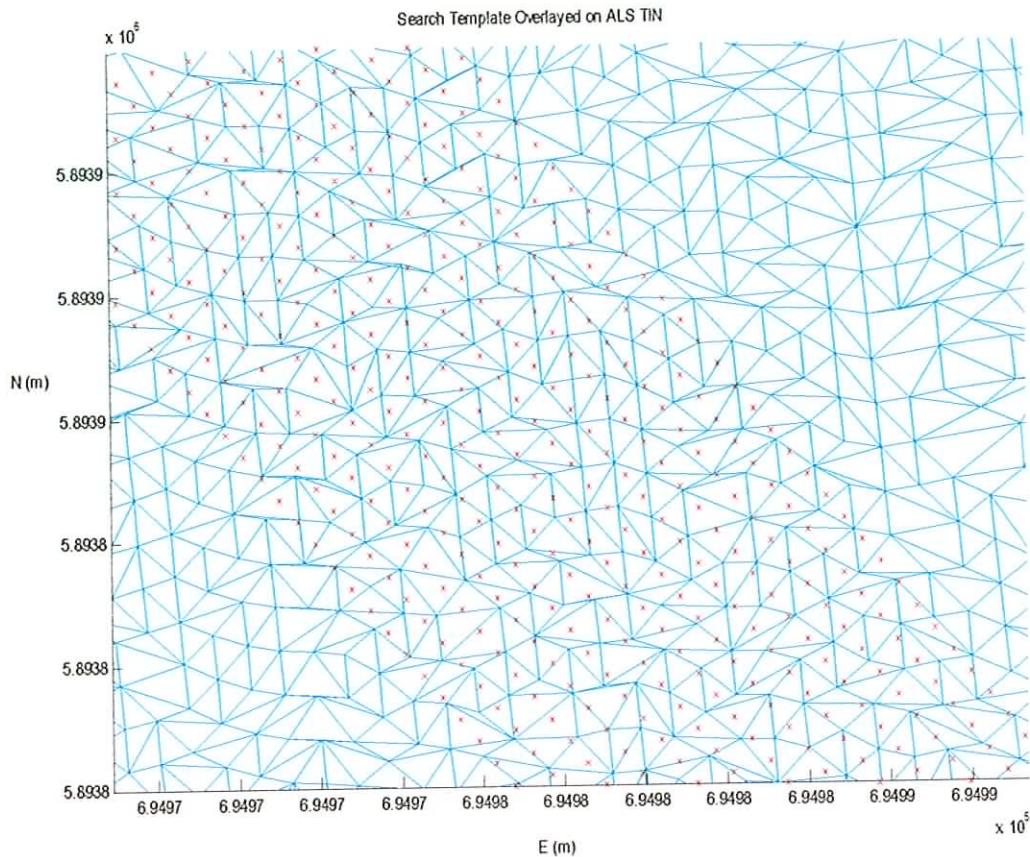
Figure: 3.4 Search Template (Left Side Road 1) Superimposed on TIN

Each "x" symbol represents a coordinated search template point at 1 m intervals. The requirement is, that for each of the search template points, the triangle nearest to it is identified and its details recorded. This process is carried out for each line of points, each line representing a cross-section. For clarity only the left side of the search template is shown, in practice, the corresponding template line on the right side of the road, along with the centre line point, would be included to form a complete cross-section from left to right. The Matlab function "tsearch" identifies the triangle that surrounds the search template point. These triangles are referred to as seed triangles. Figure 3.5 shows the seed triangles identified after using "tsearch" on one search template cross-section (left side only).
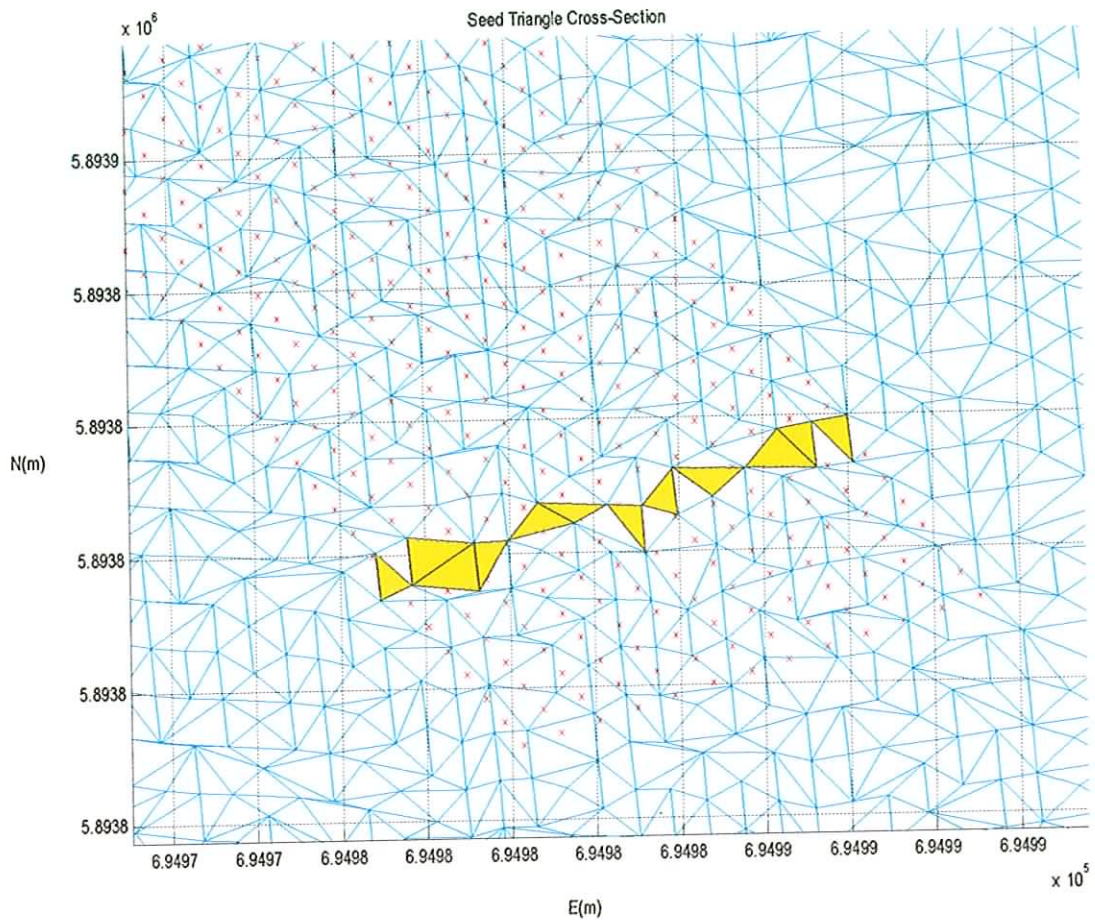
Figure: 3.5 Seed Triangle Cross-Section (Left Side only)

The 3D coordinates for each of the seed triangles vertices, along with their return intensity values, are known. From the seed triangle data a number of analysis possibilities arise.

Firstly the full dip gradient of each triangle can be determined. This is the maximum inclination exhibited by the triangle and indicates the degree of change across the surface of the triangulation. For explanatory purposes, an example of a graphical solution for the full dip gradient of a triangle is shown in figure 3.6. The highest point of the triangle is at point B. The gradient from B to A is 1:6 and from B to C is 1:4.

49
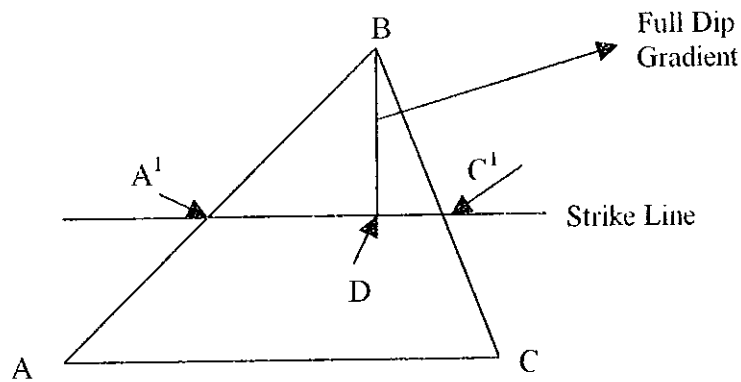
Figure: 3.6 Graphical Solution for the Full Dip Gradient of a Triangle

From point B measure down six units creating point $A^1$ and four units to create point $C^1$, these two unit lengths referring respectively to the gradient of the lines B to A and B to C. This forms a level line, known as a strike line. Drawing a line from B to D at 90 degrees to the strike line, and measuring the unit length of BD, in this case 3.3 units, gives the triangle full dip gradient of 1:3.3.

A second analysis option is to assign a height to each search template point by linear interpolation. The search template points are based on a 2D coordinate system and hence offer limited analysis options. It is however possible, as we know the coordinates of each seed triangle's vertices in 3D, and also know which seed triangle each search template point is associated with, to linearly interpolate a height for each search template point (Figure 3.7)
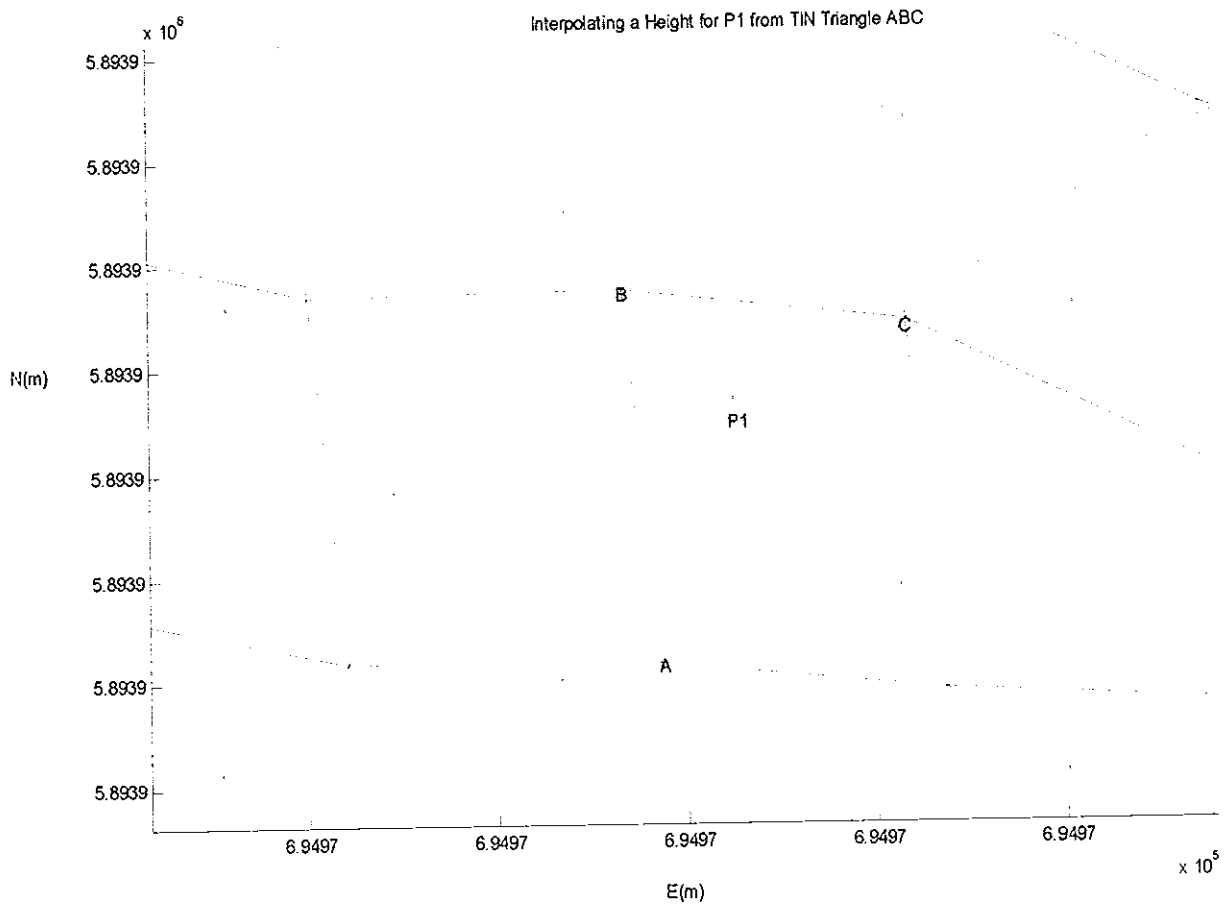
Figure: 3.7 Interpolated Height for Search Template Point

In the case of point P1 (Figure 3.7) the procedure is to extend a line from A through P1 to intersect with the triangle side BC. Determine the coordinates of this intersection point and by linear interpolation between the points B and C, calculate the height of the intersection point. The linear interpolation is then repeated between the intersection point, which now has a known height value, and the triangle vertex at A, to determine the height of the search template point P1.

As the return intensity for the vertices of all triangles in the TIN was known, it was possible to create cross-sections based on the mean of the three values for each seed

triangle and the standard deviation of this mean. The main focus for looking at the mean and standard deviation was to see if anomalies in the intensity values could be detected. For example, if the three vertices of a seed triangle had intensity values of one, one and nine, it could be concluded that the small ground area sampled by the triangle was made up of different materials. It was hoped that this would enable the detection of road markings or concrete kerbs.

An alternative to using the mean and standard deviation of the vertices of the seed triangle intensity values was also tried. This was to determine which vertex of the seed triangle was closest to the search template point, and having found this, assign the intensity value of this vertex to the search template point. Cross-sections created by this process are referred to as Nearest Neighbour Intensity cross-sections. The procedure is illustrated in Figure 3.8. The search template point P1 lies within the seed triangle ABC.
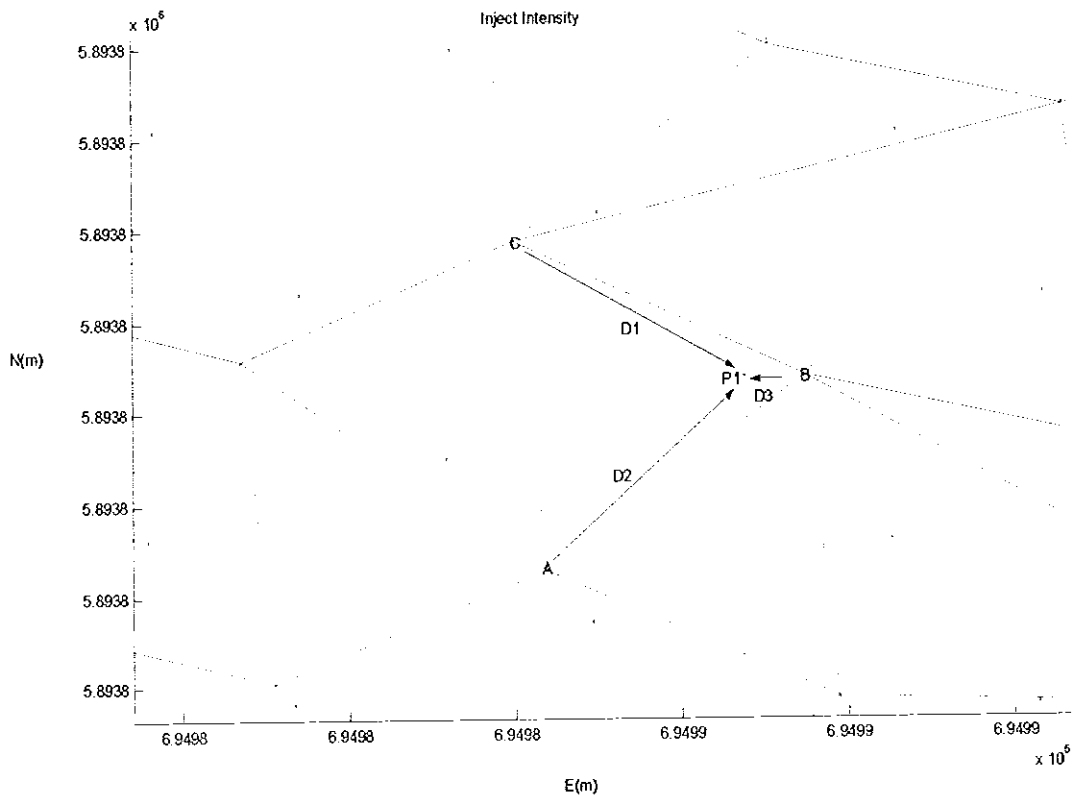
Figure: 3.8 Method of Assigning an Intensity Value to a Cross Section Template Point from the Return Intensity Values of its Bounding Triangle points.

In each case distances D1, D2 and D3 of the point P1 from A, B and C is calculated. The intensity value of P1 is set equal to the nearest vertex point value; in this case, set equal to the intensity value of point B.

Finally cross-sections were developed based on triangle groups. A region growing routine was developed that began with a seed triangle and grew this into a small group of triangles by attaching to it triangles from the TIN that shared any of the seed triangle vertices coordinates. Figure 3.9 shows a cross-section of triangle groups (left side only).

53
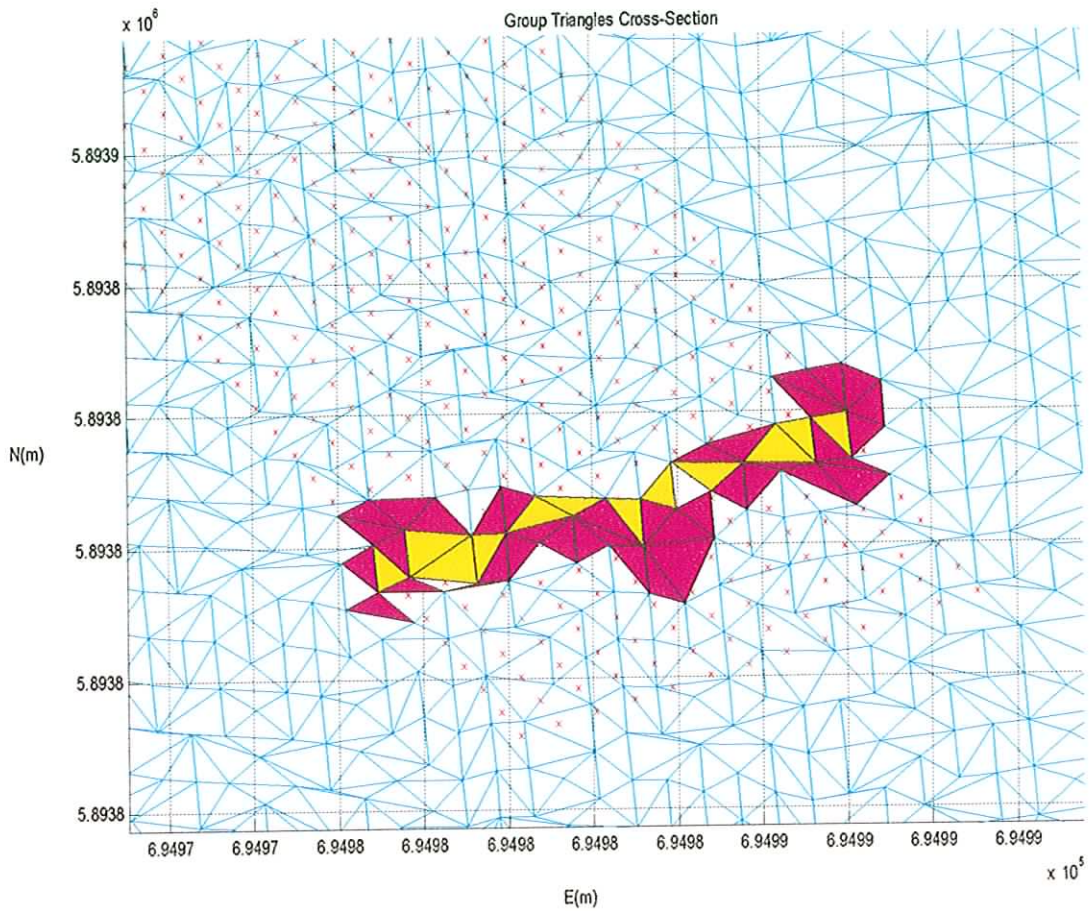
Figure: 3.9 Triangle Groups Cross-Section (Left Side only)

The cross-section types created from these triangle groups, were the mean of the full dip gradient, standard deviation of the mean full dip gradient, mean intensity of the triangle groups and standard deviation of the mean triangle group intensity

In summary there are three broad categories of cross-sections produced:

- Cross-Sections based on Seed Triangles

- Cross-Sections based on Interpolated Data from the Seed Triangles

- Cross- Sections based on Triangle Groups

With the addition of the parameters analysed the three categories can be expanded, resulting in the following cross-section types:

1.  Seed Triangle Gradient (Full Dip) Cross-Sections.

2.  Seed Triangle Mean Intensity Value Cross-Sections.

3.  Seed Triangle Standard Deviation of the Mean Intensity Value Cross-Sections.

4.  Interpolated Height Cross-Sections.

5.  Nearest Neighbour Intensity Value Cross-Sections.

6.  Triangle Groups Mean Gradient (Full Dip) Cross- Sections.

7.  Triangle Groups Standard Deviation of the Mean Gradient (Full Dip) Cross-Sections.

8.  Triangle Groups Mean Intensity Value Cross-Sections.

9.  Triangle Groups Standard Deviation of the Mean Intensity Value Cross-Sections.

The reason for producing so many cross-section types was that initially it was not known which cross-section type would provide the desired result of defining the true road extent. It became an active learning cycle, starting with cross-sections based on individual triangles in the TIN then moving to cross-sections based on small groups of triangles. After some time it became apparent that point data interpolated from the TIN, rather than an analysis of the parameters of individual or groups of TIN triangles, provided the most satisfactory results.

## 3.5 Road 1 Cross Sections based on Seed Triangles And Groups of Triangles with Gradient Parameter Analysed.

The gradient analysis for the seed triangle and triangle group cross-sections for Road 1 are based on 1m offsets extending 13m either side of the centre line, giving a total sample width, including the centre line, of 27 metres. In all, ten cross-sections were analysed with an interval of 1m between them.

Cross Sections Showing the Gradient of Seed Triangles

Figure 3.10 shows an example of a gradient cross-section for Road 1. It can be seen that the triangles showing the smallest gradient changes lie in the region between the 10-metre mark and 21-metre, and 1-metre to 3-metre, with an average gradient of approximately 11%. As the cross-section region 1m to 3m is not large enough for a road surface it is reasonable, by visual inspection, to conclude that the cross-section segment between 10m and 21m is the most likely potential road surface. To the left and right of this region the triangles are demonstrating large gradient changes compared to the small more uniform changes in the cross-section region 10m to 21m.

**Cross Section 9 (Gradient of Seed Triangles: Road 1)**
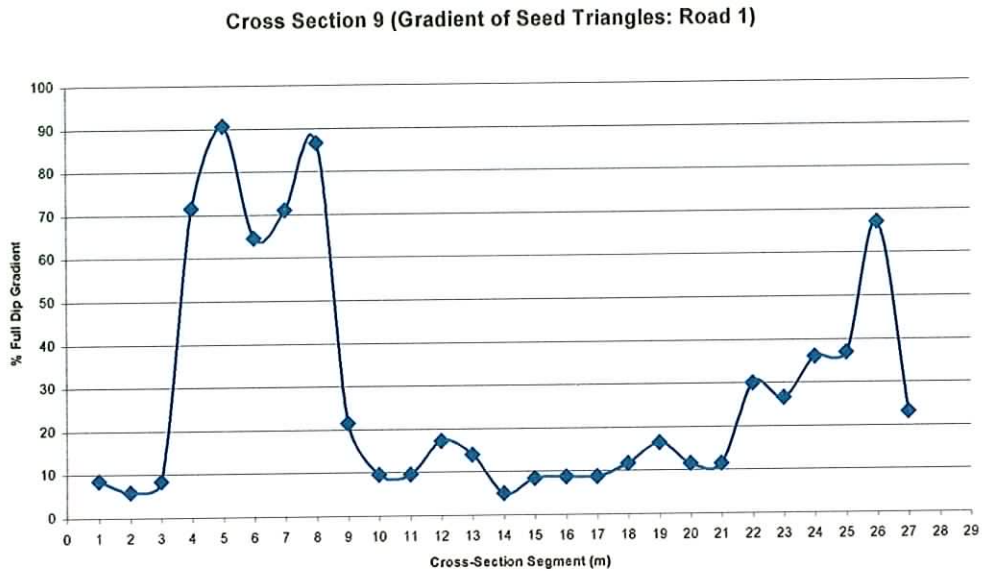


Figure: 3.10 Cross Section No 9 based on the Gradient of the Seed Triangles Road 1

A summary of all ten seed triangle gradient cross-sections is presented in Table 3.1.

| Cross Sections Based on Seed Triangles | | | |
|---|---|---|---|
| | Possible Road Surface | | |
| C/Section | From(m) | To(m) | Average Gradient % |
| 1 | 9 | 21 | 12 |
| 2 | 9 | 21 | 11 |
| 3 | 10 | 21 | 12 |
| 4 | 11 | 21 | 10 |
| 5 | 10 | 21 | 10 |
| 6 | 11 | 21 | 11 |
| 7 | 9 | 21 | 11 |
| 8 | 11 | 20 | 10 |
| 9 | 10 | 21 | 11 |
| 10 | 11 | 21 | 12 |
| Mean | 10 | 21 | 11 |

Table 3.1 Results of Visual Analysis of Ten Gradient Cross Sections for Road 1

When the results of all ten cross sections were overlaid (Figure 3.11) it was observed that the right side shows a much more definite transition at the 21m mark, from triangles having small gradient changes to triangles where the gradient was

57

increasing, whereas the left side was showing more uncertainty particularly between 9 and 10 m.

**Overlay of Cross Sections 1 to 10 (Gradient of Seed Triangles Road 1)**
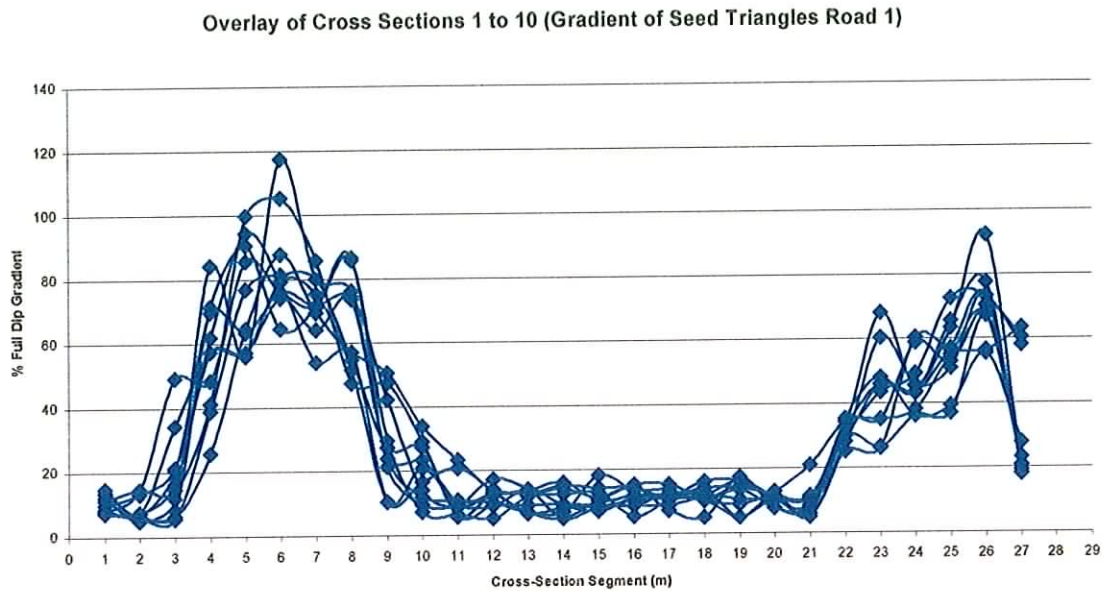


Figure: 3.11 Overlay of Ten Gradient Cross Sections for the Seed Triangles Road 1

Conclusions that could be made based on the visual inspection were that the area beyond 21m could be eliminated as a road surface and likewise the area less than 9m.

Cross Sections Showing the Mean Gradient of Triangle Groups

Inspection of the cross sections in this category showed similar results to that of the seed triangles both demonstrating that the most likely area for a road to exist is the region between 10m and 21m (Figure 3.12).

**Cross Section No 9 (Mean Gradients of Triangle Groups: Road 1)**
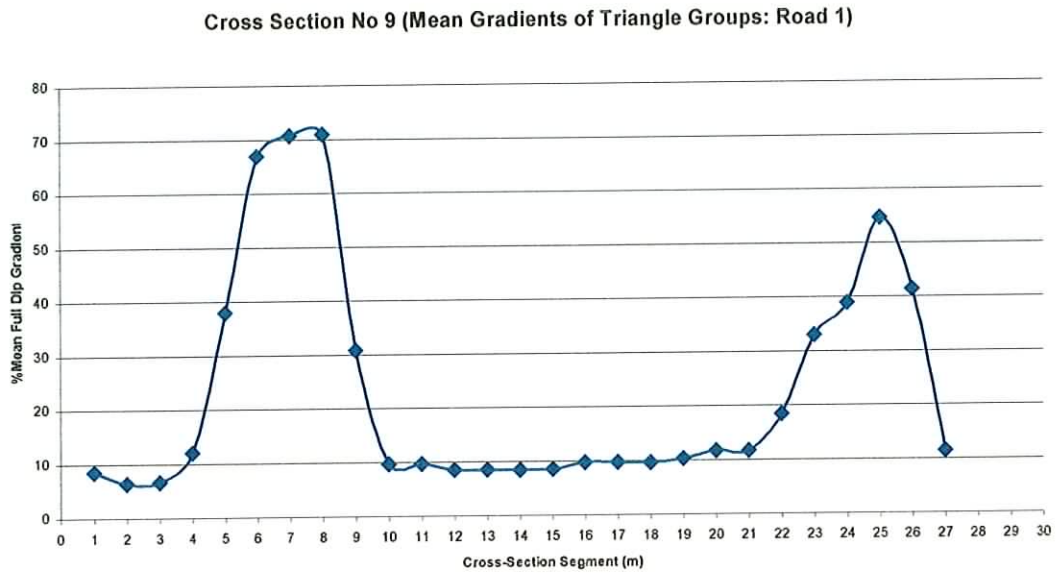


Figure: 3.12 Cross Section No 9 based on the Mean Gradient of Triangle Groups
Road 1

As the triangle groups sample a larger area of the TIN, the triangle group cross-sections show a much smoother representation when compared to those based on the seed triangles. The gradient values show less fluctuations and the region between 10m and 21m is clearly defined (Figure 3.13).

**Gradient Mean Cross Section Overlay 1to10 (Groups) R761**
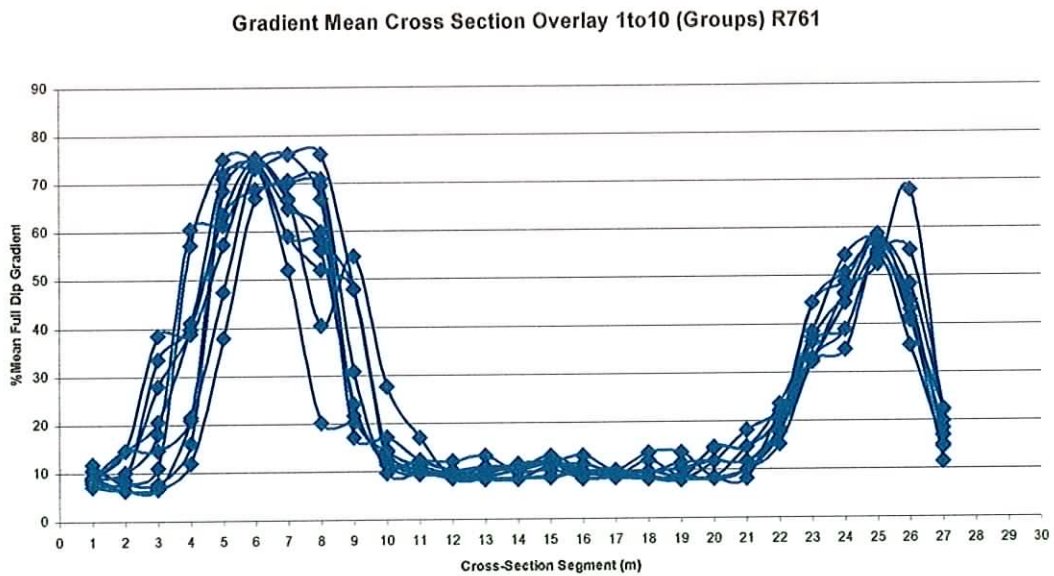


Figure: 3.13 Mean Gradient Cross Sections 1-10 (Overlay) of the Triangle Groups
Road 1

| Cross Sections Based on Triangle Groups | | | |
|---|---|---|---|
| | Possible Road Surface | | |
| C/Section | From(m) | To(m) | Average Gradient % |
| 1 | 10 | 21 | 11 |
| 2 | 10 | 21 | 11 |
| 3 | 10 | 21 | 11 |
| 4 | 10 | 21 | 11 |
| 5 | 10 | 21 | 10 |
| 6 | 10 | 21 | 10 |
| 7 | 10 | 21 | 10 |
| 8 | 9 | 21 | 11 |
| 9 | 10 | 21 | 10 |
| 10 | 12 | 21 | 11 |
| Mean | 10 | 21 | 11 |

Table 3.2 Results of Visual Analysis of Ten Gradient Cross Sections for the Triangle Groups Road 1

The visual inspection of the triangle group mean gradient cross-section provided a more confident interpretation of a potential road surface and represented an improvement in the visual analysis over the seed triangle results (Table 3.2).

Cross Sections Showing the Standard Deviation of the Gradient for the Triangle Groups

Inspection of the cross sections 1 to 10 based on the standard deviation of the gradient of triangle groups (Figure 3.14) reinforced previous results by showing very little variation between the triangles in each surface patch in the region 10m to 21m.

Figure: 3.14 Overlay of Ten Gradient Standard Deviation Cross-Sections for the Triangle Groups Road 1

Analysis of these cross sections indicated a possible road extent from between 9m and 23m. This was the first indication of a possible larger level surface with transition areas between 9m and 10m and 22m to 23m.

From the ground truth survey it was known that the road width plus the level areas on either side span approximately 13.3m. This compares favourably with the possible total extent of the level area from the inspection of these cross sections. There was not enough information provided by these results to isolate level non- road areas from the road itself.

Conclusions

It was concluded from the analysis of cross sections based on triangle slopes that a definitive statement as to where the true road extent existed was not possible with 2 points per square metre ALS data.

A new approach was therefore required to refine and enhance the boundaries of the two level regions (i.e. the footpath on the right and the level area of scrub ground on the right) that existed on either side of the true road surface.

## 3.6 Interpolated Height Cross Sections: Road 1

The preceding sections analysed the triangulated ALS ground points by taking cross-sections based on individual seed triangles, and groups of triangles in the TIN. The Interpolated Height cross-sections are a departure from analysing the TIN triangles to analysing a point within the TIN. These cross-sections are based on Interpolated heights taken from the triangulation and attached to the search template points. Cross-sections from this category (Figure 3.15) reinforce the triangle group standard deviation gradient result by confirming a level surface between the 9m and 22m marks. It can be observed from the graph that the surface between 10m and 21m has very small height variations.

**Overlay Of Cross Sections 1 to 10 (Interpolated Heights: Road 1)**
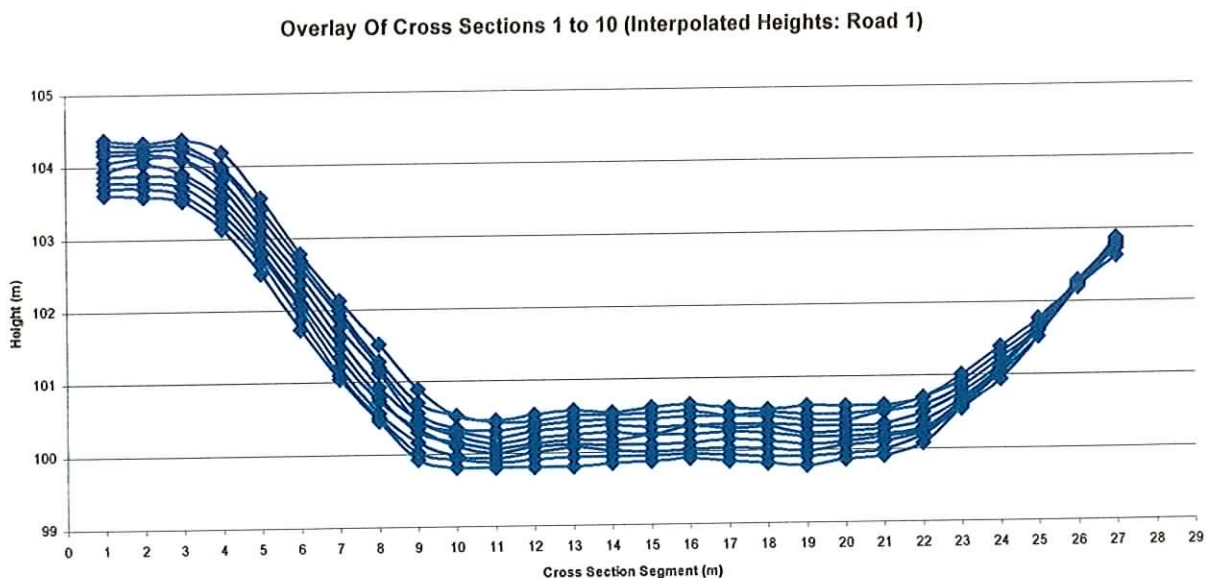


Figure: 3.15 Overlay of Ten Interpolated Height Cross-Sections for Road 1

The surface begins to show more change between 9m and 10m and also between 21m and 22m with more abrupt changes occurring at less than 9m and greater than 22m. As it is already known that there are two non-road level surfaces, at either side of the road, there is still not enough information to enable these to be identified and excluded.

## Height Differences Cross-Sections Road 1

In an effort to try to improve on the interpolated height results and resolve the ambiguity between path and road surface the height difference between each 1m-interval point across each section was examined (Table 3.3). The hypothesis was that the height differences between adjacent 1m points on the level road surface should be very small, and if a kerb and path were present, a larger height difference should occur at either side of the level road region. As a kerb is normally several centimetres above the road surface it was decided to conduct an analysis of the first instances of height differences beyond the level region that displayed a 120mm height difference.

Table 3.3 is divided into three zones, red, green and black. The red zone shows the smallest height change between adjacent offsets at a mean magnitude of approximately 40mm. Green zone shows a transition between the small height differences in the red zone to larger differences in height. As the area covered by the black zone has already been ruled out by visual inspection as qualifying as a road, the transition from red to green is investigated.

63

| | CSection1 | CSection2 | CSection3 | CSection4 | CSection5 | CSection6 | CSection7 | CSection8 | CSection9 | CSection10 |
|---|---|---|---|---|---|---|---|---|---|---|
| 1 | 0.031 | 0.006 | 0.002 | 0.010 | 0.095 | 0.065 | 0.008 | 0.008 | 0.020 | 0.045 |
| 2 | 0.056 | 0.089 | 0.053 | 0.041 | 0.146 | 0.026 | 0.072 | 0.003 | 0.007 | 0.043 |
| 3 | 0.396 | 0.374 | 0.372 | 0.362 | 0.344 | 0.394 | 0.303 | 0.273 | 0.305 | 0.175 |
| 4 | 0.622 | 0.569 | 0.586 | 0.651 | 0.616 | 0.655 | 0.649 | 0.660 | 0.584 | 0.643 |
| 5 | 0.774 | 0.802 | 0.743 | 0.719 | 0.734 | 0.690 | 0.672 | 0.684 | 0.713 | 0.774 |
| 6 | 0.693 | 0.771 | 0.812 | 0.764 | 0.734 | 0.756 | 0.726 | 0.685 | 0.700 | 0.654 |
| 7 | 0.585 | 0.594 | 0.640 | 0.602 | 0.686 | 0.670 | 0.630 | 0.721 | 0.711 | 0.608 |
| 8 | 0.531 | 0.487 | 0.404 | 0.383 | 0.479 | 0.463 | 0.673 | 0.634 | 0.572 | 0.624 |
| 9 | 0.121 | 0.094 | 0.193 | 0.260 | 0.157 | 0.232 | 0.142 | 0.215 | 0.184 | 0.374 |
| 10 | 0.006 | 0.051 | 0.039 | 0.096 | 0.086 | 0.102 | 0.094 | 0.037 | 0.096 | 0.064 |
| 11 | 0.002 | 0.029 | 0.068 | 0.078 | 0.059 | 0.067 | 0.089 | 0.058 | 0.002 | 0.066 |
| 12 | 0.002 | 0.026 | 0.066 | 0.026 | 0.048 | 0.041 | 0.036 | 0.059 | 0.077 | 0.057 |
| 13 | 0.045 | 0.003 | 0.044 | 0.010 | 0.009 | 0.020 | 0.020 | 0.004 | 0.001 | 0.034 |
| 14 | 0.016 | 0.009 | 0.030 | 0.005 | 0.058 | 0.036 | 0.030 | 0.009 | 0.015 | 0.059 |
| 15 | 0.033 | 0.019 | 0.026 | 0.021 | 0.004 | 0.109 | 0.016 | 0.030 | 0.026 | 0.033 |
| 16 | 0.044 | 0.015 | 0.015 | 0.047 | 0.035 | 0.031 | 0.011 | 0.001 | 0.066 | 0.052 |
| 17 | 0.034 | 0.037 | 0.015 | 0.032 | 0.027 | 0.010 | 0.001 | 0.009 | 0.033 | 0.025 |
| 18 | 0.031 | 0.002 | 0.036 | 0.052 | 0.054 | 0.097 | 0.027 | 0.055 | 0.028 | 0.043 |
| 19 | 0.074 | 0.035 | 0.070 | 0.040 | 0.005 | 0.030 | 0.016 | 0.013 | 0.005 | 0.014 |
| 20 | 0.047 | 0.050 | 0.046 | 0.061 | 0.025 | 0.024 | 0.032 | 0.118 | 0.045 | 0.015 |
| 21 | 0.164 | 0.195 | 0.142 | 0.091 | 0.075 | 0.104 | 0.151 | 0.090 | 0.165 | 0.092 |
| 22 | 0.471 | 0.383 | 0.348 | 0.382 | 0.344 | 0.301 | 0.269 | 0.240 | 0.225 | 0.310 |
| 23 | 0.401 | 0.459 | 0.460 | 0.449 | 0.471 | 0.416 | 0.371 | 0.382 | 0.377 | 0.383 |
| 24 | 0.581 | 0.492 | 0.473 | 0.502 | 0.514 | 0.527 | 0.510 | 0.406 | 0.395 | 0.380 |
| 25 | 0.667 | 0.690 | 0.717 | 0.624 | 0.628 | 0.569 | 0.586 | 0.653 | 0.578 | 0.479 |
| 26 | 0.437 | 0.412 | 0.485 | 0.501 | 0.523 | 0.594 | 0.611 | 0.525 | 0.458 | 0.619 |
| Mean(of Red Area) | 0.030 | 0.031 | 0.041 | 0.047 | 0.040 | 0.052 | 0.034 | 0.040 | 0.036 | 0.046 |
| Diff R to G (Top) | 0.116 | 0.393 | 0.154 | 0.164 | 0.071 | 0.130 | 0.048 | 0.178 | 0.088 | 0.310 |
| Diff R to G (Bottom) | 0.306 | 0.188 | 0.206 | 0.290 | 0.270 | 0.197 | 0.118 | 0.149 | 0.060 | 0.217 |
| Diff G to B (Top) | 0.410 | 0.108 | 0.212 | 0.123 | 0.323 | 0.231 | 0.531 | 0.419 | 0.388 | 0.250 |
| Diff G to B (Bottom) | 0.306 | 0.188 | 0.206 | 0.067 | 0.127 | 0.197 | 0.118 | 0.142 | 0.060 | 0.074 |
| StDev Red | 0.022 | 0.026 | 0.020 | 0.030 | 0.027 | 0.036 | 0.030 | 0.037 | 0.032 | 0.023 |

Table 3.3 Height Differences at Adjacent Points in Cross Sections Road 1

The nature of the change would suggest a step from a very level surface to a higher surface, the height of which may suggest a kerb. Referring to the graph of Cross Section 1 (Figure: 3.16) the small difference in height between the 10m and 20m mark can be seen. A change occurs at the 9m and 21m mark in the cross-section, where the height difference begins to increase

**Height Differences Cross Section 1 Road 1**
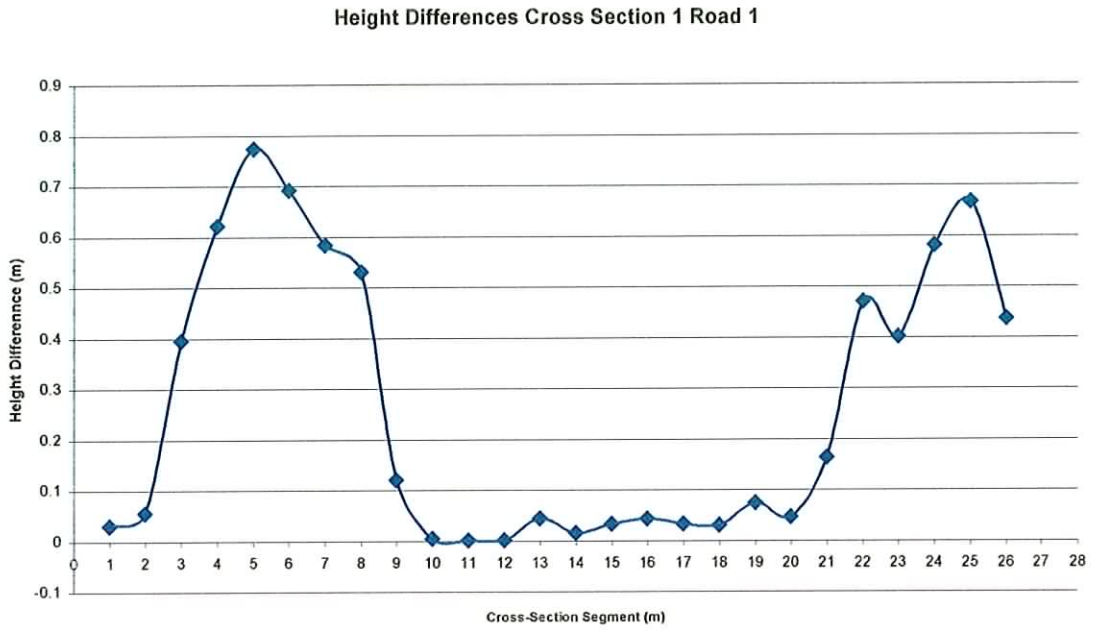


Figure: 3.16 Height Difference Cross-Section 1 Road 1

Analysing the data in Table 3.3 provided the following information:

1. The red zone showed an overall mean height difference of 40mm indicating a relatively level surface.

2. The extent of this level region ranged between road segment width of 11m and 12m.

3. There was a significant change between the red and green zones with an overall mean height difference in this region of approximately 229mm.

It was now necessary to check the location of the green zone height changes against the ground truth survey.

To test the kerb identification hypothesis the following strategy was adopted:

- Locate the green zone points in the TIN data set

- Extract the coordinates of these points and overlay them on the results of the ground truth survey.

As the ground truth survey covered a larger area than tested so far, the test area was extended to cover an additional 20m in order to see if the results achieved showed consistency over a larger distance.

Figure: 3.17 show the test results. The red lines represent the two road kerbs as determined by the ground truth survey and the pink squares represent the coordinates of the candidate kerbs inferred using the green zone points from the cross section analysis.
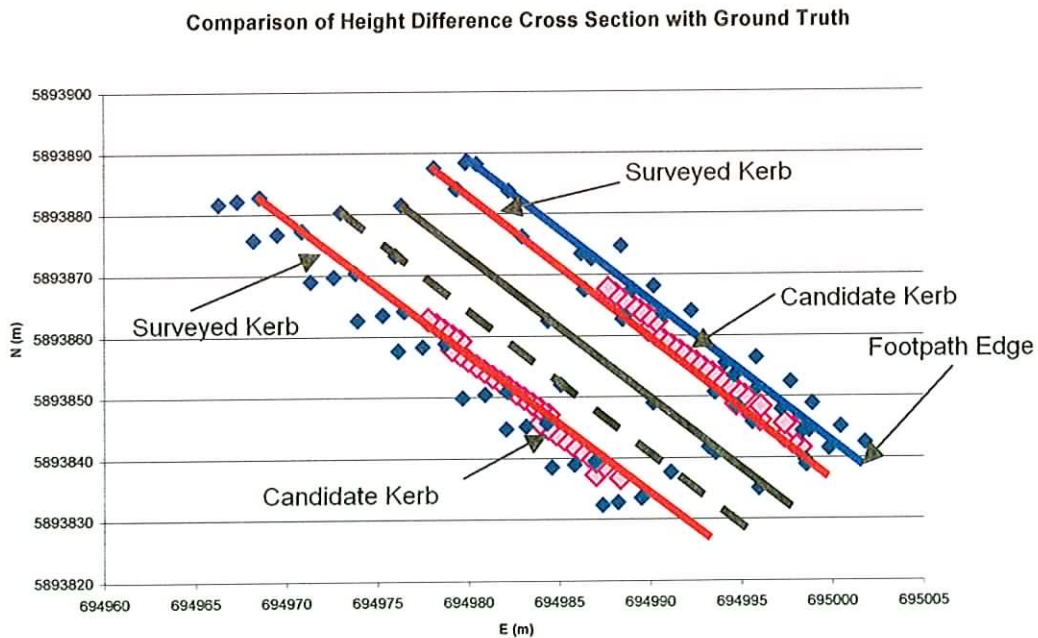


Figure: 3.17 Overlay of Candidate Kerb Lines from Cross Section Analysis on the Ground Truth Survey Data Road 1

66

The kerb in Figure 3.17 (red lines) is based on surveyed points, which have a spacing greater than one meter, joined to form a continuous line. The green zone Lidar generated point coordinates however have a one-meter spacing making a direct mathematical comparison difficult. As a visual representation of the spatial relationship between actual kerb and a candidate for a possible kerb determined by height differences it showed some promise. The magnitude of the planimetric difference between the kerb candidates and the ground truth for the right side is not greater then 1.6m (as the path width is known to be 1.6m and all kerb candidates are on the path). The left kerb candidates show a much greater coincidence with the ground truth, but some fall within the level scrub area beyond the actual kerb, this area is known to be approximately 1m wide.

In order to develop the usefulness of the method an automated process was required to identify the height change from the red to green zones of Table 3.3.

## 3.7 Automating the Process by Using a Least Squares Linear Best- Fit Algorithm –Road 1

One possible way of implementing an automatic Least Squares best fit to the height difference data was to test a range of road widths across each cross-section and choose the segment, in the cross-section, with the best linear fit. The problem with this was that with no constraints on the road width there would be many combinations of widths giving similarly good fit statistics.

For example we know that the road was approximately 10 metres wide, but road widths of 9m, 8m, 7m, 6m could also provide a best fit. There was, therefore, a requirement for some additional information to in some way confine the least squares fit. In the literature reviewed in Chapter 1 some typical sources of additional information used were:

- Intensity of the Lidar Return Signal

- Image data

- Parametric data e.g. road width.

The contribution of the Intensity data was explored in this study and is reported in Sections 3.14 and 3.15. The results from the Intensity analysis did not provide enough useful information to be incorporated into the least squares algorithm. The use of image analysis was outside the scope of this present study. It was therefore decided to introduce the road width as an example of parametric data. Road widths can often be inferred from National Road Classification data and would therefore be easily sourced.

An algorithm was developed using Matlab to fit a linear Least Squares regression line to each height difference cross-section. The road width would define the segment in the cross-section, or range of data, to be used in the least squares regression analysis. The output from this process would enable a comparison between the visual and automated processes. The steps followed were:

- Input the road width, which in this instance was ten metres,

- For each height difference cross-section collect the data for all possible ten-meter segments in the section.

- Applying the Matlab functions "polyfit" and "polyval" calculate a least squares best-fit regression line to the Height Difference data associated with each ten-metre cross-section segment.

- Calculate the root mean squared residuals (RMS) for each ten-meter cross-section segment.

- Select the cross-section segment with the smallest RMS residual.

Table 3.4 shows a comparison of the results of the road extent determination by inspection and by the semi-automatic method for the 10 m section in Table 3.4.

| Road Segments with Smallest RMS Residuals | | | |
|---|---|---|---|
| Road Segments from Semi Automatic Process | | Road Segments from Visual Inspection | |
| From m | To m | From m | To m |
| 10 | 20 | 10 | 20 |
| 10 | 20 | 9 | 20 |
| 10 | 20 | 10 | 20 |
| 11 | 21 | 10 | 21 |
| 10 | 20 | 10 | 21 |
| 10 | 20 | 10 | 20 |
| 10 | 20 | 10 | 20 |
| 10 | 20 | 10 | 21 |
| 10 | 20 | 10 | 20 |
| 10 | 20 | 10 | 21 |

Table 3.4 Comparison of the Road Segments Generated by the Least Squares Regression with those Identified by Visual Analysis Road 1

It can be seen in Table 3.4 that fitting a Least Squares regression line to the height difference cross-sections produced similar results to the visual inspections and that gave confidence in the algorithms created.

## 3.8 Generation of a Candidate Vector for the Road Centre Line

At this stage the true road extent had been defined with reference to segments within each cross-section. It was now necessary to develop a routine that could automatically coordinate these location intervals by finding their position in the search template. This resulted in kerb coordinates for the left and right sides of the road. Using these, the mid point of the road segment was calculated, giving a definition of a candidate centre line point determined from the ALS data.

Candidate vectors were then fitted to the left and right kerb points and the centre line points producing the required road vectors (Figure: 3.18).
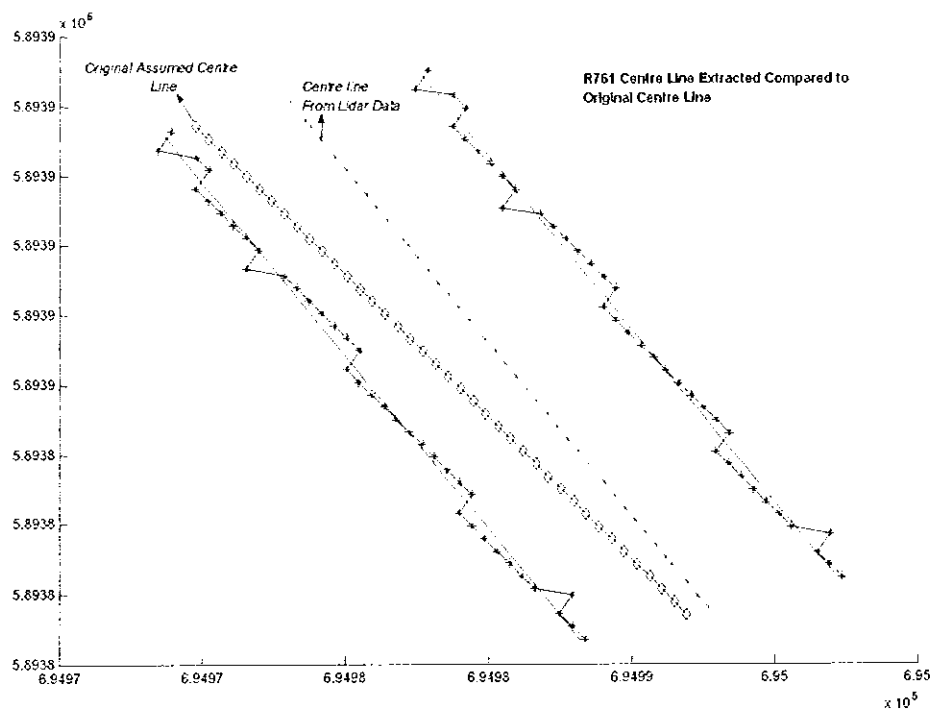


Figure: 3.18 Comparison of the Starting Centre Line with Centre Line Candidate determined from the ALS Data.

The analysis of Road 1 was complete and a methodology had been developed that gave promising results. It was now necessary to test the repeatability of the method on a second road. The methodology to be applied to Road 2 was:

- Generate Interpolated Height cross sections from the ALS data.

- From these generate Height Difference cross sections.

- Apply Least Squares best-fit regression to road segments in the height difference cross sections, using the road width as an additional given parameter.

- Identify segments giving the lowest RMS residuals.

- Calculate the mid point of the best-fit segment in each cross section as a candidate centre line point.

- Fit curves to left and right kerb points and centre line points, a candidate centre line.

- Compare this centre line with assumed centre line vector.


## 3.9 Test of the Repeatability of the Method on Road 2

The proposed workflow was applied to a different section of road to see if the results achieved on Road 1 could be repeated. The road chosen for this purpose was the Southern Cross (Road 2) that connects the R761 (Road1) and the national route N11 (Chapter 2.1) figure 2.1

Table 3.5 shows the height differences for nine cross-sections along a road length of 10m. Compared to Road 1, the kerb detection for this road appeared to be not well defined.

**Analysis of Height Difference Cross Section Data Road 2**

| 1 | 2 | 3 | 4 | 5 | 6 | 7 | 8 | 9 |
|---|---|---|---|---|---|---|---|---|
| 0.04 | 0.07 | 0.07 | 0.09 | 0.10 | 0.04 | 0.12 | 0.09 | 0.12 |
| 0.03 | 0.06 | 0.05 | 0.06 | 0.06 | 0.03 | 0.02 | 0.02 | 0.05 |
| 0.00 | 0.02 | 0.03 | 0.01 | 0.03 | 0.02 | 0.02 | 0.01 | 0.00 |
| 0.31 | 0.28 | 0.24 | 0.13 | 0.07 | 0.01 | 0.05 | 0.04 | 0.01 |
| 0.36 | 0.39 | 0.41 | 0.37 | 0.37 | 0.33 | 0.11 | 0.14 | 0.21 |
| 0.36 | 0.49 | 0.47 | 0.32 | *Back to Small Height Difference* | | 0.43 | 0.23 | 0.25 |
| 0.15 | 0.07 | 0.11 | 0.31 | | | 0.44 | 0.46 | 0.35 |
| 0.06 | 0.05 | 0.06 | 0.01 | | | 0.14 | 0.32 | 0.37 |
| 0.10 | 0.11 | 0.08 | 0.07 | | | 0.07 | 0.11 | 0.07 |
| 0.04 | 0.03 | 0.00 | 0.00 | 0.04 | 0.04 | 0.09 | 0.10 | 0.13 |
| 0.05 | 0.06 | 0.05 | *Step up to Slightly larger Height Difference* | | 0.04 | 0.04 | 0.02 | 0.06 |
| 0.13 | 0.13 | 0.19 | | | 0.02 | 0.02 | 0.06 | 0.07 |
| 0.05 | 0.04 | 0.00 | | | 0.19 | 0.26 | 0.12 | 0.07 |
| 0.02 | 0.01 | 0.01 | | | | 0.02 | 0.12 | 0.08 |
| 0.03 | 0.01 | 0.00 | *Small Height Differences (Red Zone)* | | | 0.03 | 0.06 | 0.03 |
| 0.05 | 0.06 | 0.0 | | | | 0.04 | 0.01 | 0.02 |
| 0.05 | 0.03 | 0.04 | 0.04 | 0.03 | 0.00 | 0.02 | 0.02 | 0.05 |
| 0.02 | 0.03 | 0.02 | 0.04 | 0.02 | 0.01 | 0.03 | 0.05 | 0.01 |
| 0.03 | 0.01 | 0.04 | *Step up to Slightly larger Height Difference* | | | 0.03 | 0.05 | 0.01 |
| 0.03 | 0.02 | 0.03 | | | | 0.03 | 0.01 | 0.00 |
| 0.02 | 0.01 | 0.03 | | | | 0.01 | 0.01 | 0.02 |
| 0.02 | 0.05 | 0.04 | | | | 0.05 | 0.04 | 0.02 |
| 0.05 | 0.08 | 0.00 | 0.03 | 0.03 | 0.00 | 0.03 | 0.06 | 0.03 |
| 0.11 | 0.07 | 0.07 | | | 05 | 0.01 | 0.01 | 0.03 |
| 0.03 | 0.01 | 0.12 | *Back to Small Height Difference* | | 08 | 0.13 | 0.12 | 0.06 |
| 0.05 | 0.02 | 0.02 | | | 01 | 0.13 | 0.14 | 0.09 |
| 0.11 | 0.01 | 0.03 | 0.02 | 0.04 | 0.01 | 0.05 | 0.04 | 0.06 |
| 0.60 | 0.50 | 0.32 | 0.12 | 0.16 | 0.08 | 0.03 | 0.02 | 0.00 |

Table 3.5 Height Difference Data for Nine Cross Sections on Road 2

Transitions from very small height variations (red figures) were demonstrated but in a very random pattern. What was also noticeable was a double step in some instances (green figures), which probably denoted the change from road to level areas (verge + footpaths) and the changes from these and the adjoining ground.

72

As expected therefore, the application of a Least Squares best fit regression to this data produced unacceptably poor results. Figure: 3.19 show the random distribution of candidate centre line and kerb points.
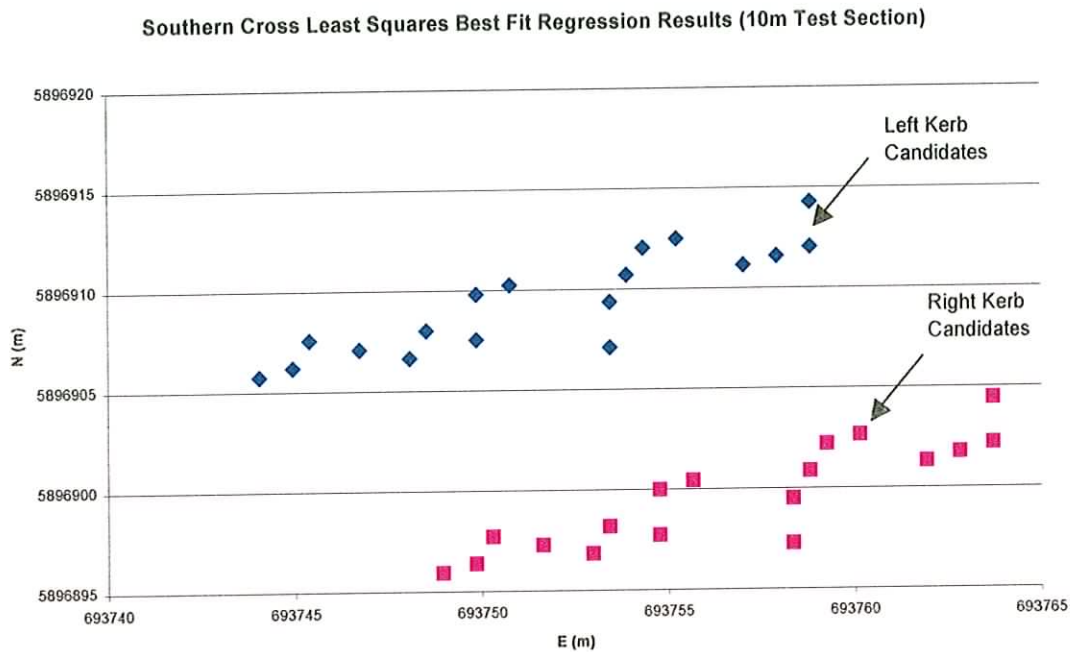


Figure: 3.19 Result of Least Squares Regression Fit of Candidate Centre Line and Kerbs Road 2.

The motivation for using the height differences was based on the fact that the visual analysis of the interpolated height cross sections of Road 1 showed a level surface, the beginnings of a transition, and a region where the height changes were so great that a road could not exist. Identifying the transition as accurately as possible was the key to determining the true road extent and as demonstrated by the height difference results and the ground truth survey the method used proved very promising. Unfortunately this approach did not work on Road 2 so an alternative was investigated.

## 3.10 Interpolated Height Analysis of Cross Sections of Road 2

Rather than look at differences in height between adjacent points the interpolated heights were reviewed for both test roads (Figure: 3.20 and 3.21). A distinct curved shape to the cross section of Road 2 was apparent compared to Road 1. On Road 2 a well-defined curve, although not smooth, is defined. It has a maximum with two minimums at the outer regions, probably a result of the drainage design specification. It now appeared that interpolated height cross sections rather than height differences, would give a more useful definition of the true road extent, when a best-fit curve was applied. The curvature stops at the extremities of the road extent similar to the height changes in the case of Road 1.
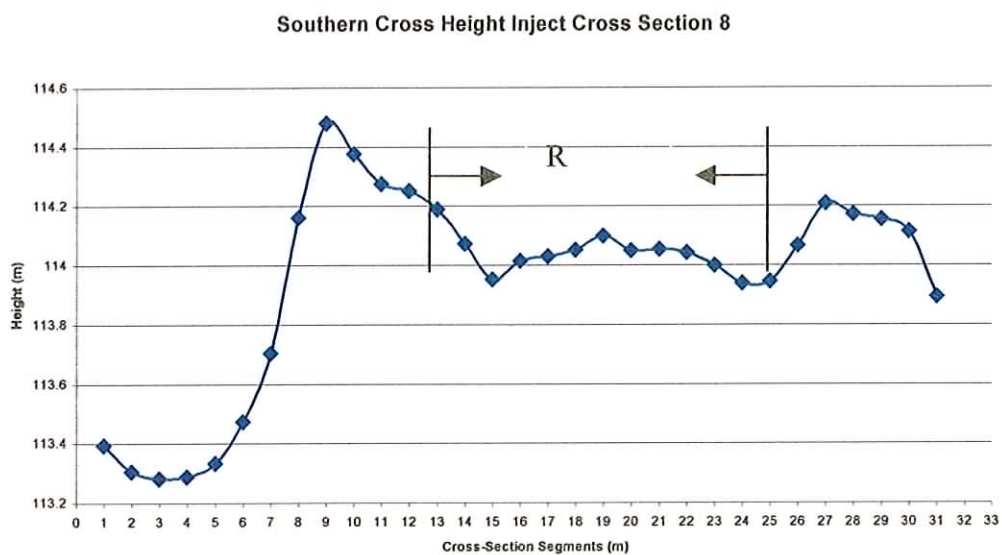


Figure: 3.20 Interpolated Heights Road 2 Section 8
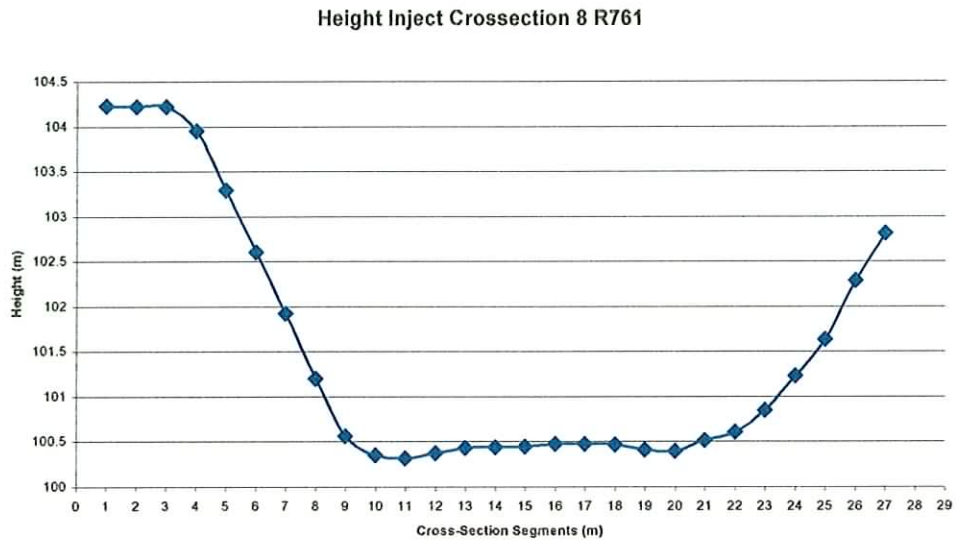
Figure: 3.21 Interpolated Heights Road 1 Cross Section 8

To model the curve in Figure 3.20 the best-fit regression algorithm was amended to fit a second order polynomial to the interpolated heights for Road 2. The resulting candidate kerbs (Figure: 3.22) show a more regular pattern. There are three identifiable blocks in the diagram that may be due to a slight change in road orientation over the sample distance.
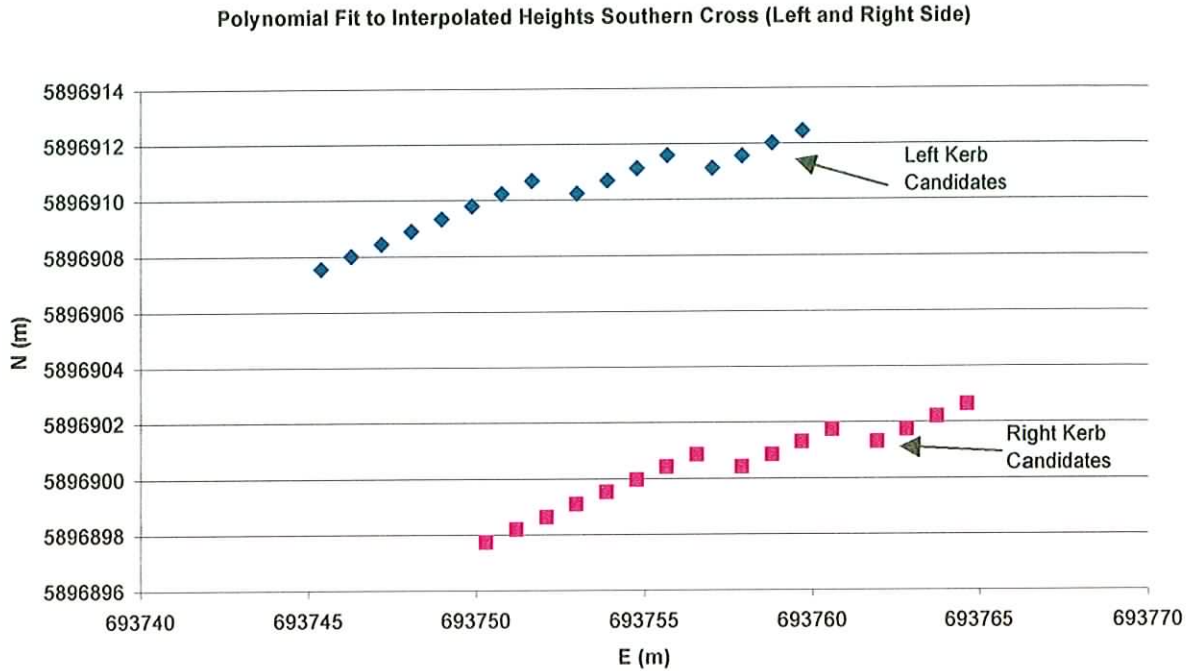
Figure: 3.22 Candidate Kerb Points from Polynomial Fit to Interpolated Height Cross Sections on Road 2

In summarising the results at this stage it can be stated that:

The height difference analysis had shown very promising results when applied to the Road 1 data and the results were verified by ground truth. The same method when applied to Road 2 did not show comparable results. A much improved result was achieved by applying a second order polynomial to interpolated height points. This raised the question of which situations should either of the methods be used, and if it were possible to determine this apriori by some pre-processing of the data. An alternative would be to assume that the design specifications for a road generally provide for a fall from the centre to the edges for drainage purposes.

The next step was to re-examine the Road 1 interpolated height cross sections, and apply the second order polynomial fit to determine if the promising height difference results could be replicated.

The same procedure as detailed for the Road 2 Interpolated Height cross-sections was followed with the added advantage of having ground truth to verify the findings. The results of the second order polynomial applied to the Interpolated Height cross-sections showed very good coincidence with the surveyed kerbs (Figure: 3.23).

**Ground Truth and Polynomial Fit to Interpolated Height Cross Sections Road 1**
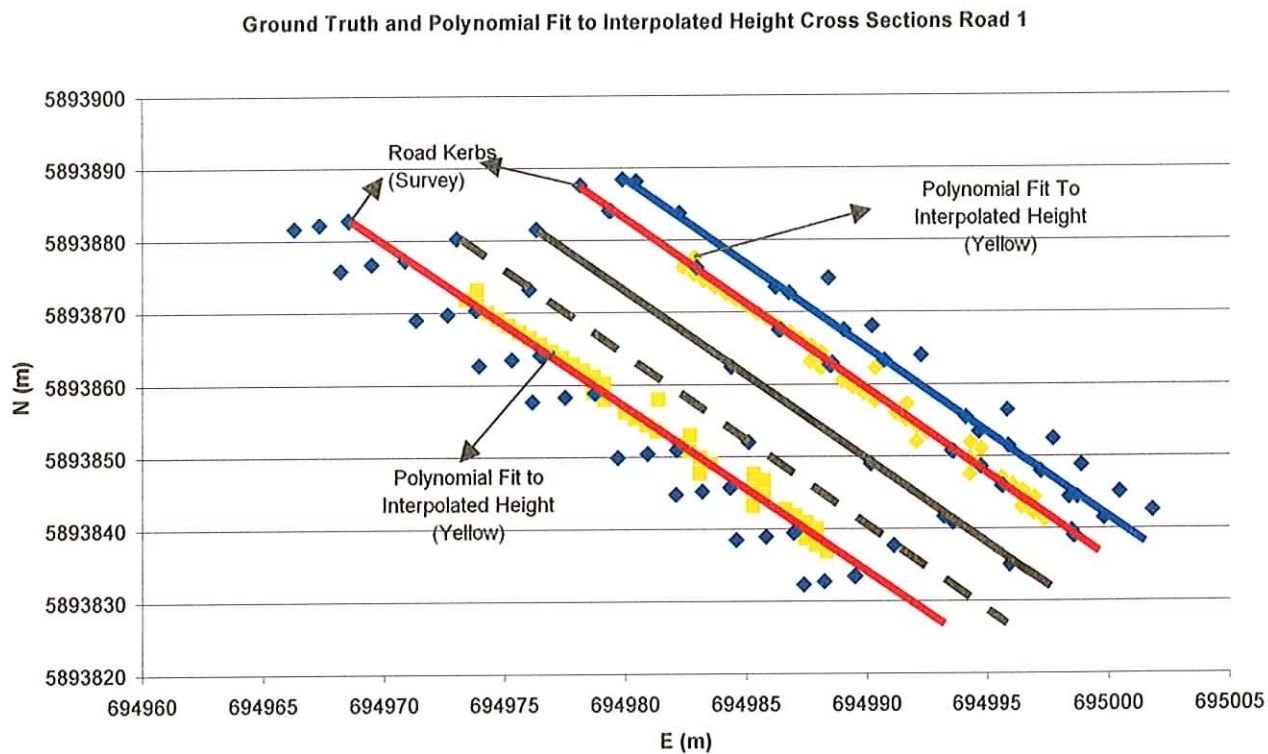


Figure: 3.23 Polynomial Fit of Interpolated Height Cross-Sections Compared with Ground Truth Road 1

It was concluded that the application of a Second Order Least Squares Polynomial best fit to the Interpolated Height cross-sections gave comparable results to the linear

fit to the Height Difference cross sections. The results were confirmed by a comparison with ground truth.

## 3.11 Observations on the Repeatability Test

The answer as to why the analysis of Height Difference cross-sections worked well on Road 1 and failed on Road 2 lay in the dissimilar terrain at the road boundaries of the two regions, and the inability of a linear fit to the data to distinguish the road segment from the edges. Studying the Height Difference cross-section for Road 1 (Figure: 3.24) reveals increasing differences on the left and right sides of the level region. There are therefore no height differences that are equal to or less than the height differences of the central level area. The linear Least Squares algorithm will work well under these circumstances as the best fit will be within the region where visual inspection suggests, somewhere between 9m and 21m.

**Height Difference Sample Road 1**
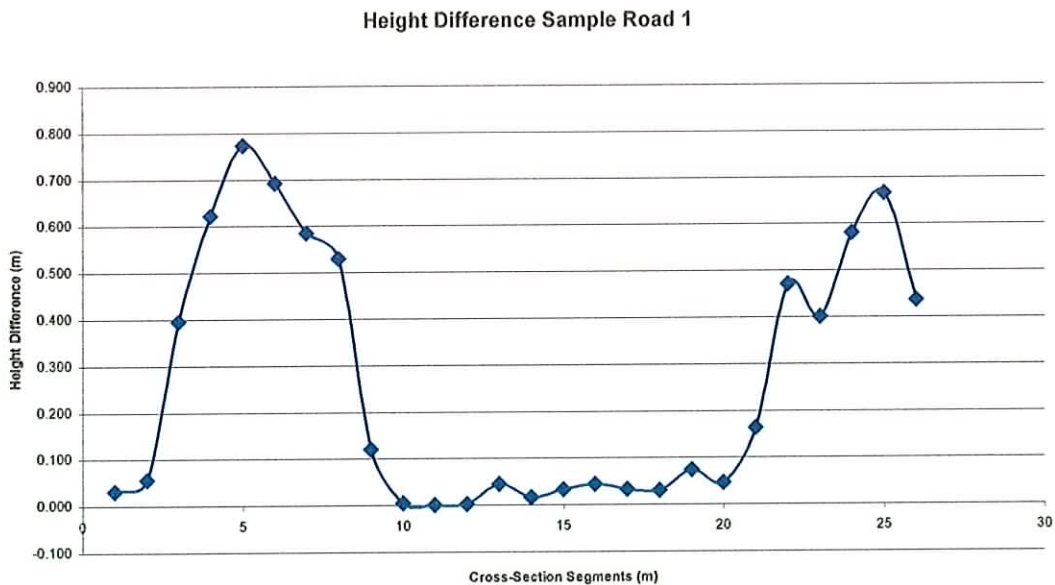


Figure: 3.24 Sample Cross-Section of Height Differences Road 1

78

A comparison of a Road 1 sample cross section to a sample from Road 2 (Figure: 3.25) reveals a different pattern. The shaded area, bounded by two peaks A and B, shows the most probable area for the road based on a visual inspection. In this case a key issue is the magnitude of the height differences on either side of the peaks. It can be seen that they are very close in magnitude to the differences that occur in the central area. In such cases the use of a linear least squares best fit to the height difference data was flawed and gave incorrect results.

**Height Difference Cross Section 1 Southern Cross Road**
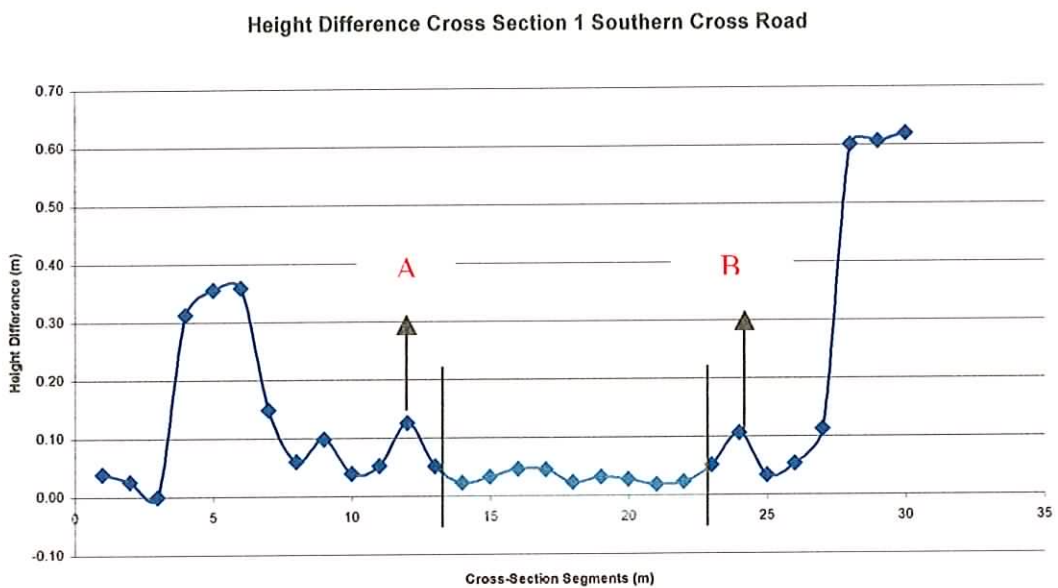


Figure: 3.25 Height Difference Cross-Section 1 Road 2

It is possible in these cases that a better fit will be found through the peaks rather than between them. Statistically it may show a better result and be flagged by the algorithm as the best candidate. Based on a visual inspection it would never be accepted.

To illustrate this flaw two tests were conducted on the above cross-section. The first test was to apply a linear Least Squares regression to the Height Differences. The second was to apply a second order polynomial Least Squares fit to the Interpolated Heights and compare the results of the two methods.

Results from the linear regression algorithm detailing the RMS for each 11 m candidate tested show that the region with the smallest RMS value is between 15m and 26m (Table 3.6).

This line extends beyond peak "B" (Figure 3.25) and would not be chosen based on a visual interpretation of the graph. The algorithm selects the most likely candidate based on the smallest RMS and in this case statistically this is the region 15m to 26 m (RMS.005407).

| RMS Residuals for 11m Segments Road 2 | | |
| Possible Kerb Candidates | | |
| From m | To m | RMS |
| --- | --- | --- |
| 5 | 16 | 0.06551 |
| 6 | 17 | 0.05408 |
| 7 | 18 | 0.01054 |
| 8 | 19 | 0.00742 |
| 9 | 20 | 0.00704 |
| 10 | 21 | 0.00646 |
| 11 | 22 | 0.00560 |
| 12 | 23 | 0.00674 |
| 13 | 24 | 0.00573 |
| 14 | 25 | 0.00542 |
| 15 | 26 | *0.00541* |

Table 3.6 Height Difference RMS for each 11m Kerb Candidate using a Linear Least Squares Fit Road 2

Referring again to Figure: 3.25 a visual inspection intuitively shows that the most probable candidate is in the region between 13m and 24m, the area bounded by peaks "A" and "B". The results of the second test conducted using a second order polynomial least squares fit to the interpolated heights confirm this region as having the smallest RMS value (Table 3.7).

| RMS Residuals for 11m Segments Road 2 | | |
|---|---|---|
| Possible Kerb Candidates | | |
| From m | To m | RMS |
| 5 | 16 | 0.24160 |
| 6 | 17 | 0.18453 |
| 7 | 18 | 0.05917 |
| 8 | 19 | 0.01394 |
| 9 | 20 | 0.01851 |
| 10 | 21 | 0.02776 |
| 11 | 22 | 0.03428 |
| 12 | 23 | 0.03044 |
| 13 | 24 | *0.01373* |
| 14 | 25 | 0.02449 |
| 15 | 26 | 0.03002 |

Table 3.7 Interpolated Height RMS for each 11m Kerb Candidate using a 2nd Order Polynomial Least Squares Fit Road 2

These results indicate that using the height difference cross-sections was not the best strategy. The second order polynomial least squares regression fitted to the interpolated height cross-sections proved a more reliable solution in both areas.

## 3.12 Second Order Polynomial Best-Fit Regression Applied to Larger Sample of Road 2

It was decided at this stage to check if the second order polynomial fitted to the Interpolated Heights was consistent over a larger sample. The routine was applied to

an 18m section of Road 2 and the results showed a large difference between cross sections 17 and 18 compared to the preceding ones (Table 3.8)

| | *Road 2* | | |
| | **2nd Order Polynomial Best Fit** | | |
| | *Best Candidate Road Segment* | | |
| **No** | **From(m)** | **To(m)** | **RMS** |
| 1 | 13 | 24 | 0.014 |
| 2 | 13 | 24 | 0.010 |
| 3 | 13 | 24 | 0.004 |
| 4 | 13 | 24 | 0.007 |
| 5 | 14 | 25 | 0.029 |
| 6 | 14 | 25 | 0.009 |
| 7 | 14 | 25 | 0.003 |
| 8 | 14 | 25 | 0.015 |
| 9 | 15 | 26 | 0.006 |
| 10 | 15 | 26 | 0.011 |
| 11 | 15 | 26 | 0.013 |
| 12 | 15 | 26 | 0.012 |
| 13 | 15 | 26 | 0.016 |
| 14 | 15 | 26 | 0.012 |
| 15 | 15 | 26 | 0.018 |
| 16 | 15 | 26 | 0.020 |
| 17 | 11 | 22 | 0.031 |
| 18 | 11 | 22 | 0.015 |

Table 3.8 Analysis of Second Order Polynomial fit to Extended Section of Road 2

In order to investigate the reason for the anomaly the interpolated height data for cross-section No18 was extracted and a curve fitting routine applied (Figure: 3.26). In the diagram the actual profile is shown in blue; successive polynomial fits are shown in cyan; and the best-fit polynomial (i.e. with the smallest RMS residual) is shown in red. Clearly the best-fit polynomial is not consistent with a visual inspection.
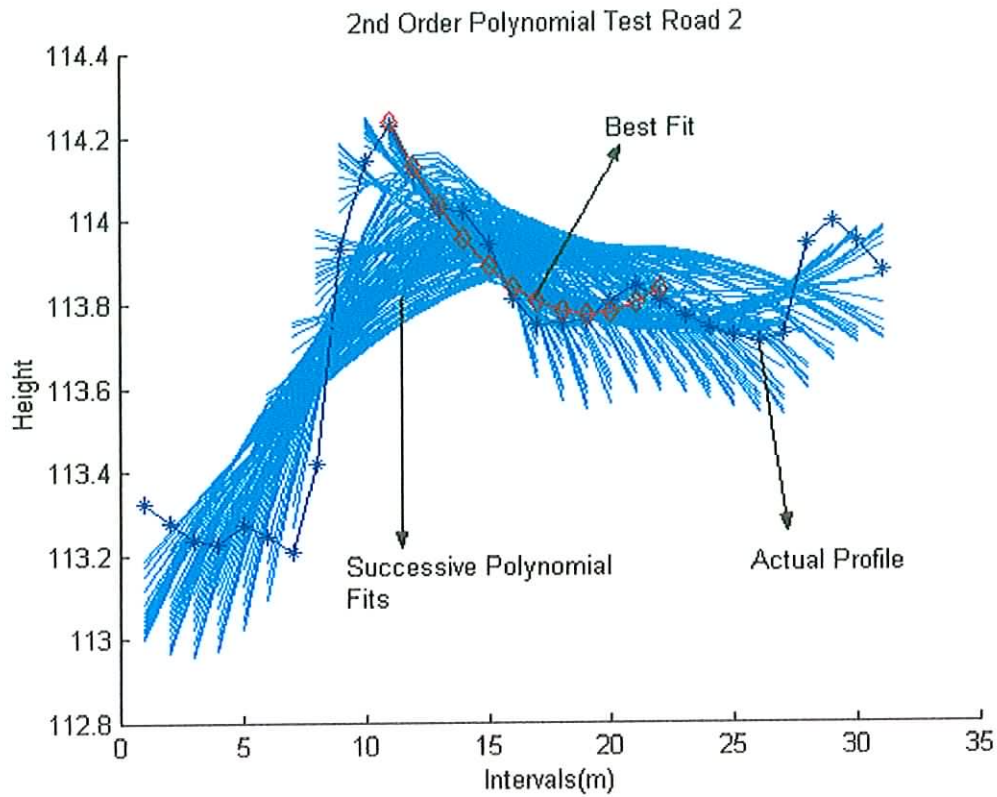
Figure: 3.26 2nd Order Polynomial Least Squares Fit to Cross Section 18 Road 2

By inspection the best fit probably lies between 15m and 25m (Figure: 3.27) and not 11m to 22m as indicated by the least squares polynomial fit.
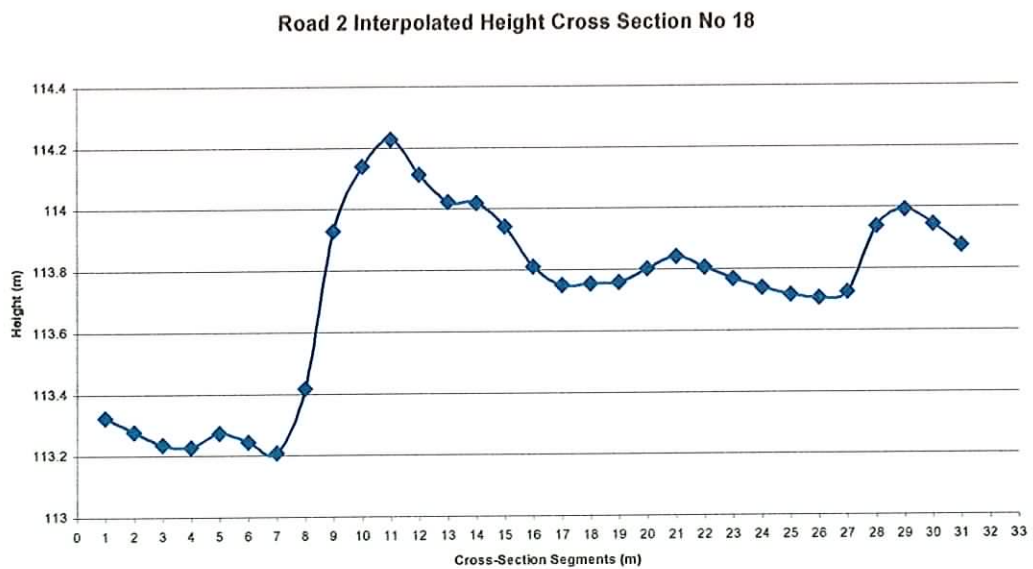


Figure: 3.27 Interpolated Heights for Cross Section No 18 Road 2

The most obvious difference between the best-fit and the visual road segments was the magnitude of the height variation. The segment between 11m and 22m showed more change compared to the 15m to 25m segments. The development of a method to detect height differences greater than a given threshold was thought to be useful as a constraint in the selection process.

A simple approach was taken:

- Calculate the RMS residuals for each candidate curve using the second order polynomial Least Squares fit.

- Determine the maximum and minimum heights in the candidate segment.

- If the height range is outside a threshold value, flag the candidate curve as excluded. In practice, height variations across typical public roads are limited and so the use of an upper threshold was considered reasonable.

The threshold value was chosen after reviewing the typical maximum and minimum heights shown in the most probable road bearing regions of the cross sections. These values ranged from between 0.09m and 0.2m so a threshold value of 0.3m was selected.

Results obtained by using the threshold value (Table 3.9) showed that the method was successful and the regions between 11m and 22m were rejected. The new value of 15m to 26m is consistent with the visual analysis and the results of the preceding cross sections.

| 2nd Order Polynomial Least Squares Fit | | | |
| --- | --- | --- | --- |
| *Best Candidate Road Segment* | | | |
| No | From(m) | To(m) | RMS |
| 1 | 13 | 24 | 0.014 |
| 2 | 13 | 24 | 0.010 |
| 3 | 13 | 24 | 0.004 |
| 4 | 13 | 24 | 0.007 |
| 5 | 14 | 25 | 0.029 |
| 6 | 14 | 25 | 0.009 |
| 7 | 14 | 25 | 0.003 |
| 8 | 14 | 25 | 0.015 |
| 9 | 15 | 26 | 0.006 |
| 10 | 15 | 26 | 0.011 |
| 11 | 15 | 26 | 0.013 |
| 12 | 15 | 26 | 0.012 |
| 13 | 15 | 26 | 0.016 |
| 14 | 15 | 26 | 0.012 |
| 15 | 15 | 26 | 0.018 |
| 16 | 15 | 26 | 0.020 |
| 17 | 15 | 26 | 0.038 |
| 18 | 15 | 26 | 0.026 |

Table 3.9 Results of $2^{nd}$ Order Polynomial Least Squares Fit with Addition of Height Threshold.

In summary the second order polynomial fit showed good results when applied to Road 1 and the 10m section of Road 2, but on the longer 18m section of Road 2, the addition of a height threshold parameter into the algorithm was required to achieve a successful outcome.

## 3.13 Linear Least Squares Best-Fit Applied to Interpolated Height Cross-Sections of both Roads.

At this stage a successful outcome had been achieved in both test areas. The problem however was that Road 2 required two addition parameters, road width and height threshold, whereas Road 1 only required the road width parameter. The preferred outcome would have been a common solution without the need to determine the

additional height threshold parameter, and to ascertain the circumstances in which to apply it.

In an effort to find a common solution a further possible method was explored. This was to apply the linear Least Squares fit to the Interpolated Height cross-sections for both roads and compare these results with previous results. The results from the linear Least Squares fit to the interpolated heights compared to the second order polynomial fit (Table 3.10) demonstrated a better linear fit to the data.

| | Road 1 | | | | | |
|---|---|---|---|---|---|---|
| | 2nd Order Polynomial Best Fit | | | Linear Best Fit | | |
| | Best Candidate Road Segment | | | Best Candidate Road Segment | | |
| NO | From(m) | To(m) | RMS | From(m) | To(m) | RMS |
| 1 | 10 | 20 | 0.002 | 10 | 20 | 0.002 |
| 2 | 10 | 20 | 0.001 | 10 | 20 | 0.003 |
| 3 | 10 | 20 | 0.003 | 10 | 20 | 0.004 |
| 4 | 11 | 21 | 0.003 | 11 | 21 | 0.006 |
| 5 | 10 | 20 | 0.004 | 10 | 20 | 0.005 |
| 6 | 10 | 20 | 0.011 | 10 | 20 | 0.011 |
| 7 | 10 | 20 | 0.001 | 10 | 20 | 0.005 |
| 8 | 11 | 21 | 0.005 | 10 | 20 | 0.012 |
| 9 | 10 | 20 | 0.009 | 10 | 20 | 0.010 |
| 10 | 10 | 20 | 0.001 | 10 | 20 | 0.001 |
| 11 | 10 | 20 | 0.005 | 10 | 20 | 0.006 |
| 12 | 11 | 21 | 0.003 | 11 | 21 | 0.003 |
| 13 | 11 | 21 | 0.015 | 11 | 21 | 0.015 |
| 14 | 11 | 21 | 0.014 | 11 | 21 | 0.016 |
| 15 | 11 | 21 | 0.005 | 11 | 21 | 0.005 |
| 16 | 11 | 21 | 0.001 | 11 | 21 | 0.004 |
| 17 | 11 | 21 | 0.003 | 11 | 21 | 0.004 |
| 18 | 11 | 21 | 0.002 | 11 | 21 | 0.003 |

Table 3.10 Comparison of Linear and Polynomial Least Squares Best-Fits on Road 2

It was clear from the comparison that the linear Least Squares yielded more consistent results than the polynomial fit.

When the results from the Road 1 (Table 3.11) were examined a similar pattern emerged with the qualification that two cross sections were not the same, but differed by one metre. As each cross section would ultimately be linked together using a second degree polynomial vector this did not represent a significant problem.

Looking at cross-section No 19 (Table 3.11), as an example the linear best fit suggested a road segment from 11m to 21m. Viewed in the context of cross-sections before and after, this appeared a true result. However other cross sections agreed for both methods, but when compared to neighbouring results they demonstrated slight inconsistency.

This was primarily due to the selection process used. The segment with the lowest RMS residual might not match the visual interpretation of the data. There could be, for instance, a very small difference in the RMS values between first and second best, but the lowest is always chosen. A higher degree of intelligent processing would be required if selections were to be made based on prior results. This may have to be considered in the future.

| | Road 1 | | | | | |
|---|---|---|---|---|---|---|
| | 2nd Order Polynomial Best Fit | | | Linear Best Fit | | |
| | Best Candidate Road Segment | | | Best Candidate Road Segment | | |
| NO | From(m) | To(m) | RMS | From(m) | To(m) | RMS |
| 1 | 10 | 20 | 0.002 | 10 | 20 | 0.002 |
| 2 | 10 | 20 | 0.001 | 10 | 20 | 0.003 |
| 3 | 10 | 20 | 0.003 | 10 | 20 | 0.004 |
| 4 | 11 | 21 | 0.003 | 11 | 21 | 0.006 |
| 5 | 10 | 20 | 0.004 | 10 | 20 | 0.005 |
| 6 | 10 | 20 | 0.011 | 10 | 20 | 0.011 |
| 7 | 10 | 20 | 0.001 | 10 | 20 | 0.005 |
| 8 | 11 | 21 | 0.005 | 10 | 20 | 0.012 |
| 9 | 10 | 20 | 0.009 | 10 | 20 | 0.010 |
| 10 | 10 | 20 | 0.001 | 10 | 20 | 0.001 |
| 11 | 10 | 20 | 0.005 | 10 | 20 | 0.006 |
| 12 | 11 | 21 | 0.003 | 11 | 21 | 0.003 |
| 13 | 11 | 21 | 0.015 | 11 | 21 | 0.015 |
| 14 | 11 | 21 | 0.014 | 11 | 21 | 0.016 |
| 15 | 11 | 21 | 0.005 | 11 | 21 | 0.005 |
| 16 | 11 | 21 | 0.001 | 11 | 21 | 0.004 |
| 17 | 11 | 21 | 0.003 | 11 | 21 | 0.004 |
| 18 | 11 | 21 | 0.002 | 11 | 21 | 0.003 |
| 19 | 10 | 20 | 0.005 | 11 | 21 | 0.006 |
| 20 | 11 | 21 | 0.003 | 11 | 21 | 0.003 |
| 21 | 11 | 21 | 0.006 | 11 | 21 | 0.006 |
| 22 | 11 | 21 | 0.007 | 11 | 21 | 0.007 |
| 23 | 12 | 22 | 0.007 | 12 | 22 | 0.009 |
| 24 | 12 | 22 | 0.011 | 12 | 22 | 0.011 |
| 25 | 12 | 22 | 0.004 | 12 | 22 | 0.005 |
| 26 | 12 | 22 | 0.005 | 12 | 22 | 0.009 |
| 27 | 12 | 22 | 0.006 | 12 | 22 | 0.007 |
| 28 | 12 | 22 | 0.009 | 12 | 22 | 0.009 |
| 29 | 12 | 22 | 0.003 | 12 | 22 | 0.004 |
| 30 | 11 | 21 | 0.004 | 11 | 21 | 0.007 |
| 31 | 12 | 22 | 0.005 | 12 | 22 | 0.005 |
| 32 | 12 | 22 | 0.005 | 12 | 22 | 0.005 |
| 33 | 12 | 22 | 0.010 | 12 | 22 | 0.010 |
| 34 | 12 | 22 | 0.003 | 12 | 22 | 0.003 |
| 35 | 12 | 22 | 0.005 | 12 | 22 | 0.005 |

Table 3.11 Comparison of Linear and Polynomial Least Squares Best-Fits to Road 1

In summary the linear Least Squares fit to the Height Differences on Road 1 worked successfully but problems were encountered when it was applied to Road 2. Success on Road 1 is attributed to the geometric nature of the road. The situation on Road 2

indicated that the algorithm was not robust enough to be used to determine the true road extent. This was due to height differences on the footpaths that were equal to differences on the road surface. In these circumstances a linear fit, satisfying the criterion of having the lowest RMS, could be achieved outside the real road segment. Modifications such as constraining the least squares regression to fit for example between peaks "A" and "B" (Figure: 3.25) would be required. Identifying these initial change regions and ignoring others would be difficult. If an algorithm could be developed to achieve this it may enable a further degree of automation. Currently the least squares fit algorithm requires an additional parameter, the road width. However, identifying "A" and "B" might serve as a first approximation of a road width. By using a loop to increase and decrease this initial value, together with a statistical analysis of each result, a most probable road width might be determined.

Using the interpolated heights and a second order polynomial fit initially gave very promising results on both test areas until the Road 2 sample was extended. The method began to fail when, due to subtle terrain changes, a better curve fit could be achieved outside of what was obviously the road segment. This was corrected by introducing a height threshold into the algorithm based on the difference between the maximum and minimum heights in the region.

As ultimately the aim was to produce an automatic method this had a disadvantage. The threshold value was decided by a visual analysis of height differences in the test area. Perhaps the value of 0.3m will work in other areas, but this would have to be proven to have confidence in the algorithm.

The linear Least Squares regression applied to the Interpolated Height cross-sections showed good consistency over the two test areas and had the advantage of only requiring the road width as an additional parameter. This method, therefore, is seen as the most promising of all methods tested. An important testing scenario would be a road section within terrain that shows very little height differences, the method has not been tested in such an area. A favourable result here would be significant.

## 3.14 Analysis of the Return Intensity Data for Road 1

In addition to studying the potential for road centre line determination by geometric analysis of the ALS data, it was also felt that the intensity data recorded with each return pulse should be explored. The analysis of the mean intensity for seed triangles and group triangles related to the same 10m-road section used in the gradient analysis. This section was extended to 30m for the analysis of standard deviations and injected intensity cross-sections.

Analysis of the Mean Intensity of Triangle Groups

Figure: 3.28 illustrates the mean intensity of triangle groups across ten cross-sections. They do not provide much useful information. This is primarily due to the nature of the intensity data which tends to fluctuate. Although the road colour is black the intensity of this surface registers as a range of values. One might generalise from the results that in the region where we know a road to exist the intensity range is between 0.5 and 4. This however is very unreliable, as intensity values will be affected by factors such as the scan angle of the laser and prevailing atmospheric conditions.

90
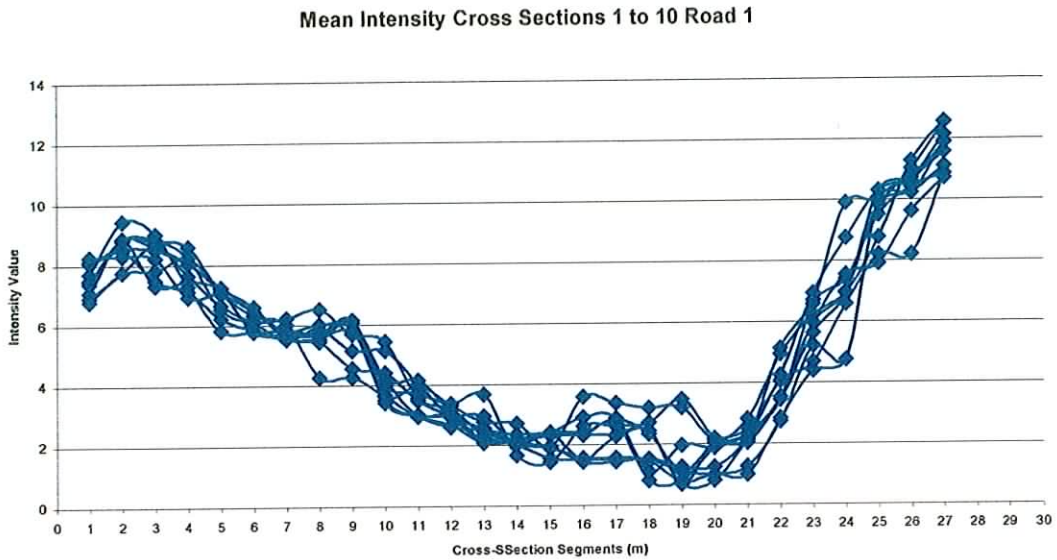
Figure: 3.28 Analysis of the Mean Intensity of Triangle Groups across Ten Cross Sections Road 1.

## Analysis of the Standard Deviation of the Intensity of Triangle Groups

Because the study deals with groups of triangles that represent small surface patches, any change in the intensity of any of the individual triangles is necessarily diluted. The standard deviations of the groups do not provide any useful information (Figure: 3.29)
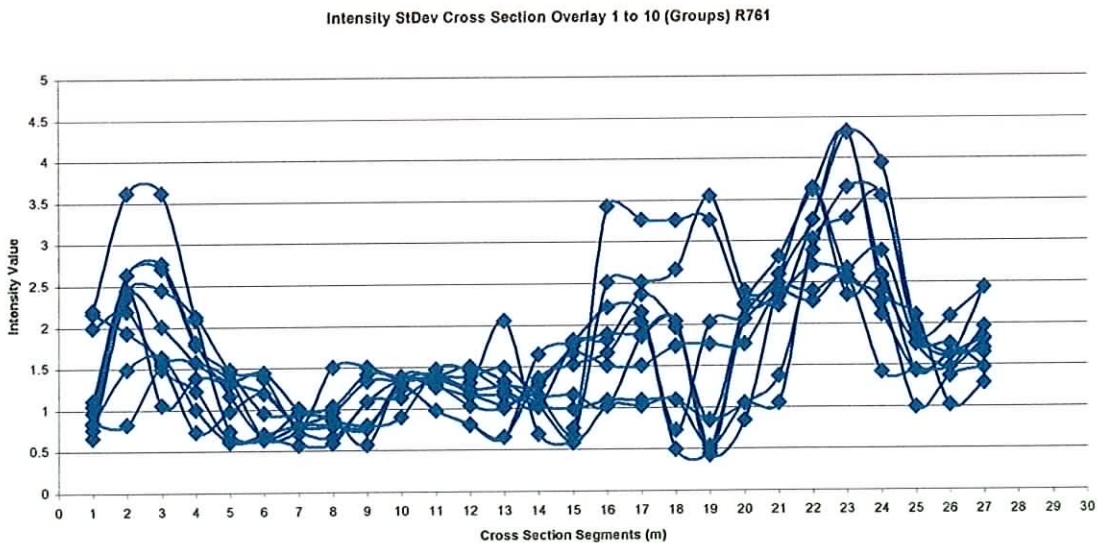


Figure: 3.29 Standard Deviation Triangle Groups Cross-Sections 1 to 10 Road 1

## Analysis of the Mean Intensity of Seed Triangles

Analysis of mean intensity of the seed triangles (Figure: 3.30) is similar to that of the group triangle in defining a general intensity range for the road surface. Because however the seed is a much more discrete area compared to the group, small peaks in the graph appear which could indicate a triangle with large intensity variations in its three vertices coordinates. As the standard deviation of the intensity of seed triangle points should highlight these changes the analysis was extended to include thirty sections.
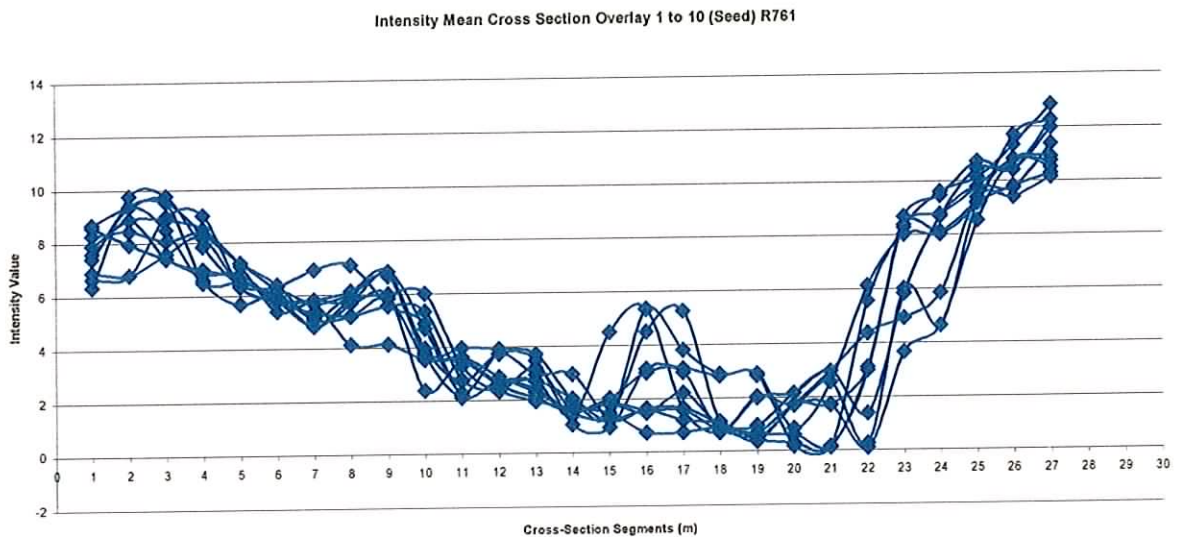


Figure: 3.30 Analysis of the Mean Intensity of the Seed Triangles for Cross Sections 1 to 10 Road 1.

## Analysis of the Standard Deviation of the Intensity of Seed Triangles

Thirty cross-sections were generated showing the standard deviations of the intensity values of the seed triangle across each section. Emphasis was placed on finding cross-sections that showed large peaks especially in areas close to the potential road centre and edges. As the road markings are white and the kerbs grey white concrete they

should have a return intensity that differs from the dark road surface. Figure: 3.31 illustrate an example of what was sought.

**Intensity StDev Cross Section 13 (Seed) R761**
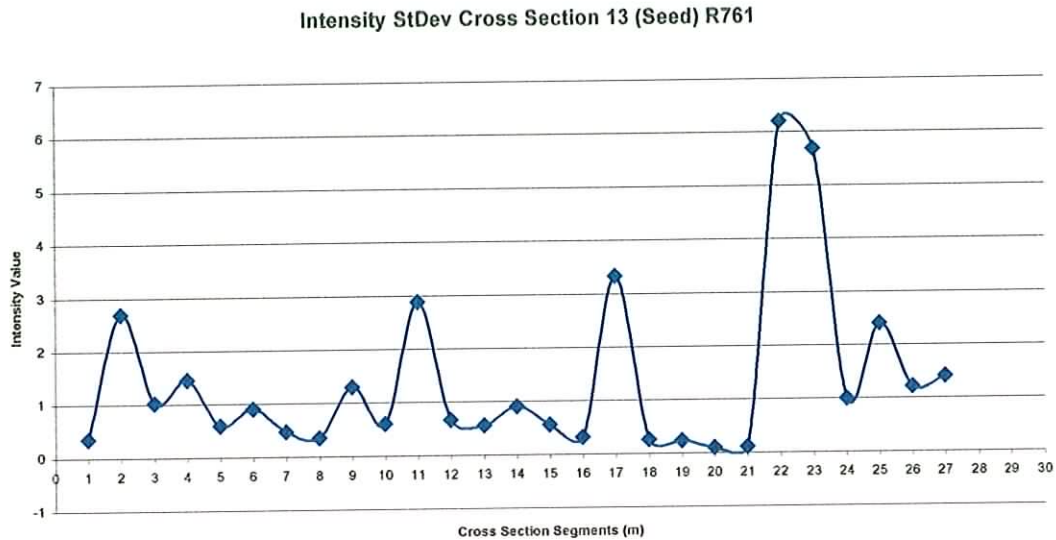


Figure: 3.31 Analysis of the Standard Deviation of the Intensity of Seed Triangle Points in Cross Section No 13

Within the segment from 10m to 21m, two peaks appear, one at 17m and the other at 11m. Of the thirty cross sections seven were found that exhibited similar properties. Similar to the kerb identification procedure each peak was traced back to the search template where they occurred. Each of the point coordinates was overlayed on the ground truth survey and the results are presented in Figure: 3.32.

Roadmarkings from Seed StdDeviations Overlayed on Ground Truth Survey R761
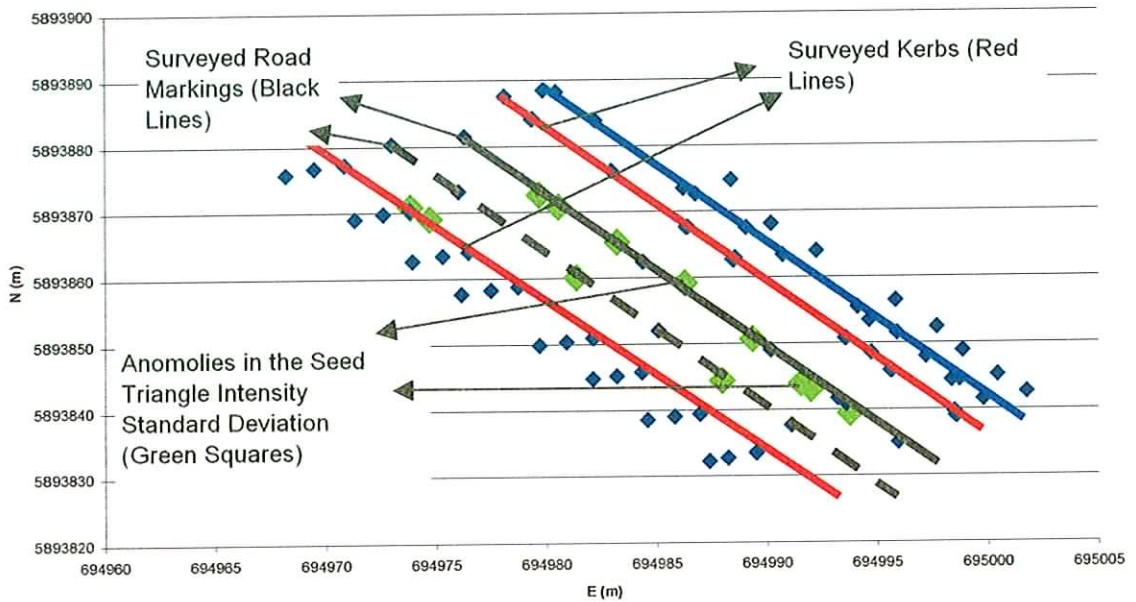
Figure: 3.32 Comparison of Peaks in the Standard Deviations of the Intensity of Triangle Points and the Position of Road Markings Road 1

The two red lines represent road kerbs; the solid black line represents the continuous white road marking, and the broken black line represents the broken white road marking. The green squares are the coordinates from the search template. It can be seen that the peaks occurring in the seed intensity standard deviation cross sections do represent anomalies within each triangle that coincide with road markings and the concrete kerb. Due to the spacing of the data and the fact that the laser hit on the ground is not a pin- point but rather a splash the results are good to within 1m.

94

An identical procedure was used in the case of the Nearest Neighbour Intensity cross-sections as was used in the case of the seed intensity standard deviations analysis. The coordinates of well-defined peaks in the cross sections were taken from the search template and overlayed on the ground truth (Figure: 3.33).
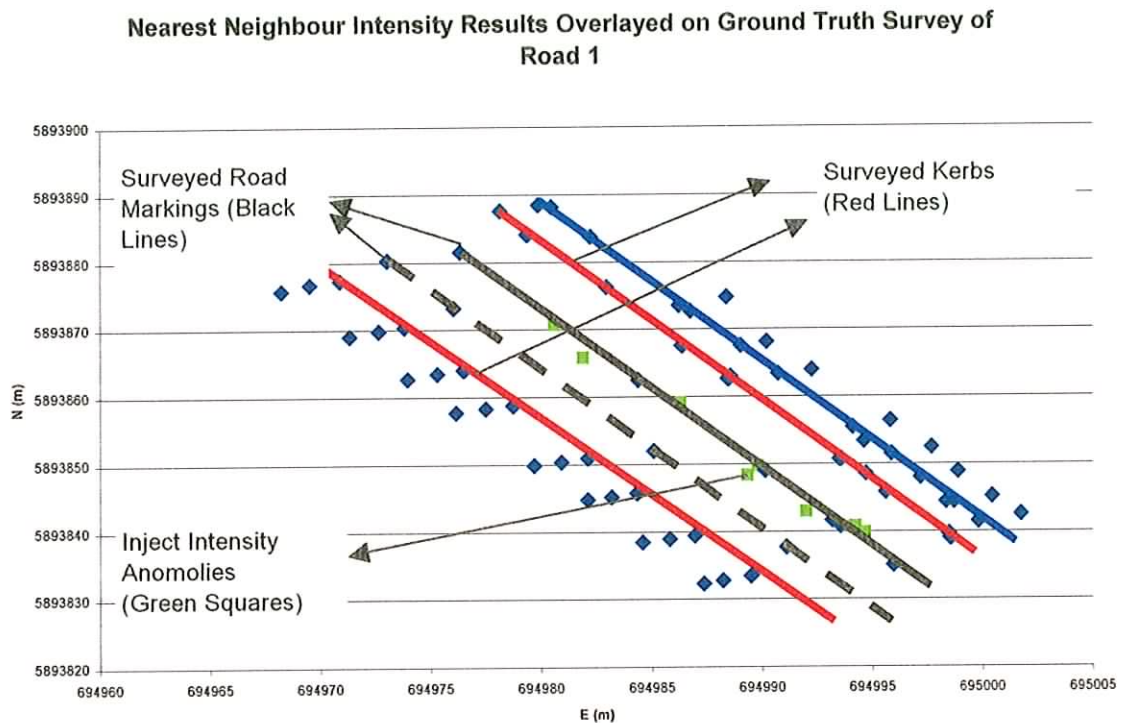


Figure: 3.33 Comparison of Peaks in the Nearest Neighbour Intensity Cross Sections and Road Markings Road 1

These results do not appear to be as good as the seed intensity standard deviation results. They do identify a possible road marking but this is confined to the continuous white centre line.

## 3.15 Analysis of the Return Intensity Data for both Roads

The intensity analysis so far had concentrated on its potential for detecting road markings. Another possible use for intensity is its use in detecting a road surface region. This could be valuable in an area where the interpolated heights are uniform. Such an area has not been tested in this study but if we concede that there might be possible problems using height data another avenue to pursue would be to try and identify surface make-up. As no one material has an exact intensity signature but rather a range of values, the surface classification would be very broad.

Roads generally are dark in colour and should have a low intensity value when compared to natural vegetation and other man made surfaces such as concrete. The possibility of using this broad distinction was explored using the intensity inject analysis for Road 1 and for comparison purposes, for a section of Road 2.

The first step was to look at Nearest Neighbour Intensity sections for the two areas (Figure: 3.34 and 3.35).

**Nearest Neighbour Intensity Cross Section 14 Southern Cross Road**
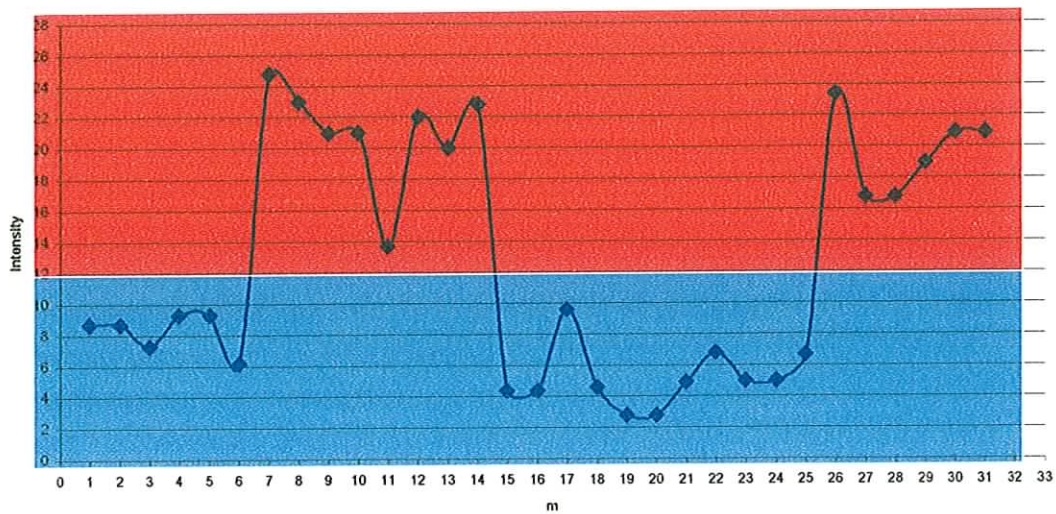


Figure: 3.34 Nearest Neighbour Intensity Cross-Section 14 Road 2

**Nearest Neighbour Intensity Cross Section 9 R761**
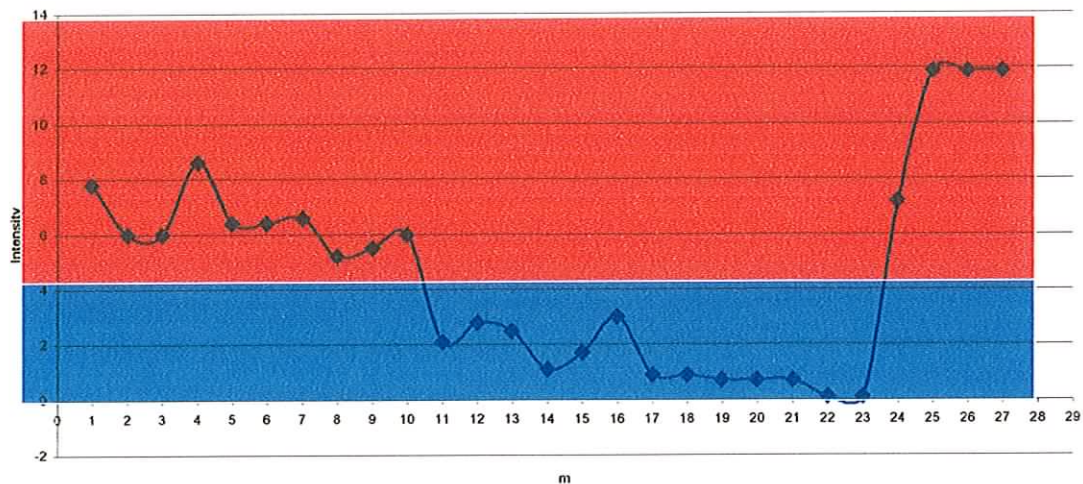


Figure: 3.35. Nearest Neighbour Intensity Cross Section 9 Road1

Both graphs can be divided into two sections; one containing high intensity values (red) the other low values (blue).

Having found that a similarity existed between the two data samples a method to analyse each cross-section was sought. It can be seen that the average of the blue area in both graphs will be less than the red area. But in the case of the Road 2 both red

97

and blue areas can be subdivided into two low value regions and two high value regions. Therefore any analysis would need to be constrained to looking at particular region sizes.

The easiest way to achieve this was to adapt the least squares regression algorithm, which used the road width parameter, to suit the purpose. Instead of calculating a best-fit line for all combinations of the road width, the amended algorithm calculated the lowest mean intensity value and outputted the location in the cross section where this occurred.

If one can imagine moving across each graph from left to right with a template of the road width, it will cover areas that incorporate high and low values, eventually it will meet an area where only low values are present and the average value here compared to previous areas will be lower. It was hoped that the results from this would be similar to the interpolated height analysis results.

For comparison purposes Tables 3.12 and 3.13 show the road extent determined from the interpolated heights and the possible road extent based on average intensity. They are not precisely the same, but do indicate a broad region where the road most probably exists based on intensity values and the additional parameter of road width.

| NO | Road 1 Interpolated Height Result Best Candidate Road Segment From(m) | To(m) | Average Intensity Best Candidate Road Segment From(m) | To(m) |
|----|------|------|------|------|
| 1 | 10 | 20 | 10 | 20 |
| 2 | 10 | 20 | 11 | 21 |
| 3 | 10 | 20 | 12 | 22 |
| 4 | 11 | 21 | 12 | 22 |
| 5 | 10 | 20 | 10 | 20 |
| 6 | 10 | 20 | 11 | 21 |
| 7 | 10 | 20 | 12 | 22 |
| 8 | 10 | 20 | 12 | 22 |
| 9 | 10 | 20 | 13 | 23 |
| 10 | 10 | 20 | 13 | 23 |
| 11 | 10 | 20 | 12 | 22 |
| 12 | 11 | 21 | 13 | 23 |
| 13 | 11 | 21 | 12 | 22 |
| 14 | 11 | 21 | 12 | 22 |
| 15 | 11 | 21 | 12 | 22 |
| 16 | 11 | 21 | 13 | 23 |
| 17 | 11 | 21 | 13 | 23 |
| 18 | 11 | 21 | 11 | 21 |

Table 3.12 Road Extent Determined by Average Intensity Compared to Interpolated Height Determination Road 1

99

| No | Road 2 Interpolated Height Result Best Candidate Road Segment From(m) | To(m) | Average Intensity Best Candidate Road Segment From(m) | To(m) |
|---|---|---|---|---|
| 1 | 13 | 24 | 14 | 25 |
| 2 | 13 | 24 | 15 | 26 |
| 3 | 13 | 24 | 11 | 22 |
| 4 | 13 | 24 | 14 | 25 |
| 5 | 14 | 25 | 12 | 23 |
| 6 | 14 | 25 | 15 | 26 |
| 7 | 14 | 25 | 15 | 26 |
| 8 | 14 | 25 | 14 | 25 |
| 9 | 15 | 26 | 13 | 24 |
| 10 | 15 | 26 | 14 | 25 |
| 11 | 15 | 26 | 15 | 26 |
| 12 | 15 | 26 | 14 | 25 |
| 13 | 15 | 26 | 14 | 25 |
| 14 | 15 | 26 | 14 | 25 |
| 15 | 15 | 26 | 14 | 25 |
| 16 | 15 | 26 | 14 | 25 |
| 17 | 15 | 26 | 15 | 26 |
| 18 | 15 | 26 | 15 | 26 |

Table 3.13  Road Extent Determined by Average Intensity Compared to Interpolated Height Determination Road 2

In the context of the flat area scenario proposed earlier this could be used as an additional filtering tool. The ALS data was extracted from the main data set using the bounding box algorithm that utilised coordinates taken from a vector map to select the required data. The extracted data set may contain more data than is needed, and in the case of the very level region, problems might be encountered. A way around this would be to further refine the selection process.

The results from the average intensity analysis could be used to set up a secondary selection procedure to filter out unwanted coordinates. A proposed method would be:

- Adjust the results of the average intensity algorithm to incorporate a degree of overlap. This would insure that no critical data is lost. Based on the results from the two test areas the addition of 3m to the cross section intervals would

suffice. Further experiment in other areas would be required to see if this was adequate.

- Coordinate the best candidate road segments from the above process

- Using the maximum and minimum values of the Easting and Northing coordinates of the best candidate road segments, use these as inputs for a second bounding box to operate on the output from the first bounding box algorithm.

- Apply the interpolated height algorithms to this new data.

Analysis of the seed intensity standard deviations and the intensity inject has shown promise in the detection of road markings in the Road 1 test area. Detection of potential markings was based purely on a visual analysis of peaks occurring in the cross section graphs. This procedure has not yet been automated.

There is a high degree of variability in the intensity data that makes it difficult to work with. This variability not only exists between cross sections in one area, but also when similar areas are compared. The two road surfaces investigated were constructed of the same material yet exhibited different ranges of intensity values. Peak values were also evident in other cross sections but were much smaller than the ones investigated. The conversion of the visual interpretation of these sections into an automatic process will be challenging.

Analysis of the standard deviation of the seed intensity had a higher success rate in detecting road markings but the procedure that calculates this is too cumbersome in its current state as it produces too many output files for analysis. Future work will involve using an amended form of the interpolated height routine that will automate

the process and store the results to a single file. The analysis of this data remains problematic.

Based on the results from the two test areas, using the intensity data as a filtering option was promising. If it functions correctly two benefits will accrue. Firstly the amount of data for processing will be reduced and secondly the problems encountered with the Least Squares regression of the height based cross sections should be minimised. The full implementation and testing of this will form future work.

# 4. Results and Discussion

The final method adopted was to use the Interpolated Height cross sections for both roads. Using the additional parameter of road width a linear Least Squares best-fit was applied to the data. The road segments demonstrating the smallest RMS residuals were extracted as potential road kerb candidates. For Road 1 the kerb candidates were compared to ground truth. The comparison of the ALS kerb candidates with the ground truth data was performed in two ways:

- Taking a sample of three Interpolated Height cross-sections compare the true kerb position relative to the segments derived from the ALS Interpolated Height analysis.

- With curves fitted to the ALS kerb candidates and the ground truth kerbs compare the same three cross-sections as used above based on the calculated join distance at the intersection of both curves with the search template.

The first comparison provided preliminary results whereby the ground truth was compared on a cross-section segment basis to the segment output from the ALS kerb detection algorithm. The procedure to interpolate the ground truth points onto the cross section was as follows:

- Import the 1m spaced Search Template coordinates into Trimble Geomatics Office. (TGO) software package. This formed a grid of all the cross sections.

- Import the ground truth kerb coordinates into TGO.

- Identify each of the three cross sections in the search template.

103

- On screen, intersect the nearest left and right ground truth kerbs onto the cross section.

- Determine the road segment for the intersected left and right ground truth kerbs.

Figures 4.1,4.2, and 4.3 show samples of the road segments where ALS kerb candidates were detected compared to their ground truth equivalent.
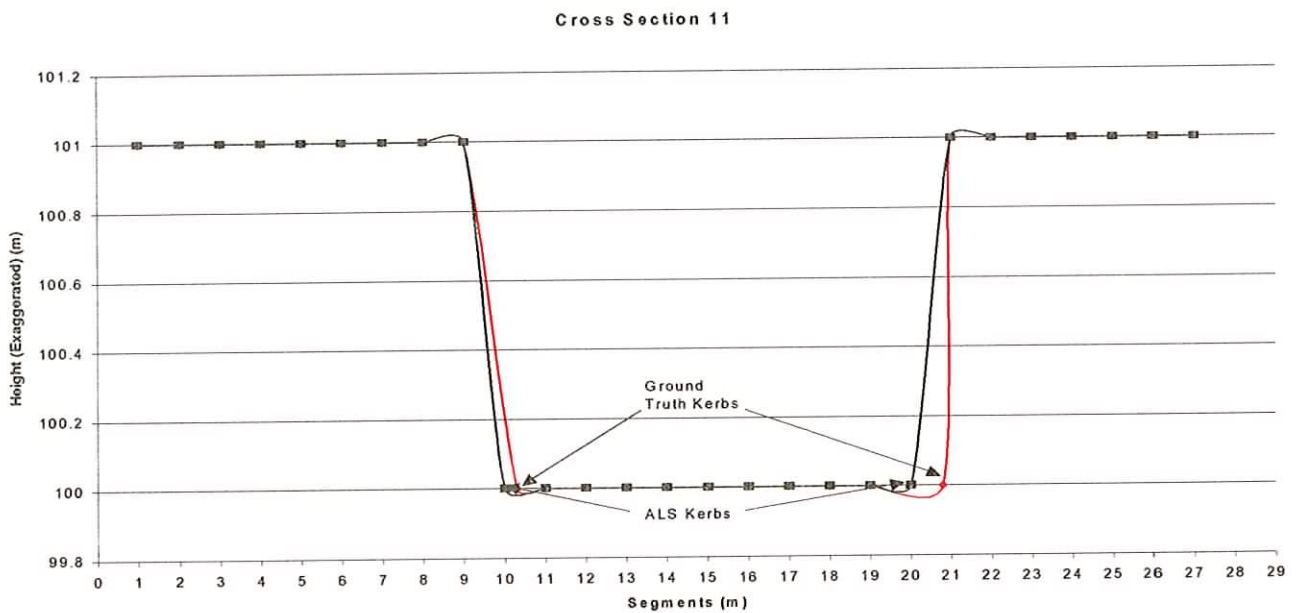
**Cross Section 11**



Figure: 4.1 ALS Kerb Candidate Road Segments Compared with Ground Truth for Cross Section 11 Road 1
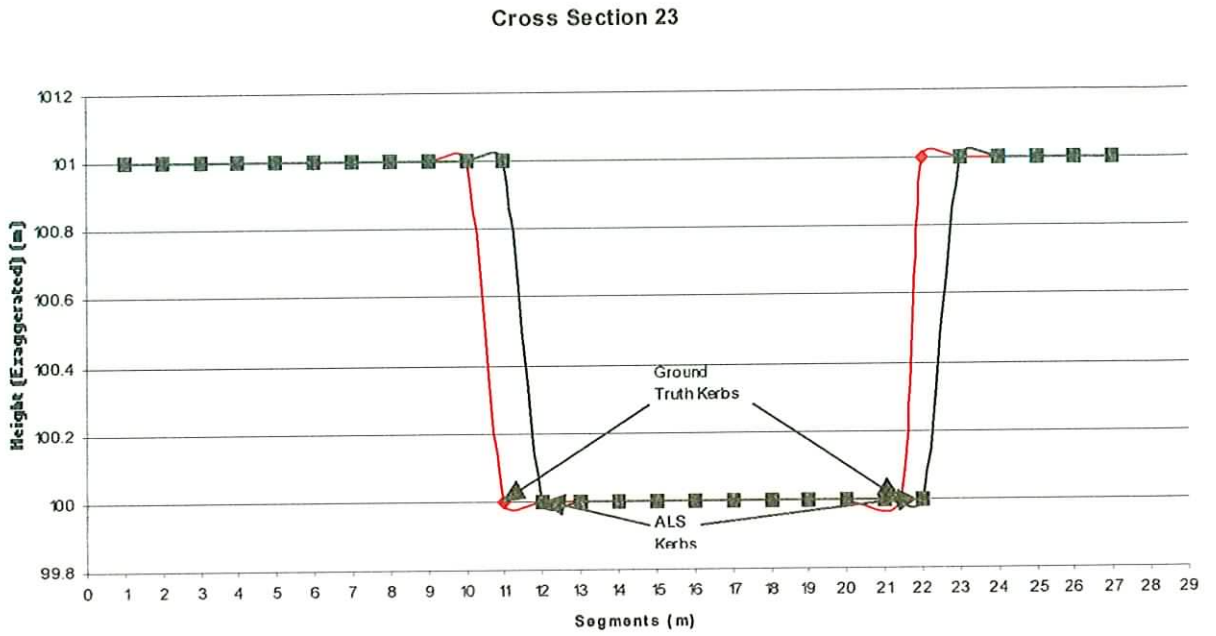
Figure: 4.2 ALS Kerb Candidate Road Segments Compared with Ground Truth for Cross Section 23
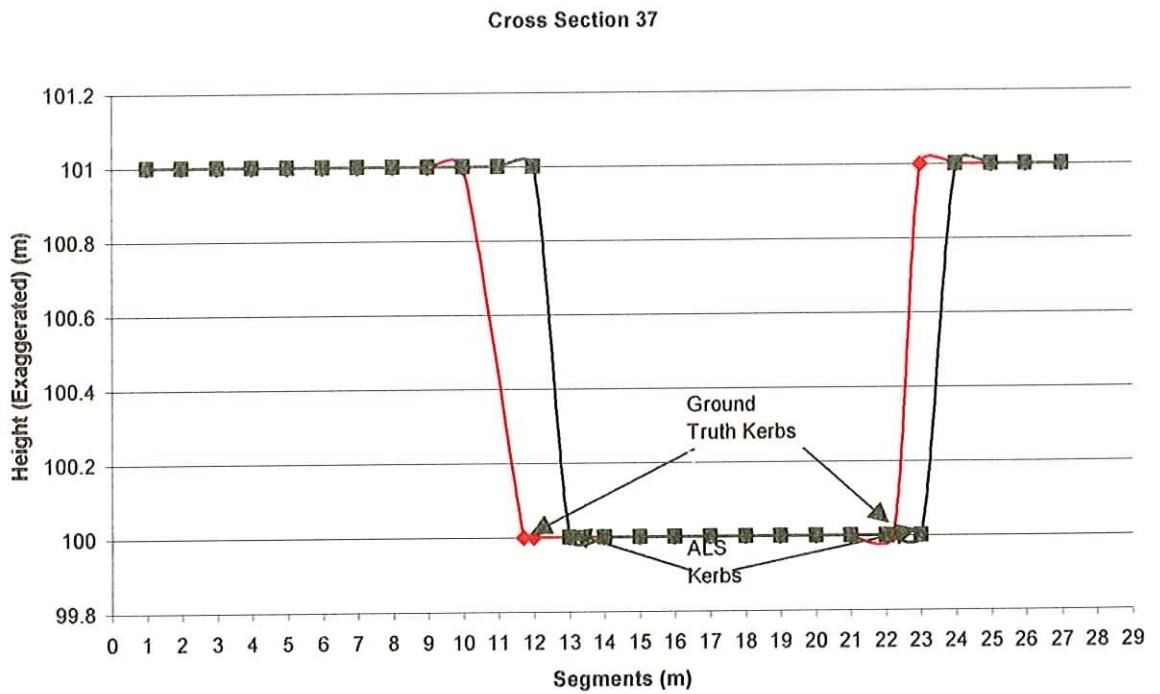
Cross Section 37



Figure: 4.3 ALS Kerb Candidate Road Segments Compared with Ground Truth for Cross Section 37

Table 4.1 shows the RMS difference values between the road segments as determined by the ALS Height Interpolation kerb detection and the true kerbs as per the ground truth data. The three cross section samples represent a road extent of approximately 40m. Over this distance the maximum RMSE difference shown is equal to the ALS data resolution of 1m.

| | Accuracy Analysis of ALS Determined Kerbs | | | | | |
| | Road Kerb Candidates from ALS Interpolated Heights | | Road Kerb Segments From Ground Truth | | Differences | |
| C/S No | From m | To m | From m | To m | From m | To m |
| --- | --- | --- | --- | --- | --- | --- |
| 11 | 10 | 20 | 10.3 | 20.8 | 0.3 | 0.8 |
| 22 | 12 | 22 | 11 | 21.4 | 1 | 0.6 |
| 37 | 13 | 23 | 11.7 | 22.2 | 1.3 | 0.8 |
| | | | | RMSE= | 1.0 | 0.7 |

Table 4.1 Accuracy Analyses of Lidar Determined Kerb Candidates for Three Cross Sections

As the proposed method fits a curve to the ALS detected kerbs, the second comparison examines the RMS differences between this curve and a curve fitted to the ground truth kerbs.

TGO is used to perform this analysis. Using the same three cross sections the points of intersection of the two curves, left and right, with the search template are determined on screen and their coordinates recorded. The join distances between these sets of coordinates is then calculated (Table 4.2)

106

| | Surveyed Kerb (Left Side) | | Lidar Kerb Candidate (Left Side) | | | Surveyed Kerb (Right Side) | | Lidar Kerb Candidate (Right Side) | | |
|---|---|---|---|---|---|---|---|---|---|---|
| CNo | E | N | E | N | Difference(m) | E | N | E | N | Difference(m) |
| 11 | 694984.2 | 5893845.9 | 694984.5 | 5893846.0 | 0.3 | 694993.6 | 5893850.5 | 694993.5 | 5893850.4 | 0.2 |
| 22 | 694979.9 | 5893856.0 | 694980.4 | 5893856.2 | 0.5 | 694989.2 | 5893860.8 | 694989.2 | 5893860.8 | 0.0 |
| 37 | 694974.0 | 5893869.9 | 694974.7 | 5893870.2 | 0.8 | 694983.4 | 5893874.5 | 694983.7 | 5893874.6 | 0.3 |
| | | | RMSE= | | 0.6 | | | RMSE= | | 0.2 |

Table 4.2 Calculated Join Distances between ALS Kerb Candidates for Cross Sections 11, 22 and 37 after Curve fitting to their equivalents on the Curve Fitted Ground Truth Data as an Accuracy Indicator of the Method.

As can be seen this analysis (Table 4.2) shows a lower RMS value than the first comparison (Table 4.1). This is as expected as the kerb detected road segments in the first analysis are determined by the search template spacing of 1m. Therefore any changes of orientation will be in 1m steps. A curve fitted to this data has a smoothing effect. Rather than using three cross sections a final analysis was conducted using forty cross sections to check for consistency in the RMSE values. As can be seen (Table 4.3) over a road extent of 40m there was an improvement in the RMSE values.

| C/No | Surveyed Kerb (Left Side) E | N | ALS Kerb Candidate (Left Side) E | N | Difference(m) | Surveyed Kerb (Right Side) E | N | ALS Kerb Candidate (Right Side) E | N | Difference(m) |
|---|---|---|---|---|---|---|---|---|---|---|
| 1 | 694988.1 | 5893836.7 | 694988.2 | 5893836.7 | 0.1 | 694997.6 | 5893841.3 | 694997.2 | 5893841.1 | 0.4 |
| 2 | 694987.8 | 5893837.6 | 694987.9 | 5893837.6 | 0.1 | 694997.2 | 5893842.2 | 694996.8 | 5893842.1 | 0.4 |
| 3 | 694987.3 | 5893838.5 | 694987.5 | 5893838.6 | 0.1 | 694996.8 | 5893843.1 | 694996.5 | 5893843.0 | 0.3 |
| 4 | 694987.0 | 5893839.4 | 694987.1 | 5893839.5 | 0.2 | 694996.4 | 5893844.1 | 694996.1 | 5893843.9 | 0.3 |
| 5 | 694986.6 | 5893840.4 | 694986.7 | 5893840.4 | 0.2 | 694996.0 | 5893845.0 | 694995.7 | 5893844.8 | 0.3 |
| 6 | 694986.2 | 5893841.3 | 694986.4 | 5893841.4 | 0.2 | 694995.6 | 5893845.9 | 694995.3 | 5893845.8 | 0.3 |
| 7 | 694985.8 | 5893842.2 | 694986.0 | 5893842.3 | 0.2 | 694995.2 | 5893846.8 | 694995.0 | 5893846.7 | 0.3 |
| 8 | 694985.4 | 5893843.1 | 694985.6 | 5893843.2 | 0.2 | 694994.8 | 5893847.7 | 694994.6 | 5893847.6 | 0.3 |
| 9 | 694985.0 | 5893844.0 | 694985.2 | 5893844.2 | 0.2 | 694994.4 | 5893848.7 | 694994.2 | 5893848.6 | 0.2 |
| 10 | 694984.6 | 5893845.0 | 694984.9 | 5893845.1 | 0.3 | 694994.0 | 5893849.6 | 694993.8 | 5893849.5 | 0.2 |
| 11 | 694984.2 | 5893845.9 | 694984.5 | 5893846.0 | 0.3 | 694993.6 | 5893850.5 | 694993.5 | 5893850.4 | 0.2 |
| 12 | 694983.8 | 5893846.8 | 694984.1 | 5893846.9 | 0.3 | 694993.2 | 5893851.4 | 694993.1 | 5893851.3 | 0.2 |
| 13 | 694983.4 | 5893847.7 | 694983.7 | 5893847.9 | 0.3 | 694992.9 | 5893852.4 | 694992.7 | 5893852.3 | 0.2 |
| 14 | 694983.1 | 5893848.7 | 694983.4 | 5893848.8 | 0.3 | 694992.5 | 5893853.3 | 694992.3 | 5893853.2 | 0.1 |
| 15 | 694982.7 | 5893849.6 | 694983.0 | 5893849.7 | 0.4 | 694992.1 | 5893854.2 | 694992.0 | 5893854.1 | 0.1 |
| 16 | 694982.3 | 5893850.5 | 694982.6 | 5893850.7 | 0.4 | 694991.7 | 5893855.1 | 694991.6 | 5893855.1 | 0.1 |
| 17 | 694981.9 | 5893851.4 | 694982.2 | 5893851.6 | 0.4 | 694991.2 | 5893856.0 | 694991.2 | 5893856.0 | 0.0 |
| 18 | 694981.5 | 5893852.3 | 694981.9 | 5893852.5 | 0.4 | 694990.9 | 5893857.0 | 694990.8 | 5893856.9 | 0.1 |
| 19 | 694981.1 | 5893853.3 | 694981.5 | 5893853.5 | 0.4 | 694990.5 | 5893857.9 | 694990.5 | 5893857.9 | 0.0 |
| 20 | 694980.7 | 5893854.2 | 694981.1 | 5893854.4 | 0.5 | 694990.1 | 5893858.8 | 694990.1 | 5893858.8 | 0.0 |
| 21 | 694980.3 | 5893855.1 | 694980.7 | 5893855.3 | 0.5 | 694989.7 | 5893859.7 | 694989.7 | 5893859.7 | 0.0 |
| 22 | 694979.9 | 5893856.0 | 694980.4 | 5893856.2 | 0.5 | 694989.2 | 5893860.8 | 694989.2 | 5893860.8 | 0.0 |
| 23 | 694979.5 | 5893856.9 | 694980.0 | 5893857.2 | 0.5 | 694988.9 | 5893861.6 | 694989.0 | 5893861.6 | 0.0 |
| 24 | 694979.1 | 5893857.9 | 694979.6 | 5893858.1 | 0.5 | 694988.5 | 5893862.5 | 694988.6 | 5893862.5 | 0.1 |
| 25 | 694978.7 | 5893858.8 | 694979.2 | 5893859.0 | 0.5 | 694988.1 | 5893863.4 | 694988.2 | 5893863.4 | 0.1 |
| 26 | 694978.3 | 5893859.7 | 694978.9 | 5893860.0 | 0.6 | 694987.8 | 5893864.3 | 694987.8 | 5893864.4 | 0.1 |
| 27 | 694978.0 | 5893860.6 | 694978.5 | 5893860.9 | 0.6 | 694987.4 | 5893865.2 | 694987.5 | 5893865.3 | 0.1 |
| 28 | 694977.6 | 5893861.6 | 694978.1 | 5893861.8 | 0.6 | 694987.0 | 5893866.2 | 694987.1 | 5893866.2 | 0.1 |
| 29 | 694977.2 | 5893862.5 | 694977.7 | 5893862.7 | 0.6 | 694986.6 | 5893867.1 | 694986.7 | 5893867.2 | 0.1 |
| 30 | 694976.8 | 5893863.4 | 694977.4 | 5893863.7 | 0.6 | 694986.2 | 5893868.0 | 694986.3 | 5893868.1 | 0.2 |
| 31 | 694976.4 | 5893864.3 | 694977.0 | 5893864.6 | 0.7 | 694985.8 | 5893868.9 | 694986.0 | 5893869.0 | 0.2 |
| 32 | 694976.0 | 5893865.2 | 694976.6 | 5893865.5 | 0.7 | 694985.4 | 5893869.9 | 694985.6 | 5893869.9 | 0.2 |
| 33 | 694975.6 | 5893866.2 | 694976.2 | 5893866.5 | 0.7 | 694985.0 | 5893870.8 | 694985.2 | 5893870.9 | 0.2 |
| 34 | 694975.2 | 5893867.1 | 694975.9 | 5893867.4 | 0.7 | 694984.6 | 5893871.7 | 694984.8 | 5893871.8 | 0.2 |
| 35 | 694974.8 | 5893868.0 | 694975.5 | 5893868.3 | 0.7 | 694984.2 | 5893872.6 | 694984.5 | 5893872.7 | 0.3 |
| 36 | 694974.4 | 5893868.9 | 694975.1 | 5893869.3 | 0.7 | 694983.8 | 5893873.5 | 694984.1 | 5893873.7 | 0.3 |
| 37 | 694974.0 | 5893869.8 | 694974.7 | 5893870.2 | 0.8 | 694983.4 | 5893874.5 | 694983.7 | 5893874.6 | 0.3 |
| 38 | 694973.7 | 5893870.8 | 694974.4 | 5893871.1 | 0.8 | 694983.0 | 5893875.4 | 694983.3 | 5893875.5 | 0.3 |
| 39 | 694973.3 | 5893871.7 | 694974.0 | 5893872.1 | 0.8 | 694982.7 | 5893876.3 | 694983.0 | 5893876.5 | 0.3 |
| 40 | 694972.9 | 5893872.6 | 694973.6 | 5893873.0 | 0.8 | 694982.3 | 5893877.2 | 694982.6 | 5893877.4 | 0.4 |
| | | | RMSE= | | 0.5 | | | RMSE= | | 0.2 |

Table 4.3 Calculated Join Distances between ALS Kerb Candidates for Cross Sections 1 to 40 after Curve fitting to their equivalents on the Curve Fitted Ground Truth Data as an Accuracy Indicator of the Method.

108

In the case of this study it has been shown that it was possible to reliably detect road kerbs by using Interpolated Heights from triangulated ALS with an RMS value better than 1m.

Referring to Figure 4.4 it can be clearly seen that for the right side of the road the ALS kerb candidates show a closer fit to the ground truth than the left side. The gradual divergence of the left side from the ground truth can also be seen as the road length increases. A question that arises, and as yet has not been investigated, what would be the outcome if the search template spacing were decreased? The first outcome envisaged could be a failure with the Least Squares fit to the increased data set. The problems encountered with Road 2 may reoccur. The best statistical fit, using the additional road width parameter, may occur off the obvious road surface. It does not seem possible that increasing the frequency of height interpolation would lead to a better determination of exactly where the kerb was detected within the one metre segment that shows the height change. An additional ALS point within the one-meter segment would be required. Therefore it would appear that if the search template spacing were decreased it would need to be matched with higher density ALS data. This should increase the accuracy of the kerb detection providing the Least Squares fit using the additional road width parameter functions correctly on the enlarged data set.
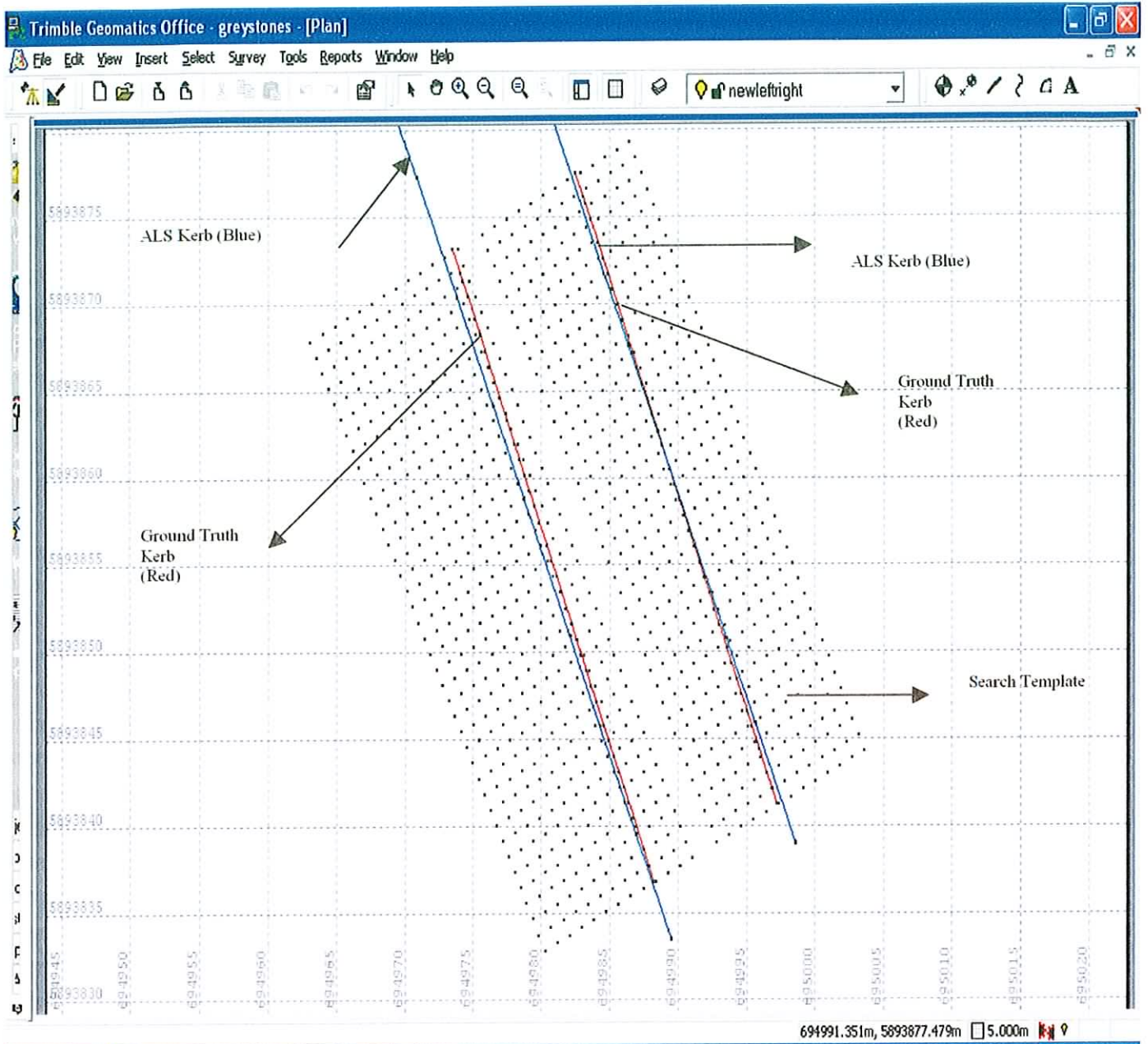
Figure: 4.4 Curve Fitted ALS Kerb Candidate Coordinates compared with Curve Fitted Ground Truth Coordinates

The method developed has produced promising results but they must be judged in the context of the following limitations:

- The test areas chosen were in a semi- rural environment. Complex urban areas would be much more challenging and no work has been done in such areas as of yet. The method is totally reliant on detecting a boundary, a footpath or a kerb, that is capable of displaying a breakline between it and the homogenous road surface. On the roads tested the kerb height was approximately 0.2m. In situations where the kerb height is closer to the height differences between each point on the road surface the method would give poor results.

- Both test areas were such that changes in the topography on either side of the road surface immediately ruled out such areas as potential roads. Possible problems could be foreseen in areas that had a combination of small kerbs and very level terrain on either side of the road. The test areas were also free from obstructions. No buildings fronted the roads and there were no overhanging trees to obscure the road or the road boundary regions. If trees or buildings were present, Terrascan would filter these from the point cloud to arrive at ground points. The Matlab Delaunay triangulation of the resulting points would lead to an irregular TIN, making it difficult to analyse cross sections taken from it. A compromise would be to grid the ALS ground points but this would lead to some interpolation of the data and has not been tried.

- The method has only been used on straight sections of road. No tests have been carried out in regions where the road exhibits large changes in direction.

- In its present state the method will not work on dual carriage way roads unless it was possible to separate each road and process them individually. A further

problem with these types of roads is that the central divide between them may be easy to detect, but in many instances the outer left and right margins are not delimitated by a hard feature, but simply merge into the adjoining terrain.

- The need for the additional road width parameter could be considered a slight flaw. Some possibilities as to how this might be dispensed with were mentioned in Section 3.12. (detecting peaks in the height difference cross sections). This will be investigated in the future, as it would constitute a major improvement to the method.

- The ALS data used for this thesis had a point spacing of 2 per square metre. It would not be possible to say if a kerb detection to an accuracy of 1m could be achieved with lower resolution data. The converse of this may also not be true, that by using higher resolution data the result would be improved. A Linear Least Squares regression to a densified data set may prove problematic. Much more research is required using a range of resolutions and various template sizes before a general accuracy statement can be made.

- A single flight strip of ALS data was used and the roads were deliberately chosen so that they were not close to the edges of the strip. If a block of ALS data were to be used it would be necessary to establish that the strips had been correctly matched.

- A priority for future work will be to acquire ground truth for Road 2 and verify the result of the kerb detection from the ALS data. A successful result

would be a major step forward. This would be an independent check and dispel any fear that having ground truth in the first instance unduly influenced the method developed for Road 1.

- The variable of the return intensity magnitudes found in the data may have been due to the scan angle and atmospheric conditions. A further factor may have been the "speckle effect" whereby certain surface areas cause scattering of the laser beam. The recorded return echo then becomes the vector sum of echoes received from a large number of points. The range to the target also has an influence on the return intensity value, the relationship between them is governed by the formula:

$$P_r = \frac{P_t D_r^2}{R^4 \beta_t^2 \Omega} \rho A_s$$

Where:

$P_r$ = Received power

$P_t$ = Transmitted power

$D_r$ = Receiver aperture size

$\beta_t$ = beam divergence

$\Omega$ = The bi-directional properties of scattering

$A_s$ = The receiving area of the scatterer

$\rho$ = reflectivity of the target surface

$R$ = Range

The recorded intensity for homogenous targets filling the footprint is proportional to $R^2$, for linear objects such as power cables it is proportional to $R^3$, and for individual large scattering targets $R^4$ (Ahokas et al, 2006).

- The factors outlined above may account for some of the fluctuation in the intensity data. However, due to the large size of the difference in the intensity returns from similar surfaces, taken from the same flight strip at the same flying altitude, it does not explain them. The most probable reason for the large differences is that the data used was had no intensity calibration tests carried out on it.

# 5. Conclusions and Recommendations

From a statistical point of view the sample size of a 40m road length with 90 ground truth points is too small to enable the method to be tested in a reliable way

With the qualification that the method developed does require more testing a successful verifiable result has been achieved on Road 1. From the results achieved the following can be concluded:

- Of all the cross-section types developed the most useful information was gained from cross-sections based on interpolated heights from the triangulated ALS ground points. By applying a linear Least Squares fit to these cross-sections, combined with the additional parameter of the road width, it was possible to detect a height change indicative of a kerb. The planimetric accuracy of the detected kerbs was at least equal to the density of the ALS data used.

- The research conducted on the ALS return intensities showed that the most useful cross-sections were those based on the standard deviation of the return intensities of the vertices of triangles in the triangulated ALS ground points, and cross-sections based on the Nearest Neighbour Intensity algorithm. The results for Road 1 showed that it was possible to detect road markings.

One criticism that can be made is the lack of an automatic quality check on the ALS kerb candidates detected. Creating a graph using the kerb candidate coordinates should show a regular pattern along the road region, but if the process is to be as automated as possible, this is not a practical solution. To resolve this it would be

preferable to introduce some mathematical function that would check the orientation of each cross section longitudinally for both sides of the road. Large changes in orientation between cross sections would immediately indicate a failure.

With future work on the return intensities a more robust process could be developed by the integration of intensity and height. In the absence of detectable height variation, intensity could be used to give an alternative solution. This solution would be less accurate but may none the less be useful. A further area to be explored is to see if the orientation of the road under investigation, when compared with the scanning direction of the aircraft, has an influence on the accuracy of the kerb detection. If possible it would also be beneficial if the scan angle for a particular road section could be determined. For example, were the good results on Road 1 achieved because the road was scanned by the laser pointing in a nadir direction.

In the context of the original scenario of being an aid to accessing the quality of an existing database of vector mapping, the method has demonstrated some promise within the limitations expressed. On a practical front it may be possible to incorporate it as a small module into a general ALS processing package.

The fact that many airborne laser scanning systems can also provide photography and video footage along with the coordinated point cloud would suggest that the integration of the data provided and not the sole use of the point cloud, could provide the optimal solution. This idea of fusion and integration of data has been a constant theme in the literature reviewed for this thesis. Of necessity this would require some image analysis that was beyond the scope of the work undertaken, but future research

could look at the possibility of using some image analysis to improve the method developed.

The FLI-MAP laser system from Fugro captures ALS data, still photography, video streams and infra-red imagery. The system uses a helicopter platform and can provide ALS data with a point density of over 20 points per square metre. Two fixed focus digital video cameras, one facing in the nadir direction and the other facing forward, collect video data in MPEG format. Alongside these two video cameras, two digital still cameras are mounted to take images at one-second intervals in the same directions. A further two digital infrared cameras record thermal data in MPEG format. Using the FLIP7 software developed by Fugro all data sets can be merged. The software provides full computer aided design capability (CAD), which sits on top of the ALS data. It also offers the capability of coordinating the video images with the ALS data to allow a full multimedia presentation of the surveyed area.

In the scenario of extracting a road centre line, it would be possible to trace a line along an image of the road and extract the ALS data for that region. Equally it would be possible to use the imagery with the ALS data to extract any feature and model it based on its 3D coordinates. This is fine for one-off projects, but because of the user interaction, extraction of features over a large area would be costly.

# References

Ahokas, E., Kaasalainen, S., Hyyppa, J., Suomalainen, J.,(2006) 'Calibration of the Optech ALTM 3100 Laser Scanner Intensity Data using Brightness Targets', *The International Archives of the Photogrammetry, Remote Sensing and Spatial Information Sciences*, Vol 34, Part XXX.

Alharthy, A., Bethel, J., Mikhail, E.M., (2004) 'Analysis And Accuracy Assessment Of Airborne Laserscanning System, Proceedings *ISPRS Congress Commission III*, 12-23 July, Istanbul.

Axelsson, P., (1999) 'Processing of Laser Scanner Data Algorithms and Applications', *ISPRS Journal of Photogrammetry and Remote Sensing*, Vol 54, pp. 138-147.

Baltsavias, E. P., (1999) 'A comparison between Photogrammetry and Laser Scanning', *ISPRS Journal of Photogrammetry and Remote Sensing*, Vol 54, pp. 83-94.

Behan, A., Maas, H-G., Vosselman, G.,(2000) 'Steps Towards Quality Improvement of Airborne Laser Scanner Data', Proceedings *26th Annual Conference of the Remote Sensing Society*, 12-14 September 2000, Leicester, UK.

Biran, A., Breiner, M., (2002) MATLAB 6 for Engineers, Prentice Hall, Pearson Education Ltd, Harlow, Essex, UK.

Brenner, C., (2003) 'Building Reconstruction from Laser Scanning and Images', Proceedings *ITC Workshop on Data Quality in Earth Observation Techniques*, November 2003, Enschede, The Netherlands.

Clode, S., Kootsookos, P., Rottensteiner, F., (2004) 'The Automatic Extraction of Roads from Lidar Data', Working Group III/3, *International Archives of the*

*Photogrammetry, Remote Sensing, and Spatial Information Sciences, Vol. XXXV, Part B3, pp. 231-236,* Istanbul, Turkey.

Hatger, C., Brenner, C., (2003) 'Extraction of Road Geometry Parameters from Laser Scanning and Existing Databases', Proceedings *ISPRS Workshop 3-D Reconstruction from Laser Scanner and InSAR Data,* 8-10 October 2003, Dresden, Germany

Haala, N., Brenner, C., (1999) 'Extraction of Buildings and Trees in Urban Environments', *ISPRS Journal of Photogrammetry and Remote Sensing,* Vol 54, pp. 130-137.

Hofmann, A.D., Maas, H-G., Streilein, A., (2002) 'Knowledge Based Building Detection Based on Laser Scanner Data and Topographic Map Information', Proceedings, *ISPRS Symposium Photogrammetric Computer Vision,* 9-13 Sept, Graz, Austria.

Hoffmann, A.D., Maas, H-G., Streilein, A., (2003) 'Derivation Of Roof Types by Cluster Analysis in Parameter Spaces of Airborne Laserscanner Point Clouds', Proceesings, *ISPRS Workshop 3-D Reconstruction from Laser Scanner and InSAR Data,* 8-10 October 2003, Dresden, Germany.

Hu, X., Tao, C.V., Hu, Y., (2003) 'Automatic Road Extraction from Dense Urban Area by Integrated Processing of High Resolution Imagery and Lidar Data', Proceedings *ISPRS Workshop 3-D Reconstruction from Laser Scanner and InSAR Data,* 8-10 October 2003, Dresden, Germany.

Katzebeisser, R., (2003a) 'About The Calibration of Lidar Sensors', ISPRS Workshop, *3-D Reconstruction from Airborne Laser-Scanner and InSAR,* 8-10 October 2003, Dresden, Germany.

Katzenbeisser, R., (2003b) 'Airborne Laser Scanning a Comparison with Terrestrial Surveying and Photogrammetry', Technical Note *TopoSys GmbH.*

Lemmens, Mathias.J.P.M., (1997) 'Accurate Height Information from Airborne Laser-Altimetry', *Proceedings of the 1997 International Geoscience and Remote Sensing Symposium*

Lohani, B., Mason, D. C., (2001) 'Application of Airborne Scanning Laser Altimetry to the Study of Tidal Channel Geomorphology', *ISPRS Journal of Photogrammetry and Remote Sensing*, Vol 56, pp. 100-120.

Maas, H-G., (2002) ' Planimetric and Height Accuracy of Airborne Laserscanner Data: User Requirements and System Performance', Proceedings 49. *Photogrammetric Week (Ed. D. Fritsch), Wichmann Verlag*, pp. 117-12

Maas, H-G., Vosselman, G., (1999) 'Two Algorithms for Extracting Building Models from Raw Laser Altimetry Data', *ISPRS Journal of Photogrammetry & Remote Sensing*, Vol 54, pp. 153-163

Morgan, M., Habib, A., (2002) 'Interpolation of Lidar Data and Automatic Building Extraction', Proceedings *ACSM-ASPRS Annual Conference 2002*.

Morin, K. W., (2002) 'Calibration of Airborne Laser Scanners', *Thesis for Degree of Master of Science*, Nov 2002, University of Calgary, Alberta, Canada

Mostafa, M., Hutton, J., Ried, B., Hill, R., (2001) 'GPS/IMU Products the Applanix Approach', *Photogrammetric Week 2001* pp. 63-83.

Rottensteiner, F., (2002) 'Automatic Extraction of Buildings From Lidar and Aerial Images', *Symposium on Geospatial Theory, Processing and Applications*, Ottawa, Canada.

Toth, C.K., Grejner-Brzezinska, D.A, (2000) 'Complimentarity of Lidar and Stereo Imagery For Enhanced Surface Extraction', *International Archives of Photogrammetry and Remote Sensing, Amsterdam*, Vol XXX111, Part B3.

Toth, C.K, Grejner-Brezezinska, D.A., Moafipoor, S., (2004) 'Precise Vehicle Topology and Road Surface Modeling Derived from Lidar Data', ION 60th Annual Meeting, 7-9 June 2004, Dayton, Ohio, U.S.A.

Vosselman, G., Maas, H-G., (2001) 'Adjustment and Filtering of Raw Laser Altimetry Data', Proceedings *OEEPE workshop on Airborne Laserscanning and Interferometric SAR for Detailed Digital Elevation Models,* 1-3 March 2001, Stockholm, Sweden.

Wehr, A., Lohr, U., (1999) 'Airborne Laser Scanning an Introduction and Overview', *ISPRS Journal of Photogrammetry and Remote Sensing,* Vol 54, pp. 68-82.

Zhan, Q., Molenaar, M., Tempfli, K., (2005) 'Building Extraction from Laser Data By Reasoning on Image Segments in Elevation Slices', Proceedings, *ISPRS Laser Scanning 2005,* 12-14 September, Enschede, Netherlands.

# Appendix A

<u>MATLAB</u>

Matlab (MATrix LABorotory) is a widely used scientific and technical programming language. The main attraction for using it in this project were some of the built in functions that lent themselves very well to the some of the key areas in creating the cross sections. Most notable were the following.

<u>Delaunay Function</u>

It was necessary to structure the scattered ALS point cloud before cross sections could be taken from it. The inputs to the routine are a list of the 3D coordinates on which to base the triangulation. The output is a very good visual of the surface, but unfortunately it does not automatically coordinate each triangle. What it does provide is a set of indexes for each triangle vertex into the original coordinate file inputted. To analyse the triangulation it is essential to have the coordinates of all three vertices so a routine was developed to do this (avectorisetricoordinates.m)

<u>Tsearch Function</u>

Given the coordinates of a point this function finds its bounding triangle in the Delaunay triangulation. It requires the output from the Delaunay, the coordinates on which the Delaunay is based, and the coordinates of the point. The result is an index into the output from the Delaunay and needs to be used in conjunction with the output from *avectorisetricoordinates.m* to get the coordinates of the triangle. Some problems were encountered with this program and an alternative was sourced via the Internet. The program *tsearchsafe.m* by Dr Charles R. Denham, Zydeco, would appear to be more reliable. This program can be downloaded and stored in the directory C:\matlab\toolbox\matlab\polyfun it can then be accessed like any other Matlab function

(http://woodshole.er.usgs.gov/staffpages/cdenham/public_html/snackbar/snackbar.html)

## Find Function

This function is used to find a particular value or a range of values in an array. It is used for instance to create the triangle groups. The coordinates of all the Delaunay triangles is held in a matrix, using the find function this matrix is searched for coordinates that match any of the vertices of the seed triangle. Matches are extracted to form a small group of triangles, a surface patch.

## Diff Function

This function is used to get the height difference between adjacent points in each of the cross sections.

## Polyfit and Polyval Function

These functions were used together to perform the Least Squares regression. Taking for example a second order polynomial (Equation 1) fitted to pairs of data $(x_i, y_i)$

$$y = c_1 x^2 + c_2 x + c_3 \qquad \text{(Equation 1)}$$

the task is to find the three coefficients that minimise the sum of the squared errors (Equation 2)

$$e = \sum_{i=1}^{m} (y_i - c_1 x_i^2 - c_2 x_i - c3)^2 \qquad \text{(Equation 2)}$$

The coefficients "$c$" can be found using the matrix operation:

$$C = (A'A)^{-1}A'Y \qquad \text{(Equation 3)}$$

Matlab solves this matrix equation using the polyfit function. It requires three inputs, an array of independent variables, dependant variables and an integer value that signifies the degree of curve to be fitted (e.g. a 2= second order polynomial, and a 1= linear). The result of the polyfit function is row containing the values of the

123

coefficients in descending orders of the powers of $x$. To solve for $y$ (Equation 1) the polyval function is used. It requires two inputs, the array of coefficients from polyfit, and the array of independent variable values (Biran & Breiner, 2002)

MATLAB PROGRAMS

For anyone wishing to use the Matlab programs there are a few complications with the data file inputs to some of the processes developed. These mainly stem from timing differences in receiving the Lidar data and lack of expertise in programming and in using Matlab. The data available at the start of the project had no return intensities. Programming began with this data but provision should have been made in the code for the eventual arrival of the intensity data. The net result is that, although some data files should be common to programs, a certain amount of duplication was required to overcome the problem. It is important that the processing sequence below is accurately followed to insure that essential files are created.

- The Lidar point cloud (with X,Y,Z and Intensity columns) is classified using Terrascan and the point class "Ground" is saved as an X,Y,Z,I tab delimited text file.

- The ground points file created above is reloaded into Terrascan and a region in the vicinity of the road is selected using the Fence Tool.

- The points within the fence must now be saved as an X,Y,Z tab delimited text file named "gridback.txt", they must also be saved as an X,Y,Z,I tab delimited text file named "gstonesiintensity.txt"

- Run the program "adodelaunay.m" this program performs a Delaunay Triangulation and stores the result in "triangles2.txt". The result is an index into the coordinate file on which the triangulation is based (gridback.txt)

- Run "avectorisetricoordinates.m". This coordinates all the triangle vertices in the triangulation. The output is stored in "tricoordinates.txt"

- Run "trapzerointjan.m". The purpose of this program is to scan through the file "gstonesiintensity.txt (created above in Terrascan) and replace any zero value with a very small value (.001). A zero intensity value caused some subsequent programs to crash so this was the easiest way to resolve it. The output is stored in "gstonesiintensity2.txt".

- Run program "ainserttriint.m" this creates a file "triint.txt" which is necessary for any programs using return intensities.

Lack of time prevented the rationalising and amending of programs to dispense with the above. A schematic of the processing is included at the end of this Appendix that hopefully may prove useful.

Many of the programs developed follow a strategy of processing the centre line then process left of the centre line then right of centre line. This enabled easy troubleshooting of the algorithms. The downside however was that each processing stage created output files that did become daunting, particularly when collecting and analysing results. It also meant that the final results would ultimately be held in three separate locations, centre line result, left of centre line and right of centre line. As all output files were stored as text files, much use was made of Microsoft Excel to combine the three areas, as a text file for input into other algorithms, and as an Excel file to produce cross section graphs and further analysis.

Program 1 (Gradient Cross Sections for Triangle Groups)

Program1 contains many individual programs that were simply strung together to make running them easier. This program calculates the gradient for the group triangles and the centre line group triangles. The inputs to the program are:

- The start and end coordinates of the centre line section.
- The interval distance (in metres) to be taken along the centre line section.

- The interval distance (in metres) to be taken left and right of the centre line.
- The number of intervals left and right of the centre line

The total number of cross sections generated is equal to the length of the centre line section divided by the interval distance along the section. These inputs define the Search Template.

Outputs from the program are:

- *crossection"n".txt* ("n" is an increasing number starting at 1 and signifies the cross section number). There is one file for each cross section that contains the points left and right of the centre, and does not contain the centre line point

- *clinecrossection"n".txt.* Contains the centre line points. This is one file and "n" will be the total number of cross sections. If for example the number of cross sections generated was thirteen the file will be named *"clinecrossection13.txt"*

Open *"clinecrossection.txt"* in Excel . The file will have six columns and the number of rows will be equal to the number of cross sections.

Open the *"crossection1.txt"* this file will also have six columns and the number of rows will be equal to the number of intervals taken across the road.

The first entry in *clinecrossection.txt* must now be copied and inserted into the middle of *crossection1.txt.* This now represents one cross section where the first row is the outer most left point and the last row is the outermost right point of the cross section. This text file can now be saved as an Excel file. The operation is repeated until each centre line point has been inserted into its correct cross section. Each column contains the following information:

| Mean Area Of Triangle Groups | Mean Side Length | Standard Deviation of Area | Standard Deviation of Side Lengths | Mean Gradient of Triangle Groups | Standard Deviation of Gradient |
|---|---|---|---|---|---|

The percentage mean gradient and standard deviations were calculated in Excel as an additional two columns. It must be stressed that the files mentioned above are the overall result but many other files will be created by this program, some are used for

other algorithms the others store interim results. The two last columns (Mean Gradient and Gradient Standard Deviation) are the important ones, the others can be omitted.

## Program 2

As stated above Program 1 creates some files used by other algorithms, so rather than running this, program Program 2 offers a shortcut to creating these essential files, without the necessity of creating many of the data files. Program 2 is made up of blocks of code taken from Program 1. There is no need to state the output files, but suffice it to say that if Program 1 is not executed then it is necessary to run Program 2. The user inputs will be the same as for Program 1.

## Program 3 (Seed Triangle Gradient and Intensity Cross Sections)

No user inputs are required for this program.

Outputs from the program are:

Gradient Cross Sections

- *crossectionseed"n".txt* ("n" is an increasing number starting at 1 and signifies the cross section number). There is one file for each cross section that contains the points left and right of the centre, and does not contain the centre line point

- *clineseedcrossection"n".txt*. Contains the centre line points. This is one file and "n" will be the total number of cross sections. If for example the number of cross sections generated was thirteen the file will be named *"clineseedcrossection13.txt"*

The centre line point for each cross section must be inserted as per the instructions for Program 1 using Excel. All columns bar the last one on the right (column "E" in Excel) can be ignored. The percentage gradient can calculated in Excel.

127

Intensity Cross Sections

- *intcrossectionseeds"n".txt* ("n" is an increasing number starting at 1 and signifies the cross section number). There is one file for each cross section that contains the points left and right of the centre, and does not contain the centre line point

- *clineintseedssection"n".txt.* Contains the centre line points. There is one file for each point along the centre line. The numbering scheme is as above.

Here again the centre line point has to be inserted into the centre of each cross section. In this case it is slightly different in so far as the centre line points are not in one file but individual files. There will therefore be the same number of *"intcrossectionseeds.txt"* files as there are *"clineintseedssection.txt"* files. Both sets of files will have two columns. The first column is the Mean Intensity and the second the Intensity Standard Deviation.

## Program 4 (Intensity Cross Sections for Triangle Groups)

No user inputs required. This program produced Intensity cross sections for groups of triangles. The outputs from this program are:

- *intcrossection"n".txt* ("n" is an increasing number starting at 1 and signifies the cross section number). There is one file for each cross section that contains the points left and right of the centre, and does not contain the centre line point

- *statsresultclineint"n".txt.* Contains the centre line points. There is one file for each point along the centre line. The numbering scheme is as above.

Inserting the centre line is the same as Program 3. Each file will have two columns. Mean Intensity and Intensity standard Deviation.

128

## Programs "ainjectheight.m" and "ainjectheightcline.m"

These two programs are used to interpolate the heights for each point in the search template from the Lidar TIN in order to generate height cross sections. No user inputs are required. The output files from these programs are:

*"hleftcoords.txt"*

*"hrightcoords.txt"*

*"clineheights.txt"*

These three text files must be combined in Excel in the following manner:

- Open *"hleftcoords.txt"* in Excel

- Open *"clineheights.txt"* in Excel

- Copy the single row of file *"clineheights.txt"* and paste it as the last entry in *"hleftcoords.txt"*

- Open *"hrightcoords.txt"* select all the entries and copy them into the space in *"hleftcoords.txt."* immediately after the position where *"clineheights.txt"* was pasted

Save this file as an Excel file so that cross section graphs can be created and also save the combined files as:

- *"heightinject.txt"* a tab delimited text file that is used for other programs.

## Program "heightdifference.m"

This is used to calculate the height difference between adjacent points in the search template. The output from this program is:

- *"hdiff.txt"*

This file can be used as is in Excel to create Height Difference graphs.


Program "linearfittohdiff.m"


This program is used to fit a Least Squares Linear Regression best fit to the Height Difference cross sections. The road width is required as an input. The output from this program is a file containing the segments in the cross section where the best fit occurred:

- *"bestfit.txt"*


Program "searchtemplatecoordshdiff.m"


No user inputs required. The above program must be executed first as *"bestfit.txt"* is required. This program coordinates the best fit segments from the search template. The coordinates are stores in:

- *"bestfitcoords.txt"*


Program "linearfittoheights.m"


This program fits a Least Squares Linear Regression to the Interpolated Height Cross Sections. The road width is required as an input. The text file "heightinject.txt" must have been created before this program is executed (see above) The output from this program is a file containing the segments in the cross section where the best fit occurred:

- "bestfitheight.txt"

Program "searchtemplatecoordsheight.m"

No user inputs required. The above program must be executed first as *"bestfitheight.txt"* is required. This program coordinates the best fit segments from the search template. The coordinates are stores in:

- *"bestfitcoordsheight.txt"*

Program "ainjectintensity.m" and "ainjectclineintensity.m"

These two programs are used to get an Intensity value for each of the search template coordinates and the centre line. They are very similar to the programs used to interpolate the heights so some of the variable names may be misleading as they are simply the code used in the interpolated height program with some minor changes.

The procedure for combining the text files is exactly the same as for the interpolated height algorithms ("ainjectheight.m" and "ainjectheightcline.m" above )

The output files are:

- *"intinjectleft.txt"*
- *"intinjectright.txt"*
- *"intinjectcline.txt"*

Combine files using Excel and save as an .xls file for cross section graphs. Also save as a text file:

- *"injectint.txt"*

Program "averageintensity.m"

This program uses the text file from the above program ("injectint.txt" ) and also requires the user to input the road width. It calculates the average intensity value and outputs the segments where the lowest average value occurred. The output from the program is held in:

- "averageint.txt"

Program "getcline.m"

No user inputs. This program fits a curve to the left and right coordinates from the above program, calculates a centre line between them, and shows the original centre line for comparison (Matlab visual).

Programs "eastnorthlefttemplate.m and "eastnorthrighttemplate.m"

The Search Template coordinates were in a structure that proved difficult to plot. In the latter stages of the thesis it was necessary to use the package Trimble Geomatics Office and there was a need to see the positional relationship of the search template to the ground truth. These programs organise the data so that it is easily plotted. The data is collected into two columns, Easting and Northing coordinates, for left and right sides of the centre line. The centre line is not included, this makes it identifiable as the large gap between the two when a visual is created. The output is in the following files:

- "eastnorthlefttemplate.txt"
- "eastnorthrighttemplate.txt"

Program "boxnew4.m"

This program was not used in the thesis but may prove useful to further automate the method developed. It is essentially a means of reducing the ground points to an area of interest based on the coordinates of the assumed centre line. By using this there is no need to use the fence tool in TerraScan. The user inputs required are

- Start coordinates of centre line
- End coordinates of centre line
- Threshold value in metres

Using the bearing of the start and end coordinates and the threshold value a box is constructed around the road centre line. The coordinates of the corners of this box are used to determine coordinates that qualify as being inside. The program code

132

currently expects the ALS ground points to be in a file named *lidarscross.txt* and the output from the process is stored in *road2005.txt*. These names should be changed to suite.

**Initial Processing Sequence**
These programs must be executed first, as they provide essential files for all other algorithms.

```
                    ┌─────────────────────┐
                    │ Lidar Ground Points │
                    └─────────────────────┘
                               │
                               ▼
                    ┌─────────────────────┐
                    │ Use Terrascan to Fence │
                    │ off Required Area in the │
                    │ Vicinity of the Road │
                    └─────────────────────┘
                      ╱                   ╲
                     ▼                     ▼
    ┌──────────────────────┐      ┌──────────────────────┐
    │ Save Points as an X.Y.Z │   │ Save Points as an      │
    │ tab delimited text file │   │ X.Y.Z.I tab delimited  │
    │ named                  │    │ text file named        │
    │                        │    │                        │
    │ "gridback.txt"         │    │ "gstonesiintensity.txt" │
    └──────────────────────┘      └──────────────────────┘
                   ╲                      ╱
                    ▼                    ▼
```

| Run Program | Output File |
|---|---|
| adodelaunay.m | → triangles2.txt |

| Run Program | Output File |
|---|---|
| avectorisetricoordinates.m | → tricoordinates.txt |

| Run Program | Output File |
|---|---|
| trapzerointjan.m | → gstonesiintensity2.txt |

| Run Program | Output File |
|---|---|
| ainserttriint.m | → triint.txt |

134

# Appendix B

Notes on Least Squares Best Fit Algorithm

The following is an explanation of how the least squares regression is performed and is common to all algorithms that use a least squares best fit to data. Matlab is very efficient at manipulating data stored in a matrix or tabular format. To exploit this feature the data is organised as far as possible in matrices, then these are used in matrix operations to achieve the final result. The algorithm only uses one input, other than the data file to be processed, the road width. In essence what the program must achieve is to automatically process each cross section in turn, finding the intervals in each cross section that achieves the best least squares fit to a string of data equal to the inputted road width.

The solution detailed below may appear overly complex but it does reduce the amount programming and interim storage of data that would otherwise be required if each cross section were processed individually. Each iteration of the routine equals one cross section processed. Three matrices are created all having the same dimensions

The program code for the algorithm *"linearfittoheights.m"* should be viewed in conjunction with the following paragraphs and figures, or any program that solves a least squares regression

Following the heading "Fill Array with Distance Intervals" are eight lines of code that build a matrix called *"a"* based on the input file *"heightinject.txt"*. The input file is an array that contains the Interpolated Height cross sections for all the points in the search template. Table AB.1 is an example of an *"a"* matrix for one iteration of the routine. The diagonals represent distance intervals across the cross section. For clarity an additional column titled *"From"* and an extra row *"To"* have been inserted, but it must be remembered that they are not part of the actual matrix, this consists only of the rows and columns in italics.

135

The "From" row begins with the first one metre interval and progress towards the centre of the cross section at fifteen metres. The "To" columns work from the end of the cross section at thirty metres back towards the centre. With the data structured in this manner the metre intervals for any road width can determined using their location within this matrix.

| From \ TO | 30 | 29 | 28 | 27 | 26 | 25 | 24 | 23 | 22 | 21 | 20 | 19 | 18 | 17 | 16 |
|---|---|---|---|---|---|---|---|---|---|---|---|---|---|---|---|
| 1 | 29 | 28 | 27 | 26 | 25 | 24 | 23 | 22 | 21 | 20 | 19 | 18 | 17 | 16 | 15 |
| 2 | 28 | 27 | 26 | 25 | 24 | 23 | 22 | 21 | 20 | 19 | 18 | 17 | 16 | 15 | 14 |
| 3 | 27 | 26 | 25 | 24 | 23 | 22 | 21 | 20 | 19 | 18 | 17 | 16 | 15 | 14 | 13 |
| 4 | 26 | 25 | 24 | 23 | 22 | 21 | 20 | 19 | 18 | 17 | 16 | 15 | 14 | 13 | 12 |
| 5 | 25 | 24 | 23 | 22 | 21 | 20 | 19 | 18 | 17 | 16 | 15 | 14 | 13 | 12 | 11 |
| 6 | 24 | 23 | 22 | 21 | 20 | 19 | 18 | 17 | 16 | 15 | 14 | 13 | 12 | 11 | 10 |
| 7 | 23 | 22 | 21 | 20 | 19 | 18 | 17 | 16 | 15 | 14 | 13 | 12 | 11 | 10 | 9 |
| 8 | 22 | 21 | 20 | 19 | 18 | 17 | 16 | 15 | 14 | 13 | 12 | 11 | 10 | 9 | 8 |
| 9 | 21 | 20 | 19 | 18 | 17 | 16 | 15 | 14 | 13 | 12 | 11 | 10 | 9 | 8 | 7 |
| 10 | 20 | 19 | 18 | 17 | 16 | 15 | 14 | 13 | 12 | 11 | 10 | 9 | 8 | 7 | 6 |
| 11 | 19 | 18 | 17 | 16 | 15 | 14 | 13 | 12 | 11 | 10 | 9 | 8 | 7 | 6 | 5 |
| 12 | 18 | 17 | 16 | 15 | 14 | 13 | 12 | 11 | 10 | 9 | 8 | 7 | 6 | 5 | 4 |
| 13 | 17 | 16 | 15 | 14 | 13 | 12 | 11 | 10 | 9 | 8 | 7 | 6 | 5 | 4 | 3 |
| 14 | 16 | 15 | 14 | 13 | 12 | 11 | 10 | 9 | 8 | 7 | 6 | 5 | 4 | 3 | 2 |
| 15 | 15 | 14 | 13 | 12 | 11 | 10 | 9 | 8 | 7 | 6 | 5 | 4 | 3 | 2 | 1 |

Table AB.1 Example of "a" Matrix

For example, if the road width parameter was 26m, the diagonals that contain 26 are located at *From* 4 *TO* 30, *From* 3 *TO* 29 etc.

The second matrix, "rresid", is created by the code following the heading in the code listing "Processing loop Inner" to the third "end" command. The purpose of this part of the program is calculate a least squares best fit (polyfit and polyval commands) to the data that relates to each of the intervals in the "a" matrix. Table AB.2 shows the results of this operation, a matrix of the RMS residual values. If one could imagine the matrix "a" and "rresid" printed on transparent material, overlaying "a" on "rresid" would enable you to get the RMS residual values for each road segment.

136

With the creation of an additional matrix, Matlab can perform this procedure automatically

| From | TO 30 | 29 | 28 | 27 | 26 | 25 | 24 | 23 | 22 | 21 | 20 | 19 | 18 | 17 | 16 |
|---|---|---|---|---|---|---|---|---|---|---|---|---|---|---|---|
| 1 | 1.3567 | 1.3284 | 1.2615 | 1.1369 | 1.012 | 0.98688 | 0.97327 | 0.96385 | 0.95649 | 0.94993 | 0.94158 | 0.92996 | 0.92793 | 0.92504 | 0.90368 |
| 2 | 1.3316 | 1.2974 | 1.2199 | 1.0778 | 0.93118 | 0.89414 | 0.87033 | 0.85122 | 0.83414 | 0.81726 | 0.79628 | 0.76842 | 0.75635 | 0.75611 | 0.75051 |
| 3 | 1.3268 | 1.2895 | 1.2056 | 1.0515 | 0.888 | 0.84006 | 0.8059 | 0.77802 | 0.74723 | 0.71703 | 0.67918 | 0.62912 | 0.59866 | 0.5911 | 0.5911 |
| 4 | 1.3248 | 1.2889 | 1.2056 | 1.0486 | 0.87735 | 0.82273 | 0.78122 | 0.74277 | 0.70366 | 0.66062 | 0.6054 | 0.53096 | 0.47646 | 0.45235 | 0.44635 |
| 5 | 1.3013 | 1.2712 | 1.1955 | 1.0457 | 0.87734 | 0.82189 | 0.77793 | 0.73532 | 0.6899 | 0.63753 | 0.56782 | 0.47052 | 0.38952 | 0.3417 | 0.31852 |
| 6 | 1.2488 | 1.2289 | 1.1635 | 1.0284 | 0.87116 | 0.81968 | 0.77763 | 0.73512 | 0.68758 | 0.62986 | 0.54924 | 0.43119 | 0.32166 | 0.24269 | 0.18927 |
| 7 | 1.0785 | 1.0687 | 1.0272 | 0.92345 | 0.79692 | 0.76085 | 0.73175 | 0.70128 | 0.66516 | 0.61797 | 0.54601 | 0.43104 | 0.31442 | 0.21895 | 0.1414 |
| 8 | 0.64764 | 0.64734 | 0.63294 | 0.57596 | 0.50071 | 0.48872 | 0.48073 | 0.47221 | 0.4607 | 0.44252 | 0.40707 | 0.33665 | 0.25931 | 0.19248 | 0.13327 |
| 9 | 0.18664 | 0.18046 | 0.17972 | 0.15898 | 0.12677 | 0.1266 | 0.12648 | 0.12631 | 0.1263 | 0.12592 | 0.12111 | 0.099825 | 0.07372 | 0.052237 | 0.033383 |
| 10 | 0.093872 | 0.080794 | 0.080463 | 0.070886 | 0.052851 | 0.051785 | 0.048149 | 0.04372 | 0.039902 | 0.037928 | 0.037927 | 0.032118 | 0.02325 | 0.016361 | 0.010172 |
| 11 | 0.084091 | 0.067238 | 0.066937 | 0.059664 | 0.045689 | 0.043243 | 0.036997 | 0.02899 | 0.020911 | 0.014772 | 0.0133 | 0.012094 | 0.009154 | 0.007033 | 0.004936 |
| 12 | 0.080929 | 0.065855 | 0.06492 | 0.057463 | 0.040997 | 0.039674 | 0.034986 | 0.028299 | 0.020878 | 0.014566 | 0.012634 | 0.011834 | 0.00915 | 0.006598 | 0.002927 |
| 13 | 0.079986 | 0.065724 | 0.064879 | 0.068977 | 0.038795 | 0.038036 | 0.034289 | 0.028239 | 0.020576 | 0.013174 | 0.009832 | 0.009704 | 0.008319 | 0.006535 | 0.002261 |
| 14 | 0.079869 | 0.066639 | 0.064666 | 0.066972 | 0.037914 | 0.037444 | 0.034178 | 0.028154 | 0.019502 | 0.009185 | 0.002188 | 0.00165 | 0.001649 | 0.001646 | 0.000789 |
| 15 | 0.073303 | 0.061925 | 0.06152 | 0.051326 | 0.026419 | 0.026409 | 0.025392 | 0.022464 | 0.01702 | 0.008898 | 0.001945 | 0.000863 | 0.000633 | 2.89E-06 | 2.63E-27 |

Table AB.2 Example of "rresid" Matrix (RMS Values)

To illustrate this step the diagonal in Table AB.2, highlighted in red, is the results an 11 metre road width for one cross section. The matrix named *"na"* is used to extract the required data, and was created using the code *"na=a= = 11"*. This piece of code can be translated as "create a new matrix *"na"*, with the same dimensions as *"a"*, the diagonal in *"a"* with values equal to 11 are to be replaced in *"na"* with the numeral 1, all other entries are set to zero"(Table AB.3).

137

| From\To | 30 | 29 | 28 | 27 | 26 | 25 | 24 | 23 | 22 | 21 | 20 | 19 | 18 | 17 | 16 |
|---|---|---|---|---|---|---|---|---|---|---|---|---|---|---|---|
| 1 | 0 | 0 | 0 | 0 | 0 | 0 | 0 | 0 | 0 | 0 | 0 | 0 | 0 | 0 | 0 |
| 2 | 0 | 0 | 0 | 0 | 0 | 0 | 0 | 0 | 0 | 0 | 0 | 0 | 0 | 0 | 0 |
| 3 | 0 | 0 | 0 | 0 | 0 | 0 | 0 | 0 | 0 | 0 | 0 | 0 | 0 | 0 | 0 |
| 4 | 0 | 0 | 0 | 0 | 0 | 0 | 0 | 0 | 0 | 0 | 0 | 0 | 0 | 0 | 1 |
| 5 | 0 | 0 | 0 | 0 | 0 | 0 | 0 | 0 | 0 | 0 | 0 | 0 | 0 | 1 | 0 |
| 6 | 0 | 0 | 0 | 0 | 0 | 0 | 0 | 0 | 0 | 0 | 0 | 0 | 1 | 0 | 0 |
| 7 | 0 | 0 | 0 | 0 | 0 | 0 | 0 | 0 | 0 | 0 | 0 | 1 | 0 | 0 | 0 |
| 8 | 0 | 0 | 0 | 0 | 0 | 0 | 0 | 0 | 0 | 0 | 1 | 0 | 0 | 0 | 0 |
| 9 | 0 | 0 | 0 | 0 | 0 | 0 | 0 | 0 | 0 | 1 | 0 | 0 | 0 | 0 | 0 |
| 10 | 0 | 0 | 0 | 0 | 0 | 0 | 0 | 0 | 1 | 0 | 0 | 0 | 0 | 0 | 0 |
| 11 | 0 | 0 | 0 | 0 | 0 | 0 | 0 | 1 | 0 | 0 | 0 | 0 | 0 | 0 | 0 |
| 12 | 0 | 0 | 0 | 0 | 0 | 0 | 1 | 0 | 0 | 0 | 0 | 0 | 0 | 0 | 0 |
| 13 | 0 | 0 | 0 | 0 | 0 | 1 | 0 | 0 | 0 | 0 | 0 | 0 | 0 | 0 | 0 |
| 14 | 0 | 0 | 0 | 0 | 1 | 0 | 0 | 0 | 0 | 0 | 0 | 0 | 0 | 0 | 0 |
| 15 | 0 | 0 | 0 | 1 | 0 |  |  |  |  |  |  |  |  |  |  |

Table AB.3  Example of Matrix "na" (Mask)

This matrix forms a mask that can be combined with the matrix "rresid" (whatsse=rresid(na) ) which takes only those results relating to the 11 metre road width. The result is a single column matrix ("whatsse") from which the minimum value is taken

The final task is to determine the interval that this minimum refers by finding its location in the matrix "rresid". Because of the way the data is organised it is not possible to do this directly and a little manipulation is required. The Matlab function "Find" will give an index into the array where the value occurs in the form of a row and column number. Row values are in the correct order, but the column value will have to be adjusted. In Table AB.2 the smallest RMS value is the underlined value 0.020911 using this value combined with the "Find" function

*(find(rresid==(minsse)))* will give an index into *"rresid"*. The row index will be 11 and the column index 9, but by adding the road width to the row index value will give the correct location, the interval between 11m and 22m. This result is then written to a file and the complete process repeated for all cross sections.

# Appendix C

<u>Matlab Program Code</u>

See attached CD

# Appendix D

Excel Charts

See attached CD